

These notes are taken for the Compressible Flow course taught by Professor Emeritus J. Craig Dutton at the University of Illinois at Urbana-Champaign.

## Compressible Flow – Course Notes

### 1 Review of Thermodynamic and Fluid Mechanic Principles

#### 1.1 Thermodynamics of Ideal Gases

##### 1.1.1 Equation of State

A gas in which intermolecular forces are neglected is defined as an *ideal gas*. For an ideal gas pressure  $p$ , density  $\rho$  and temperature  $T$  are related by the following *equation of state*:

$$p = \rho RT \quad (1)$$

where  $R = R^0/M$  is the specific gas constant,  $R^0 = 8.314 \text{ J} \cdot \text{mol}^{-1} \cdot \text{K}^{-1}$  is the universal gas constant and  $M$  is the molecular weight of the gas. For air at standard conditions  $M = 28.966 \text{ g/mol}$ , hence  $R = 287 \text{ J} \cdot \text{kg}^{-1} \cdot \text{K}^{-1} = 53.35 \text{ ft} \cdot \text{lb}_f \cdot \text{lb}_m^{-1} \cdot {}^{\circ}\text{R}^{-1} = 1716 \text{ ft}^2 \cdot \text{s}^{-2} \cdot {}^{\circ}\text{R}^{-1}$ . For most compressible flow applications, as long as the pressure is not too high ( $P < 100 \text{ bar}$ ) and the temperature is not too low ( $T > 100 \text{ K}$ ), the assumption of perfect gas is accurate.

##### 1.1.2 Energy/Specific Heat Reactions

The internal energy of a gas is the sum of the energy of all its molecules (which can be stored in the form of translational, rotational, and vibrational motion). The specific internal energy  $e$  of a gas, *i.e.*, the internal energy per unit mass is related to the gas enthalpy by

$$h = e + pv = e + \frac{p}{\rho} = e + RT \quad (2)$$

where  $v = 1/\rho$  is the specific volume of the gas.

A *calorically perfect gas* is one in which the ideal gas equation of state (1) is satisfied and the specific internal energy and the enthalpy are linearly proportional to the temperature, that is

$$e = c_v T \quad (3)$$

$$h = c_p T \quad (4)$$

where  $c_v = \left(\frac{\partial e}{\partial T}\right)_p = \frac{de}{dT} = \text{const.}$  and  $c_p = \left(\frac{\partial h}{\partial T}\right)_p = \frac{dh}{dT} = \text{const.}$ , are the specific heats at constant volume<sup>1</sup> and constant pressure, respectively.

The differentials of  $e$  and  $h$  are

$$de = c_v dT \quad (5)$$

$$dh = c_p dT \quad (6)$$

Therefore, differentiating the definition of enthalpy (2), yields the well-known Mayer's relation for calorically perfect gas:

$$dh = de + RdT \Rightarrow c_p dT = c_v dT + RdT \Rightarrow c_p - c_v = R \quad (7)$$

<sup>1</sup> Note that  $\rho = 1/v$  so can use indifferently the notation  $(\dots)_\rho = (\dots)_v$  to indicate quantities “at constant density” or “at constant specific volume”.

Dividing (7) by  $c_p$  and defining  $\gamma \equiv c_p/c_v$  (adiabatic coefficient or ratio of specific heats,  $\gamma = 1.4$  for air at standard conditions) we have

$$1 - \frac{1}{\gamma} = \frac{R}{c_p} \Rightarrow c_p = \frac{\gamma R}{\gamma - 1} \quad (8)$$

Similarly, dividing (7) by  $c_v$  gives:

$$c_v = \frac{R}{\gamma - 1} \quad (9)$$

A *thermally perfect gas* is one in which the ideal gas equation of state (1) is satisfied and the internal energy is a sole – but not linear – function of the temperature, namely:

$$de = c_v(T)dT \Rightarrow e_2 - e_1 = \int_{T_1}^{T_2} c_v(T)dT \quad (10)$$

with  $c_v = c_v(T) = \left(\frac{\partial e}{\partial T}\right)_p = \frac{de}{dT} \neq \text{const.}$  a specific heat at constant volume varying with temperature. Eq. (7) still holds, therefore:

$$dh = de + d\left(\frac{P}{\rho}\right) = c_v dT + R_g dT = c_p(T) dT \Rightarrow h_2 - h_1 = \int_{T_1}^{T_2} c_p(T) dT \quad (11)$$

with  $c_p = c_p(T) \neq \text{const.}$  a specific heat at constant volume varying with temperature. Correspondingly, the adiabatic coefficient

$$\gamma = \gamma(T) = \frac{c_p(T)}{c_v(T)} = 1 + \frac{R}{c_v(T)} = \frac{1}{1 - \frac{R}{c_p(T)}} \quad (12)$$

is not constant and varies with  $T$ .

### 1.1.3 First Law of Thermodynamics

We define a fixed mass of gas as the *system* and the region outside the system as the *surrounding*, with the interface between the two being the *boundary*. The *first law of thermodynamics* states that the sum of the incremental heat  $\delta q$  added to the system and the incremental work  $\delta w$  done on the system by the surrounding, cause a change in internal energy

$$\delta q + \delta w = de \quad (13)$$

Note that  $e$  is a state variable, therefore here  $de$  is an exact differential, whereas  $\delta q$  and  $\delta w$  depend on the path in going from the initial to the final state. For an *adiabatic process* no heat is added or subtracted to the system, *i.e.*,  $\delta q = 0$ . For a *reversible process*, where dissipative effects of viscosity, thermal conductivity and mass diffusion are negligible, it can be shown that  $\delta w = -pdv$ , where  $dv$  is an incremental change in volume, therefore

$$\delta q - pdv = de \quad (14)$$

A process that is both adiabatic and reversible is called an *isentropic process*.

### 1.1.4 Second Law of Thermodynamics

The entropy  $s$  of a system is defined such that

$$ds = \frac{\delta q}{T} + ds_{irrev} \quad (15)$$

where  $ds_{irrev} > 0$  is the generation of entropy due to irreversible, dissipative processes and  $ds_{irrev} = 0$  for reversible processes. The *second law of thermodynamics* tells us that the entropy of the universe always increases, therefore for an isolated system

$$ds \geq \frac{\delta q}{T} \quad (16)$$

or  $ds \geq 0$  for adiabatic processes.

### 1.1.5 Entropy Changes/Isentropic Processes

The first and second laws of thermodynamics are conveniently used to calculate entropy changes for thermodynamic processes. For reversible processes, combining (14) and (16), we have

$$Tds = de + pdv = de + pd\left(\frac{1}{\rho}\right) = de - \frac{p}{\rho^2}d\rho = c_v dT - \frac{p}{\rho^2}d\rho \quad (17)$$

Using the equation of state (1) and dividing by  $T$ , (17) gives

$$Tds = c_v dT - \frac{RT}{\rho} d\rho \Rightarrow ds = c_v \frac{dT}{T} - R \frac{d\rho}{\rho} \quad (18)$$

Integrating:

$$\int_{s_1}^{s_2} ds = \int_{T_1}^{T_2} c_v \frac{dT}{T} - R \int_{\rho_1}^{\rho_2} \frac{d\rho}{\rho} \quad (19)$$

Alternatively, using the definition of enthalpy (2)

$$h = e + pv \Rightarrow dh = de + pdv + vdp \quad (20)$$

plugging it into (17) gives and dividing by  $T$

$$\begin{aligned} Tds = dh - pdv - vdp + pdv \Rightarrow Tds = dh - vdp \Rightarrow ds = c_p \frac{dT}{T} - \frac{v}{T} dp \Rightarrow \\ ds = c_p \frac{dT}{T} - R \frac{dp}{p} \end{aligned} \quad (21)$$

Integrating:

$$\int_{s_1}^{s_2} ds = \int_{T_1}^{T_2} c_p \frac{dT}{T} - R \int_{p_1}^{p_2} \frac{dp}{p} \quad (22)$$

For a calorically perfect gas  $c_p$ ,  $c_v$  and  $R$  are constant, therefore (19) and (22) yield

$$s_2 - s_1 = c_v \ln\left(\frac{T_2}{T_1}\right) - R \ln\left(\frac{\rho_2}{\rho_1}\right) \quad (23)$$

$$s_2 - s_1 = c_p \ln \left( \frac{T_2}{T_1} \right) - R \ln \left( \frac{p_2}{p_1} \right) \quad (24)$$

For *isentropic process*  $s_2 - s_1 = 0$ , therefore

$$c_p \ln \left( \frac{T_2}{T_1} \right) - R \ln \left( \frac{p_2}{p_1} \right) = 0 \Rightarrow \frac{R}{\gamma - 1} \ln \left( \frac{T_2}{T_1} \right) = R \ln \left( \frac{p_2}{p_1} \right) \quad (25)$$

$$c_p \ln \left( \frac{T_2}{T_1} \right) - R \ln \left( \frac{p_2}{p_1} \right) = 0 \Rightarrow \frac{\gamma R}{\gamma - 1} \ln \left( \frac{T_2}{T_1} \right) = R \ln \left( \frac{p_2}{p_1} \right) \quad (26)$$

which give:

$$\frac{T_2}{T_1} = \left( \frac{\rho_2}{\rho_1} \right)^{\gamma-1} \quad (27)$$

$$\frac{T_2}{T_1} = \left( \frac{p_2}{p_1} \right)^{\frac{\gamma-1}{\gamma}} \quad (28)$$

Equating (27) and (28):

$$\frac{p_2}{p_1} = \left( \frac{\rho_2}{\rho_1} \right)^{\gamma} = \left( \frac{T_2}{T_1} \right)^{\frac{\gamma}{\gamma-1}} \quad (29)$$

In conclusion, for isentropic processes:

$$\frac{p}{\rho^{\gamma}} = \text{const.} \quad (30)$$

#### 1.1.6 Speed of Sound and Mach Number

The speed of sound  $a$  of any substance is a thermodynamic derivative property, defined as

$$a = \left( \frac{\partial p}{\partial \rho} \right)_s^{1/2} \quad (31)$$

Because from (30)  $p/\rho^{\gamma} = \text{const.} = c \Rightarrow p = c\rho^{\gamma}$  for an isentropic process, then

$$a^2 = \left( \frac{\partial p}{\partial \rho} \right)_s = \left[ \frac{\partial (c\rho^{\gamma})}{\partial \rho} \right]_s = c\gamma\rho^{\gamma-1} = \frac{\gamma(c\rho^{\gamma})}{\rho} = \frac{\gamma p}{\rho} \quad (32)$$

that is

$$a = \left( \frac{\gamma p}{\rho} \right)^{1/2} = (\gamma RT)^{1/2} \quad (33)$$

This expression highlights that for a calorically perfect gas the speed of sound is only a function of temperature. For air at standard sea level:  $a = 340.29 \text{ m/s} = 1117 \text{ ft/s}$ .

The ratio of the local fluid velocity by the local speed of sound is the *Mach number*:

$$\text{Ma} \equiv \frac{U}{a} \quad (34)$$

Remember that  $a$  is not generally a constant but rather varies with  $T$  through the flowfield.

Based on the Mach number we identify the following regimes:

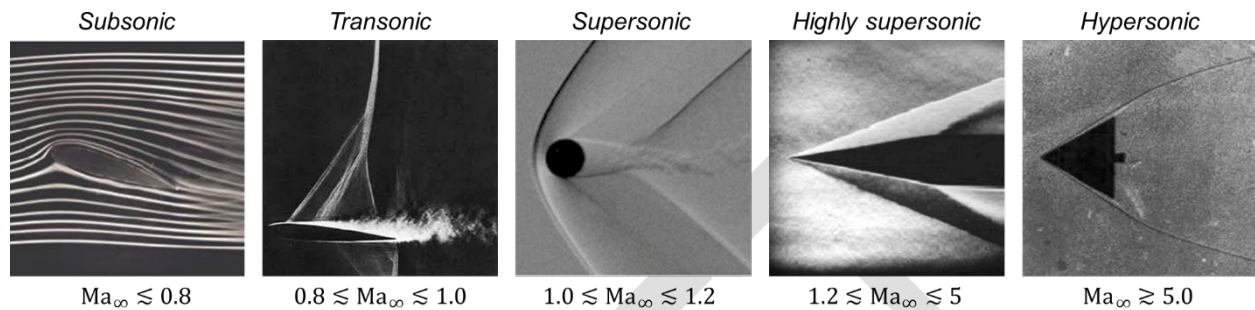


**Figure 1. Flow field around aerodynamic shapes at increasing freestream Mach number.**

### 1.1.7 Compressibility

Consider a fluid element of volume  $v$  at pressure  $p$ , subjected to an infinitesimal increase in pressure  $dp$  causing a corresponding change in volume  $dv$ . We define *compressibility*  $\tau$  the fractional change in volume of the fluid element per unity change of pressure:

$$\tau \equiv -\frac{1}{v} \frac{dv}{dp} = \frac{1}{\rho} \frac{dp}{dp} \quad (35)$$

For an isentropic process (not heat added to or removed from the fluid and no friction),  $\tau$  is defined as isentropic compressibility

$$\tau_s = -\frac{1}{v} \left( \frac{\partial v}{\partial p} \right)_s = \frac{1}{\rho} \left( \frac{\partial \rho}{\partial p} \right)_s = \frac{1}{\gamma p} \quad (36)$$

Combining (31) and (36) we find that the compressibility and speed of sound are related as

$$a = \left( \frac{1}{\rho \tau_s} \right)^{1/2} \quad (37)$$

## 1.2 Governing Equations

We define a fixed set of identifiable particles of fluid matter with constant mass as the systems (sys) followed throughout the analysis. We also define a control volume  $V(t)$  as a region of space which may or may not be moving with the flow and through which fluid may flow, with the control surface  $S$  being the geometric surface bounding the control volume. To derive the governing equations we write the equations in a known system form, we then apply the Reynold's Transport Theorem and finally obtain the corresponding equations in control volume form.

### 1.2.1 Reynold's Transport Theorem

The Reynold's transport theorem relates the time rate of change of an extensive property following a system to appropriate terms for a control volume, the latter form being more useful for flow problems. Let  $\Phi$  be an arbitrary extensive property (i.e. proportional to mass) of the fluid and  $\phi = d\Phi/dm$  the corresponding specific property, i.e. the amount of  $\Phi$  per unit mass. By considering the situation in which a system and control volume coincide at time  $t_0$  and an infinitesimal

increment of time  $\Delta t$  later during which the control volume remains fixed, but the system moves in the general direction of the mean streamlines, Reynolds' Transport Theorem (RTT) can be derived

$$\frac{d\Phi_{sys}(t)}{dt} = \frac{D\Phi}{Dt} = \frac{d}{dt} \int_{sys} \rho \phi dV = \frac{d}{dt} \int_V \rho \phi dV + \oint_S \rho \phi \vec{U} \cdot \hat{n} dS \quad (38)$$

which tells us that the time rate of change of an extensive property  $\Phi$  of a fluid system results from the time rate of change of  $\Phi$  within the control volume and the flux of  $\Phi$  through the control surface. Here  $D(\dots)/Dt$  is the substantial (or material) derivative,  $\vec{U}$  is the flow velocity and  $dS$  is an infinitesimal element of the control surface with normal  $\hat{n}$  pointing outward of the control surface. In (38),  $\vec{U}$  is measured with respect to the control volume.

### 1.2.2 Conservation of Mass

Choose:

$$\Phi = \text{mass} = m \quad (39)$$

$$\phi = \frac{d\Phi}{dm} = \frac{dm}{dm} = 1 \quad (40)$$

Physical principle: *mass can be neither created nor destroyed.*

System form:

$$m_{sys} = \text{const.} \Rightarrow \frac{dm_{sys}}{dt} = 0 \quad (41)$$

Applying the RTT to the LHS of (41) the **conservation of mass** is

$$\frac{d}{dt} \int_V \rho dV + \oint_S \rho \vec{U} \cdot \hat{n} dS = 0 \quad (42)$$

The sum of the time rate of change of the mass in the control volume and the next flux of mass through the control surface is equal to zero.

### 1.2.3 Conservation of Momentum

Choose:

$$\vec{\Phi} = \text{linear momentum} = \vec{P} \quad (43)$$

$$\vec{\phi} = \frac{d\vec{\Phi}}{dm} = \frac{d\vec{P}}{dm} = \vec{U} = \text{velocity} \quad (44)$$

Physical principle: *Force = time rate of change of momentum.*

System form:

$$\frac{d\vec{P}_{sys}}{dt} = \sum \vec{F} = \vec{F}_V + \vec{F}_S \quad (45)$$

with  $\vec{F}_V$  = body forces (e.g., gravity, electromagnetic forces, Coriolis forces, etc.) acting on the fluid within the control volume, and  $\vec{F}_S$  = surface forces (e.g., pressure and shear stress) active on the control surface).

Applying the RTT to the LHS of (45)

$$\frac{d}{dt} \int_V \rho \vec{U} dV + \oint_S \rho \vec{U} \vec{U} \cdot \hat{n} dS = \vec{F}_V + \vec{F}_S \quad (46)$$

Let us now evaluate the right-hand side of (46). We express the volume forces as:

$$\vec{F}_V = \int_V \rho \vec{f} dV \quad (47)$$

where  $\vec{f}$  is a specific force (i.e., force per unit mass, such as gravity for example), whereas the surface forces are the sum of pressure and viscous forces (shear and normal viscous stresses):

$$\vec{F}_S = - \oint_S p \hat{n} dS + \vec{F}_{\text{visc}} \quad (48)$$

Finally, plugging (47) and (48) into (46), we obtain the **conservation of linear momentum** as

$$\frac{d}{dt} \int_V \rho \vec{U} dV + \oint_S \rho \vec{U} \vec{U} \cdot \hat{n} dS = \int_V \rho \vec{f} dV - \oint_S p \hat{n} dS + \vec{F}_{\text{visc}} \quad (49)$$

The sum of the time rate of change of the momentum in the control volume and the next flux of momentum through the control surface is equal to the sum of the body forces, the pressure force and the viscous forces on the control volume.

#### 1.2.4 Conservation of Energy

Choose:

$$\Phi = \text{total energy} = E \quad (50)$$

$$\phi = \frac{d\Phi}{dm} = \frac{dE}{dm} = \epsilon = \text{specific total energy} \quad (51)$$

Physical principle: *energy can be neither created nor destroyed; it can only change in form.*

System form:

$$dE_{\text{sys}} = \delta Q + \delta W \quad (52)$$

Dividing by  $dt$  we can rewrite the principle on a rate base:

$$\frac{dE_{\text{sys}}}{dt} = \dot{Q} + \dot{W} \quad (53)$$

where

$$\dot{Q} = \text{heat transfer rate} \quad \begin{cases} \dot{Q} > 0 \text{ for heat transfer to the system} \\ \dot{Q} < 0 \text{ for heat transfer from the system} \end{cases} \quad (54)$$

$$\dot{W} = \text{work rate (power)} \quad \begin{cases} \dot{W} > 0 \text{ for work done on the system} \\ \dot{W} < 0 \text{ for work done by the system} \end{cases}$$

Applying the RTT to the LHS of (53)

$$\frac{d}{dt} \int_V \rho \epsilon dV + \oint_S \rho \epsilon \vec{U} \cdot \hat{n} dS = \dot{Q} + \dot{W} \quad (55)$$

Let us now evaluate the right-hand side of (55). Recall the different components of volume and surface forces in (47) and (48). Consider for example the first term  $dF_V = \rho \vec{f} dV$ , which is the body force on the infinitesimal volume  $dV$ . Multiplying by the velocity  $\vec{U}$  we obtain the associated power (rate of work), that is

$$dF_V \cdot \vec{U} = \rho \vec{f} \cdot \vec{U} dV \quad (56)$$

or for the entire volume:

$$\dot{W}_V = \int_V dF_V \cdot \vec{U} = \int_V \rho \vec{f} \cdot \vec{U} dV \quad (57)$$

We can do the same for all terms in (48) and obtain

$$\dot{W} = \int_V \rho \vec{f} \cdot \vec{U} dV - \oint_S p \vec{U} \cdot \hat{n} dS + \dot{W}_{\text{visc}} \quad (58)$$

For the heat rate (thermal power) we consider both a volume and surface contribution,  $\dot{Q} = \dot{Q}_V + \dot{Q}_S$ . The volume component is:

$$\dot{Q}_V = \int_V \rho \dot{q} dV \quad (59)$$

where  $\dot{q}$  is the thermal power per unit mass, whereas the surface component is the heat addition due to viscous effects  $\dot{Q}_S = \dot{Q}_{\text{visc}}$ . Therefore

$$\dot{Q} = \int_V \rho \dot{q} dV + \dot{Q}_{\text{visc}} \quad (60)$$

Plugging (58) and (60) into (55), we obtain

$$\begin{aligned} \frac{d}{dt} \int_V \rho \epsilon dV + \oint_S \rho \epsilon \vec{U} \cdot \hat{n} dS &= \\ &= \int_V \rho \dot{q} dV + \dot{Q}_{\text{visc}} + \int_V \rho \vec{f} \cdot \vec{U} dV - \oint_S p \vec{U} \cdot \hat{n} dS + \dot{W}_{\text{visc}} \end{aligned} \quad (61)$$

Lastly, we need to find a closure for the equation by defining what contributes to the specific total energy  $\epsilon$ . The total energy has a kinetic, internal and potential component, that is

$$\epsilon = \frac{|\vec{U}|^2}{2} + e + gz \quad (62)$$

Plugging (62) into (61) we obtain the **conservation of energy** as

$$\begin{aligned}
 \frac{d}{dt} \int_V \rho \left( \frac{|\vec{U}|^2}{2} + e + gz \right) dV + \oint_S \rho \left( \frac{|\vec{U}|^2}{2} + e + gz \right) \vec{U} \cdot \hat{n} dS = \\
 = \int_V \rho \dot{q} dV + \dot{Q}_{\text{visc}} + \int_V \rho \vec{f} \cdot \vec{U} dV - \oint_S p \vec{U} \cdot \hat{n} dS + \dot{W}_{\text{visc}}
 \end{aligned} \tag{63}$$

This is the conservation of energy in integral form.

### 1.2.5 Governing Equations Inviscid Compressible Flow

For an inviscid flow, compressible flow, with negligible changes in potential energy the conservation equations (42), (49), and (63) reduce to:

*Continuity:*

$$\frac{d}{dt} \int_V \rho dV + \oint_S \rho \vec{U} \cdot \hat{n} dS = 0 \tag{64}$$

*Momentum:*

$$\frac{d}{dt} \int_V \rho \vec{U} dV + \oint_S \rho \vec{U} \cdot \hat{n} dS = \int_V \rho \vec{f} dV - \oint_S p \hat{n} dS \tag{65}$$

*Energy:*

$$\begin{aligned}
 \frac{d}{dt} \int_V \rho \left( e + \frac{|\vec{U}|^2}{2} \right) dV + \oint_S \rho \left( e + \frac{|\vec{U}|^2}{2} \right) \vec{U} \cdot \hat{n} dS = \\
 = \int_V \rho \dot{q} dV + \int_V \rho \vec{f} \cdot \vec{U} dV - \oint_S p \vec{U} \cdot \hat{n} dS
 \end{aligned} \tag{66}$$

Equations (64)-(66), together with the equation of state (1) and the definition of internal energy (3), form a closed system of 5 equations in the 5 unknowns:  $p$ ,  $\vec{U}$ ,  $\rho$ ,  $T$  and  $e$ .

### 1.3 Static and Stagnation Properties

In high-speed, compressible gas flows, it is important to distinguish between the static and stagnation values of the thermodynamic properties  $p$ ,  $\rho$ ,  $T$ . In addition, we will find that the stagnation properties serve as useful reference values in our compressible flow analyses.

The static thermodynamic properties are those properties measured when moving along with the flow at the local fluid velocity  $\vec{U}$ , i.e., when there is no relative velocity between the observer and the flow. Thus, there is no flow deceleration involved in the measurement of static properties.

In order to define the stagnation properties and to relate them to the local static properties, consider the streamtube control volume shown below and assume: (1) steady flow, (2) no shear or shaft work, (3) negligible changes in gravitational potential energy, and (4) an adiabatic process. In this control volume, the flow is decelerated from local velocity  $\vec{U}$  and static properties  $p$ ,  $\rho$ ,  $T$  to zero velocity adiabatically (isentropically). In this latter state, the properties are labeled  $p_0$ ,  $\rho_0$ ,  $T_0$ .

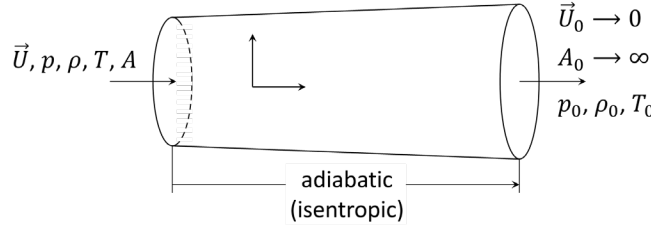


**Figure 2. Adiabatic processes within a streamtube control volume.**

Applying continuity (64):

$$\frac{d}{dt} \int_V \rho dV + \oint_S \rho \vec{U} \cdot \hat{n} dS = 0 \Rightarrow -\rho U A + \rho_0 U_0 A_0 = 0 \quad (67)$$

or

$$\dot{m} = \text{mass flow rate} = \rho U A = \rho_0 U_0 A_0 = \text{const. (in steady flow)} \quad (68)$$

Applying energy (66) and using (2):

$$\begin{aligned} & \frac{d}{dt} \int_V \rho \left( e + \frac{|\vec{U}|^2}{2} \right) dV + \oint_S \rho \left( e + \frac{|\vec{U}|^2}{2} \right) \vec{U} \cdot \hat{n} dS \\ &= \int_V \rho \dot{q} dV + \int_V \rho \vec{f} \cdot \vec{U} dV - \oint_S p \vec{U} \cdot \hat{n} dS \Rightarrow \\ & \Rightarrow \oint_S \rho \left( e + \frac{p}{\rho} + \frac{|\vec{U}|^2}{2} \right) \vec{U} \cdot \hat{n} dS = 0 \Rightarrow \oint_S \rho \left( h + \frac{|\vec{U}|^2}{2} \right) \vec{U} \cdot \hat{n} dS = 0 \\ & \Rightarrow - \left( h + \frac{U^2}{2} \right) (\rho U A) + \left( h_0 + \frac{U_0^2}{2} \right) (\rho_0 U_0 A_0) = 0 \end{aligned} \quad (69)$$

Noting that  $U_0 \rightarrow 0$  and that from continuity  $\rho U A = \rho_0 U_0 A_0$  (69) simplifies to

$$- \left( h + \frac{U^2}{2} \right) (\rho U A) + \left( h_0 + \frac{U_0^2}{2} \right) (\rho_0 U_0 A_0) = 0 \quad (70)$$

or

$$h_0 = \text{stagnation enthalpy} = h + \frac{U^2}{2} = \text{const. (in steady, adiabatic flow)} \quad (71)$$

Using (11), for a calorically perfect gas

$$h_0 - h = c_p (T_0 - T) \quad (72)$$

Substituting above:

$$c_p T_0 = c_p T + \frac{U^2}{2} \Rightarrow T_0 = T + \frac{U^2}{2c_p} \quad (73)$$

or

$$\frac{T_0}{T} = 1 + \frac{U^2}{2c_p T} \quad (74)$$

Substituting (8) into (74):

$$\frac{T_0}{T} = 1 + \frac{\gamma - 1}{2} \frac{U^2}{\gamma RT} \quad (75)$$

Using (33):

$$\frac{T_0}{T} = 1 + \frac{\gamma - 1}{2} Ma^2 \quad (76)$$

From this derivation, we see that the stagnation temperature  $T_0$  (sometimes referred to as total temperature  $T_t$ ) is the temperature measured when the flow is decelerated adiabatically to zero velocity. In addition, the stagnation temperature in a steady, adiabatic flow is constant, and the relation between the local static and stagnation temperatures is that given above. If, in addition to being adiabatic, the deceleration is also reversible, *i.e.*, isentropic, we can use the previously derived isentropic relations to relate the stagnation pressure  $p_0$  and stagnation density  $\rho_0$  to their corresponding static values,  $p$  and  $\rho$ .

$$\frac{p_0}{p} = \left( \frac{T_0}{T} \right)^{\frac{1}{\gamma-1}} = \left( 1 + \frac{\gamma - 1}{2} Ma^2 \right)^{\frac{1}{\gamma-1}} \quad (77)$$

$$\frac{\rho_0}{\rho} = \left( \frac{T_0}{T} \right)^{\frac{1}{\gamma-1}} = \left( 1 + \frac{\gamma - 1}{2} Ma^2 \right)^{\frac{1}{\gamma-1}} \quad (78)$$

From those expressions we see that the stagnation pressure  $p_0$  and stagnation density  $\rho_0$  (or  $p_t$  and  $\rho_0$ ) are those values measured when the flow is decelerated isentropically to zero velocity.

These relations for  $p_0/p$ ,  $\rho_0/\rho$ , and  $T_0/T$  are tabulated in most fluid mechanics and gas dynamics texts as a function of  $Ma$  for  $\gamma = 1.4$ . These are called the Isentropic Flow Tables and can be found in the well known NACA 1135 report<sup>2</sup>. The stagnation properties  $p_0$ ,  $\rho_0$ ,  $T_0$  are local point functions which can always be determined given the local static properties  $p$ ,  $\rho$ ,  $T$  and the Mach number  $Ma$ . In general,  $p_0$ ,  $\rho_0$ ,  $T_0$  may vary from point-to-point in a compressible flow, but by knowing their variation, we gain a good deal of qualitative information, *e.g.*, if  $T_0$  is constant, the flow is adiabatic, etc.

<sup>2</sup> <https://www.grc.nasa.gov/www/BGH/Images/naca1135.pdf>

## 2 One-dimensional Wave Motion; Normal Shock Wave

### 2.1 Introduction

A normal shock (NS) wave is a thin  $\mathcal{O}(10^{-5}$  in) planar discontinuity across which finite usually large changes in velocity, pressure, temperature, etc. occur. It is the NS wave that we will now study.

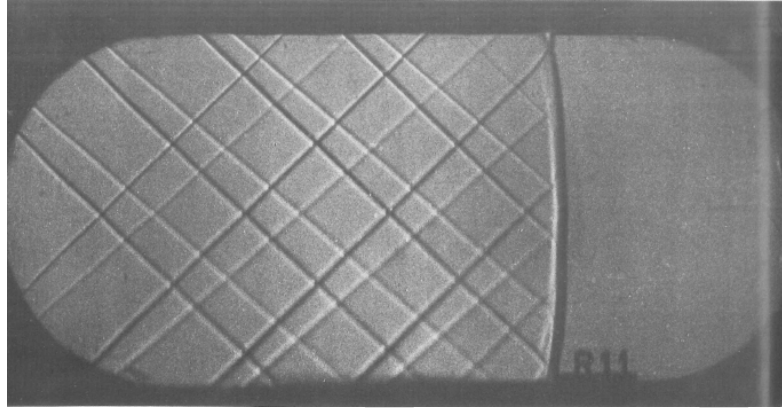


**Figure 3.** Normal-shock wave at  $Ma = 1.5$ . A pattern of pairs of weak oblique shock waves is produced by strips of tape on the floor and ceiling of a supersonic nozzle. They terminate at an almost straight and NS wave, showing that the flow is subsonic downstream. U. S. Air Force photograph, courtesy of Arnold Engineering Development Center.

Consider the piston-cylinder arrangement shown in Figure 4. If we give the piston an infinitesimal increment of velocity  $dU_1$ , to the right, an acoustic (sound) wave will propagate into the undisturbed fluid at the speed of the sound  $a_1$  relative to the fluid it moves into. Since fluid “piles up” at the piston face due to its motion, the density, pressure and temperature behind this first wave are higher than in front and its velocity is  $dU_1$ . Now, if the piston gives a second increment of velocity  $dU_2$  to the right, a second wave will move to the right. However, it will move at a higher absolute velocity ( $a_2 + dU_1$ ) with respect to the cylinder walls than the first wave because the fluid into which it moves is already moving to the right at  $dU_1$ , and since this fluid has been compressed by the passage of the first wave and therefore has a higher temperature and speed of sound ( $a_2 > a_1$ ). A third wave will move even faster ( $a_3 + dU_1 + dU_2$ ) than a second, etc. Eventually, the faster moving trailing waves will overtake and coalesce (combine) with the leading waves in a nonlinear manner with the result being a single, finite, *normal shock wave* that can be modeled as a discontinuity. For a final piston velocity  $U$ , which is the summation of an infinite number of infinitesimals  $dU_i$ , the situation eventually looks like that shown in Figure 5.

Compression waves tend to coalesce to form a single finite compression wave (NS wave).

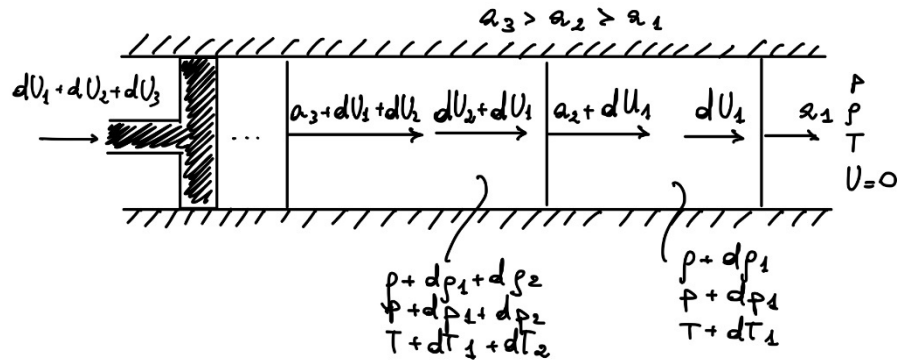


Figure 4. Progressive compression in piston-cylinder system.

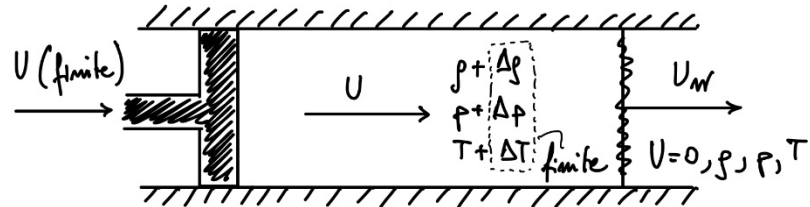


Figure 5. Compression waves tend to coalesce to form a single finite compression wave (NS wave).

On the other hand, if we move the piston to the left (Figure 6), successive acoustic *expansion* waves will propagate to the right at the speed of sound relative to the fluid they move into. The first wave induces a velocity to the left at  $dU_1$ , and lift the temperature, pressure, and density two  $T - T_1$ ,  $p - dp_1$  and  $\rho - d\rho_1$ . Therefore, the second wave will move at a lower absolute velocity ( $a_2 - dU_1$ ) than the first because it is moving into the fluid that is itself moving to the left at  $dU_1$ , and the fluid into which it is moving has been expanded and its temperature lowered by the passage of the first wave,  $a_2 < a_1$ . A third wave will move slower ( $a_3 - dU_1 - dU_2$ ) than the second, etc. Therefore, for a finite piston velocity  $U$  to the left, the expansion waves will spread out and will not coalesce (Figure 7).

Expansion waves spread out (diverge) and do not coalesce.

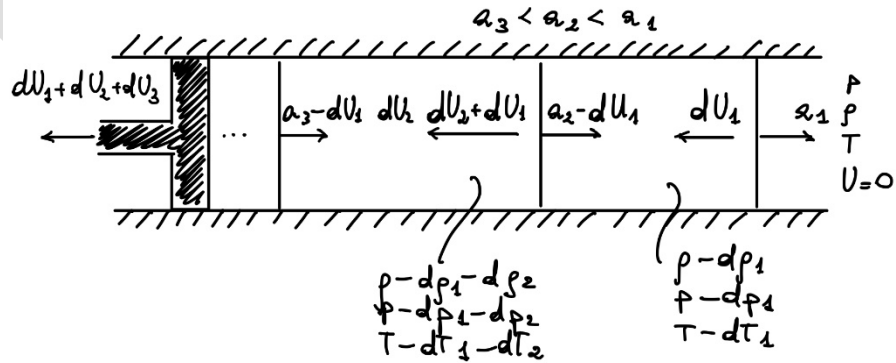


Figure 6. Progressive compression in piston-cylinder system.

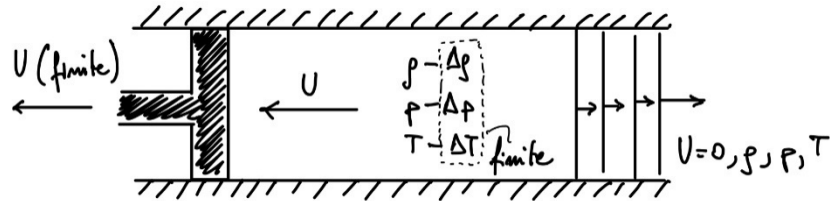


Figure 7. Expansion waves spread out (diverge) and do not coalesce.

## 2.2 Normal Shock Wave Analysis

We will now do the analysis for the finite (coalesced) compression NS wave. Most books do separate analyses for moving and stationary waves, but we will just do a single, general analysis for the moving case, which has the stationary wave as a special case. In addition, we will obtain information about infinitesimal acoustic waves along the way.

Consider the situation shown in Figure 8 in which the wave moves to the right at constant velocity  $U_w$  in the absolute ( $X, Y$ ) reference frame. By definition  $X$  is assumed positive in the direction of  $U_w$  and the absolute velocity  $U_1$  and  $U_2$  of the undisturbed and disturbed regions are also assumed positive. We must assume  $U_w > U_1$ , however, so that the wave overruns the undisturbed fluid.

Objective: for purposes of the analysis, assume that the undisturbed properties  $U_1, p_1, \rho_1, T_1$  are known, and it is the properties in the disturbed region  $U_2, p_2, \rho_2, T_2$  that we want to solve for.

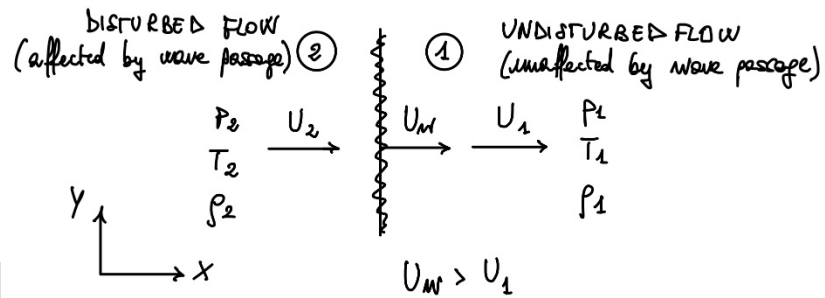


Figure 8. Disturbed and undisturbed flow across a NS wave moving at a velocity  $U_w$

In this absolute ( $X, Y$ ) reference frame, we have an unsteady problem. We then convert it to a steady flow problem by attaching the observer/coordinate system ( $x, y$ ) to the wave, i.e., we add  $U_w$  to the left everywhere, as shown in Figure 9.

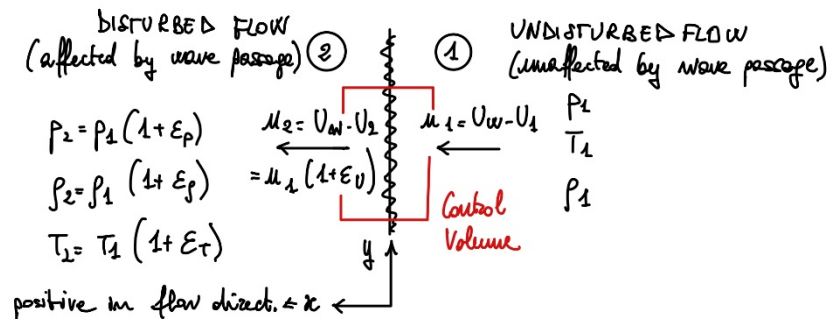


Figure 9. Modified (steady) reference frame for the analysis of the flow across a NS wave.

Also, defined the finite  $\varepsilon_\alpha$  operators, as

$$\varepsilon_\alpha = \frac{\alpha_2 - \alpha_1}{\alpha_1} = \frac{\alpha_2}{\alpha_1} - 1 \Rightarrow \alpha_2 = \alpha_1(1 + \varepsilon_\alpha) \quad (79)$$

with  $\alpha = [U, p, \rho, T]$ . Thus, the problem of finding the disturbed properties, is now transformed to finding the  $\varepsilon_\alpha$ . Also, note that the  $\varepsilon_\alpha$  are not infinitesimal in general, so higher order terms (H.O.T.) cannot be discarded.

Assumptions:

- (1) steady,
- (2) uniform, 1D flow on both undisturbed and disturbed sides,
- (3) neglect friction,
- (4) neglect body forces,
- (5) adiabatic,
- (6) neglect gravitational potential energy,
- (7) wave is thin, *i.e.*, control volume of constant, unit area  $A = 1$ ,
- (8) calorically perfect gas.

### 2.2.1 Governing Equations

We apply the governing equations (64)-(66) to the control volume shown in Figure 9. From continuity (64) we obtain

$$\begin{aligned} \cancel{\frac{d}{dt} \int_V p dV} + \oint_S \rho \vec{U} \cdot \hat{n} dS &= 0 \Rightarrow \\ \Rightarrow -\rho_1 u_1 + \rho_1(1 + \varepsilon_\rho) u_1 (1 + \varepsilon_U) &= 0 \Rightarrow \\ \Rightarrow \rho_1 u_1 [-1 + (1 + \varepsilon_\rho)(1 + \varepsilon_U)] &= 0 \Rightarrow \\ \Rightarrow -1 + 1 + \varepsilon_\rho + \varepsilon_U + \varepsilon_\rho \varepsilon_U &= 0 \end{aligned} \quad (80)$$

or

$$\varepsilon_\rho + \varepsilon_U + \varepsilon_\rho \varepsilon_U = 0 \quad (81)$$

From  $x$ -momentum conservation (65) we obtain

$$\begin{aligned} \cancel{\frac{d}{dt} \int_V \rho \vec{U} dV} + \oint_S \rho \vec{U} \cdot \hat{n} dS &= \cancel{\int_V \rho \vec{f} dV} - \oint_S p \hat{n} dS \Rightarrow \\ \Rightarrow p_1 - p_1(1 + \varepsilon_p) &= -\rho_1 u_1 u_1 + \rho_1(1 + \varepsilon_\rho)(u_1(1 + \varepsilon_U))(u_1(1 + \varepsilon_U)) \Rightarrow \\ \Rightarrow p_1(1 - 1 - \varepsilon_p) &= \rho_1 u_1^2 [-1 + (1 + \varepsilon_\rho)(1 + \varepsilon_U)(1 + \varepsilon_U)] \end{aligned} \quad (82)$$

Since  $(1 + \varepsilon_\rho)(1 + \varepsilon_U) = 1$  from continuity, then (82) gives

$$-p_1 \varepsilon_p = \rho_1 u_1^2 (-1 + 1 + \varepsilon_U) \Rightarrow \varepsilon_p + \frac{\rho_1 u_1^2}{p_1} \varepsilon_U = 0 \quad (83)$$

or

$$\varepsilon_p + \gamma M a_1^2 \varepsilon_U = 0 \quad (84)$$

From *energy* conservation (66):

$$\begin{aligned}
& \cancel{\frac{d}{dt} \int_V \left( e + \frac{|\vec{U}|^2}{2} \right) dV} + \oint_S \rho \left( e + \frac{|\vec{U}|^2}{2} \right) \vec{U} \cdot \hat{n} dS \\
&= \cancel{\int_V \rho \dot{q} dV} + \cancel{\int_V \rho \vec{f} \cdot \vec{U} dV} - \oint_S p \vec{U} \cdot \hat{n} dS \\
&\Rightarrow \oint_S \rho \left( h + \frac{|\vec{U}|^2}{2} \right) \vec{U} \cdot \hat{n} dS = 0 \Rightarrow \quad (85) \\
&\Rightarrow \oint_S \rho \left( T + \frac{|\vec{U}|^2}{2c_p} \right) \vec{U} \cdot \hat{n} dS = 0 \Rightarrow \\
&\Rightarrow -\rho_1 \left( T_1 + \frac{u_1^2}{2c_p} \right) u_1 + \rho_1 (1 + \varepsilon_p) \left[ T_1 (1 + \varepsilon_T) + \frac{u_1^2 (1 + \varepsilon_U)^2}{2c_p} \right] u_1 (1 + \varepsilon_U) = 0
\end{aligned}$$

Since  $(1 + \varepsilon_p)(1 + \varepsilon_U) = 1$  from continuity, then (85) gives

$$\begin{aligned}
& -\rho_1 u_1 \left( T_1 + \frac{u_1^2}{2c_p} \right) + \rho_1 u_1 \left[ T_1 (1 + \varepsilon_T) + \frac{u_1^2 (1 + \varepsilon_U)^2}{2c_p} \right] = 0 \Rightarrow \quad (86) \\
& \Rightarrow T_1 (-1 + 1 + \varepsilon_T) + \frac{u_1^2}{2c_p} (-1 + 1 + 2\varepsilon_U + \varepsilon_U^2) = 0
\end{aligned}$$

Dividing by  $T_1$  and using (8):

$$\varepsilon_T + \left( \frac{\gamma - 1}{2} \right) \frac{u_1^2}{\gamma R T_1} (2\varepsilon_U + \varepsilon_U^2) = 0 \quad (87)$$

or

$$\varepsilon_T + \left( \frac{\gamma - 1}{2} \right) \text{Ma}_1^2 (2\varepsilon_U + \varepsilon_U^2) = 0 \quad (88)$$

Using the equation of state (1) for the undisturbed flow:

$$p_1 = \rho_1 R T_1 \quad (89)$$

while for the disturbed flow:

$$p_1 (1 + \varepsilon_p) = \rho_1 (1 + \varepsilon_p) R T_1 (1 + \varepsilon_T) \quad (90)$$

Dividing (90) by (89):

$$\varepsilon_p - \varepsilon_p - \varepsilon_T - \varepsilon_p \varepsilon_T = 0 \quad (91)$$

Equations (81), (84), (88), (91) form a system of 4 nonlinear algebraic equations in the 4 unknowns  $\varepsilon_U$ ,  $\varepsilon_p$ ,  $\varepsilon_p$ ,  $\varepsilon_T$  with  $\text{Ma}_1^2$  and  $\gamma$  treated as known independent variables. It is these four equations that we will now need to solve for the  $\varepsilon_\alpha$ .

### 2.2.2 Strong Waves

Since these algebraic equations are nonlinear, standard techniques for linear algebra do not apply, and we have to be creative. Our technique is to solve continuity for  $\varepsilon_\rho$ , momentum for  $\varepsilon_p$ , and energy for  $\varepsilon_T$  as functions of  $\gamma$  and  $\text{Ma}_1$ . Then substitute these into the equation of state to solve for  $\varepsilon_U$ . We then back-substitute into continuity, momentum, energy to find  $\varepsilon_p$ ,  $\varepsilon_\rho$ ,  $\varepsilon_T$  as  $f(\gamma, \text{Ma}_1)$ .

From (81):

$$\varepsilon_\rho + \varepsilon_U + \varepsilon_\rho \varepsilon_U = 0 \Rightarrow \varepsilon_\rho = -\frac{\varepsilon_U}{(1 + \varepsilon_U)} \quad (92)$$

From(84):

$$\varepsilon_p + \gamma \text{Ma}_1^2 \varepsilon_U = 0 \Rightarrow \varepsilon_p = -\gamma \text{Ma}_1^2 \varepsilon_U \quad (93)$$

From (88):

$$\varepsilon_T + \left(\frac{\gamma - 1}{2}\right) \text{Ma}_1^2 (2\varepsilon_U + \varepsilon_U^2) = 0 \Rightarrow \varepsilon_T = -\left(\frac{\gamma - 1}{2}\right) \text{Ma}_1^2 (2\varepsilon_U + \varepsilon_U^2) \quad (94)$$

Substituting into (91)

$$\begin{aligned} -\gamma \text{Ma}_1^2 \varepsilon_U + \frac{\varepsilon_U}{(1 + \varepsilon_U)} + \left(\frac{\gamma - 1}{2}\right) \text{Ma}_1^2 (2\varepsilon_U + \varepsilon_U^2) - \frac{\varepsilon_U}{(1 + \varepsilon_U)} \left(\frac{\gamma - 1}{2}\right) \text{Ma}_1^2 (2\varepsilon_U + \varepsilon_U^2) \\ = 0 \end{aligned} \quad (95)$$

The first thing we would do is multiply through by the factor  $(1 + \varepsilon_U)$  to clear the denominator, so this looks like a cubic equation. However, there is a common factor of  $\varepsilon_U$  in every term, and we are not interested in the trivial solution  $\varepsilon_U = 0$ , so we can cancel it. The remaining quadratic terms cancel, so the solution is linear in  $\varepsilon_U$ . After some algebra:

$$\varepsilon_U = \frac{u_2 - u_1}{u_1} = \frac{u_2}{u_1} - 1 = -\left(\frac{2}{\gamma + 1}\right) \frac{\text{Ma}_1^2 - 1}{\text{Ma}_1^2} \quad (96)$$

or

$$\frac{u_2}{u_1} = 1 + \varepsilon_U = 1 - \left(\frac{2}{\gamma + 1}\right) \frac{\text{Ma}_1^2 - 1}{\text{Ma}_1^2} \quad (97)$$

Back-substituting (97) into (92):

$$\varepsilon_\rho = -\frac{\varepsilon_U}{(1 + \varepsilon_U)} = \frac{\left(\frac{2}{\gamma + 1}\right) \frac{\text{Ma}_1^2 - 1}{\text{Ma}_1^2}}{1 - \left(\frac{2}{\gamma + 1}\right) \frac{\text{Ma}_1^2 - 1}{\text{Ma}_1^2}} = \frac{\rho_2}{\rho_1} - 1 \quad (98)$$

which gives

$$\frac{\rho_2}{\rho_1} = 1 + \varepsilon_\rho = \left[1 - \left(\frac{2}{\gamma + 1}\right) \frac{\text{Ma}_1^2 - 1}{\text{Ma}_1^2}\right]^{-1} \quad (99)$$

Back-substituting (97) into (93):

$$\varepsilon_p = -\gamma Ma_1^2 \varepsilon_U = \left( \frac{2\gamma}{\gamma+1} \right) (Ma_1^2 - 1) = \frac{p_2}{p_1} - 1 \quad (100)$$

which gives

$$\frac{p_2}{p_1} = 1 + \varepsilon_p = 1 + \left( \frac{2\gamma}{\gamma+1} \right) (Ma_1^2 - 1) \quad (101)$$

Back-substituting (97) into (94), after some algebra:

$$\varepsilon_T = \left[ \frac{2(\gamma-1)}{(\gamma+1)^2} \right] \left( \frac{Ma_1^2 - 1}{Ma_1^2} \right) (\gamma Ma_1^2 + 1) = \frac{T_2}{T_1} - 1 \quad (102)$$

which gives

$$\frac{T_2}{T_1} = 1 + \varepsilon_T = 1 + \left[ \frac{2(\gamma-1)}{(\gamma+1)^2} \right] \left( \frac{Ma_1^2 - 1}{Ma_1^2} \right) (\gamma Ma_1^2 + 1) \quad (103)$$

An important parameter that we need is  $Ma_1$ , the Mach number of the disturbed or downstream fluid relative to the wave. Using continuity, *i.e.*,  $\rho_1 u_1 = \rho_2 u_2$

$$\frac{Ma_2^2}{Ma_1^2} = \frac{u_2^2 / (\gamma p_2 / \rho_2)}{u_1^2 / (\gamma p_1 / \rho_1)} = \frac{u_2/p_2}{u_1/p_1} = \frac{u_2/u_1}{p_2/p_1} \quad (104)$$

which gives

$$Ma_2^2 = Ma_1^2 \frac{1 + \varepsilon_U}{1 + \varepsilon_p} = \frac{Ma_1^2 + \left( \frac{2}{\gamma-1} \right)}{\left( \frac{2\gamma}{\gamma-1} \right) Ma_1^2 - 1} \quad (105)$$

Now let us investigate the stagnation properties. Note that these depend on the reference frame because they depend on the deceleration to zero velocity. Using (77) we find:

$$\frac{p_{02}}{p_{01}} = \frac{p_{02}/p_2}{p_{01}/p_1} \frac{p_2}{p_1} = \frac{\left( 1 + \frac{\gamma-1}{2} Ma_2^2 \right)^{\frac{\gamma}{\gamma-1}}}{\left( 1 + \frac{\gamma-1}{2} Ma_1^2 \right)^{\frac{\gamma}{\gamma-1}}} \left[ 1 + \left( \frac{2\gamma}{\gamma+1} \right) (Ma_1^2 - 1) \right] \quad (106)$$

After some algebra (106) gives:

$$\frac{p_{02}}{p_{01}} = \left( \frac{\frac{\gamma+1}{2} Ma_1^2}{1 + \frac{\gamma-1}{2} Ma_1^2} \right)^{\frac{\gamma}{\gamma-1}} \left( \frac{2\gamma}{\gamma+1} Ma_1^2 - \frac{\gamma-1}{\gamma+1} \right)^{\frac{-1}{\gamma-1}} \quad (107)$$

Also, going back to the energy equation (85), since  $T_0 = T + \frac{u_1^2}{2c_p}$ , we find:

$$\oint_S \rho \left( T + \frac{|\vec{U}|^2}{2c_p} \right) \vec{U} \cdot \hat{n} dS = 0 \Rightarrow -\rho_1 T_{01} u_1 + \rho_2 T_{02} u_2 = 0 \quad (108)$$

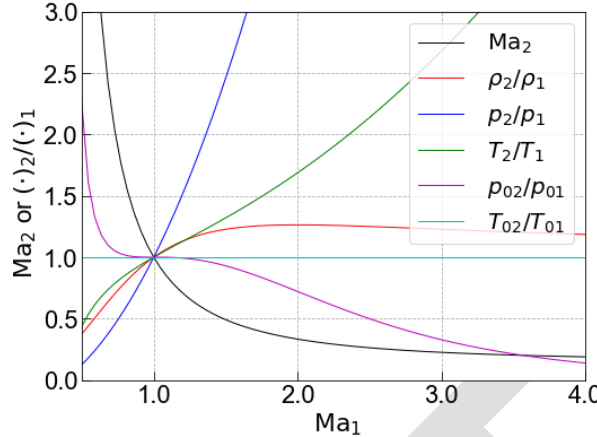


**Figure 10. Behavior of flow properties across a NS wave.  $Ma_1 < 1$  (expansion shock),  $Ma_1 > 1$  (compression shock).**

Then, because of continuity:

$$T_{01} = T_{02} \quad (109)$$

which tells us that for a steady, adiabatic, calorically perfect gas the stagnation temperature remains constant across the shock. Remember, however, that these results for the stagnation properties apply only in the reference frame relative to the wave. Previously, we defined a stagnation temperature as the temperature measured when adiabatically decelerate the flow to zero velocity, and similarly for the stagnation pressure with isentropic deceleration. Thus, these properties depend on the reference frame/coordinate system because they depend on the velocity.

The results above for  $p_0$  and  $T_0$  apply only in the steady, relative reference frame. On the other hand, the static thermodynamic properties are independent of the reference frame, so those results are generally applicable. These equations for  $Ma_2^2$ ,  $\frac{p_2}{p_1}$ ,  $\frac{\rho_2}{\rho_1}$ ,  $\frac{T_2}{T_1}$ ,  $\frac{p_{02}}{p_{01}}$ , and  $\frac{p_2}{p_{02}}$  are summarized in

Table 1, plotted in Figure 10 and tabulated in the handout tables for ease of use, on exams and homework, for  $\gamma = 1.4$ . Oftentimes you may be given values of these parameters and want to calculate  $Ma_1$ . But not all these equations are explicitly invertible for the Mach number  $Ma_1$ , so the tables are useful for that, as well. There is also many software available on the web that allows calculating for all these quantities (in either direction usually). Careful though, the notation for the upstream/undisturbed side and downstream/disturbed side might be different.

**Table 1. NS functions**

$$\frac{\rho_2}{\rho_1} = 1 + \varepsilon_\rho = \left[ 1 - \left( \frac{2}{\gamma + 1} \right) \frac{Ma_1^2 - 1}{Ma_1^2} \right]^{-1} \quad (110)$$

$$\frac{p_2}{p_1} = 1 + \varepsilon_p = 1 + \left( \frac{2\gamma}{\gamma + 1} \right) (Ma_1^2 - 1) \quad (111)$$

$$\frac{T_2}{T_1} = 1 + \varepsilon_T = 1 + \left[ \frac{2(\gamma - 1)}{(\gamma + 1)^2} \right] \left( \frac{Ma_1^2 - 1}{Ma_1^2} \right) (\gamma Ma_1^2 + 1) \quad (112)$$

$$Ma_2^2 = Ma_1^2 \frac{1 + \varepsilon_U}{1 + \varepsilon_p} = \frac{Ma_1^2 + \left(\frac{2}{\gamma-1}\right)}{\left(\frac{2\gamma}{\gamma-1}\right) Ma_1^2 - 1} \quad (113)$$

$$\frac{p_{02}}{p_{01}} = \left( \frac{\frac{\gamma+1}{2} Ma_1^2}{1 + \frac{\gamma-1}{2} Ma_1^2} \right)^{\frac{\gamma}{\gamma-1}} \left( \frac{2\gamma}{\gamma+1} Ma_1^2 - \frac{\gamma-1}{\gamma+1} \right)^{\frac{-1}{\gamma-1}} \quad (114)$$

$$T_{01} = T_{02} \quad (115)$$

$$\frac{p_1}{p_{02}} = \frac{\left( \frac{2\gamma}{\gamma+1} Ma_1^2 - \frac{\gamma-1}{\gamma+1} \right)^{\frac{1}{\gamma-1}}}{\left( \frac{\gamma+1}{2} Ma_1^2 \right)^{\frac{\gamma}{\gamma-1}}} \quad (116)$$

Obviously in using these equations and tables it is most convenient if we know  $Ma_1 = Ma_x$ .

Also, in looking at the normal shock tables, we see that they start at  $Ma_1 = Ma_x = 1$ . Why? to answer such question let us investigate the entropy change across the shock. From (24), using (8):

$$s_2 - s_1 = c_p \ln \left( \frac{T_2}{T_1} \right) - R \ln \left( \frac{p_2}{p_1} \right) \Rightarrow \frac{s_2 - s_1}{R} = \ln \left( \frac{T_2}{T_1} \right)^{\frac{\gamma}{\gamma-1}} - \ln \left( \frac{p_2}{p_1} \right) \quad (117)$$

Since the static and stagnation states have the same entropy we can rewrite (24) as

$$\begin{aligned} \frac{s_2 - s_1}{R} &= \ln \left( \frac{T_{02}}{T_{01}} \right)^{\frac{\gamma}{\gamma-1}} - \ln \left( \frac{p_{02}}{p_{01}} \right) \\ &= - \ln \left[ \left( \frac{\frac{\gamma+1}{2} Ma_1^2}{1 + \frac{\gamma-1}{2} Ma_1^2} \right)^{\frac{\gamma}{\gamma-1}} \left( \frac{2\gamma}{\gamma+1} Ma_1^2 - \frac{\gamma-1}{\gamma+1} \right)^{\frac{-1}{\gamma-1}} \right] \end{aligned} \quad (118)$$

Note that we have used that  $\frac{T_{02}}{T_{01}} = 1$ . Therefore:

$$\frac{\Delta s}{R} = f(\gamma, Ma_1) \quad (119)$$

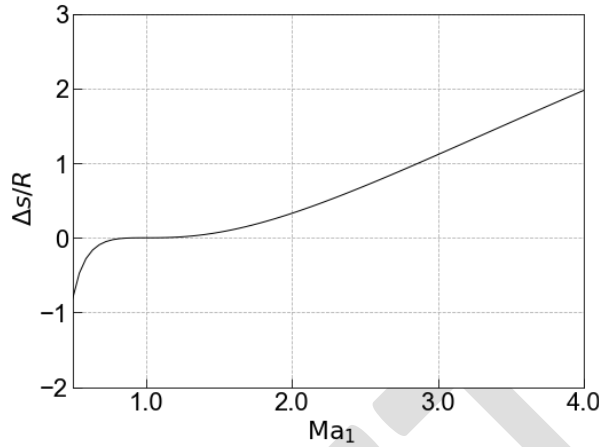
This function is plotted in

Figure 11. We have  $\Delta s/R < 0$  for expansion shocks,  $\Delta s/R > 0$  for compression shocks, and  $\Delta s/R = 0$  for  $Ma_1 = 1$  (weak waves). Recall now the Second Law of Thermodynamics (cf. section 1.1.4), which tells us that  $ds \geq 0$  for adiabatic process. If we apply the RTT to the second law of thermodynamics we obtain

$$\begin{aligned} \frac{d}{dt} \int_V \rho s dV + \oint_S \rho s \vec{U} \cdot \hat{n} dS - \oint_S \frac{\dot{q}''}{T} dS &\geq 0 \Rightarrow \\ \Rightarrow -\rho_1 u_1 s_1 + \rho_2 u_2 s_2 &\geq 0 \end{aligned} \quad (120)$$

which becomes (because of continuity):

$$(s_2 - s_1) \geq 0 \quad (121)$$



**Figure 11.** Expansion shocks ( $Ma_1 < 1$ ) are not possible because they violate the second law of thermodynamics (recall that entropy cannot decrease...).

We note that only  $Ma_1 \geq 1$  (compression shocks and unit Mach number) is possible, while expansion shocks are impossible. Note also that, because  $\frac{\Delta s}{R} = -\ln\left(\frac{p_{02}}{p_{01}}\right)$ , an increase in entropy across a NS wave is equivalent to a loss in stagnation pressure. In general, in steady, adiabatic, calorically perfect gas flows, we may use the losses that measure pressure as a measure of the irreversibilities present, since stagnation pressure generally has more physical meaning (measurable) than does entropy.

The effects as the flow goes through a NS, from the supersonic undisturbed side to the subsonic disturbed side in the relative frame, are summarized in Table 2 and Figure 1.

**Table 2.** Variation of flow quantities across a NS wave

$$\text{Mach number: decreases } (Ma_1 \leq 1) \quad (122)$$

$$\text{Velocity: decreases } (u_2/u_1 \leq 1) \quad (123)$$

$$\text{Static pressure: increases } (p_2/p_1 \geq 1) \quad (124)$$

$$\text{Static density: increases } (\rho_2/\rho_1 \geq 1) \quad (125)$$

$$\text{Static temperature: increases } (T_2/T_1 \geq 1) \quad (126)$$

$$\text{Stagnation pressure: decreases } (p_{02}/p_{01} \leq 1) \quad (127)$$

$$\text{Stagnation temperature: const. } (T_{01} = T_{02}) \quad (128)$$

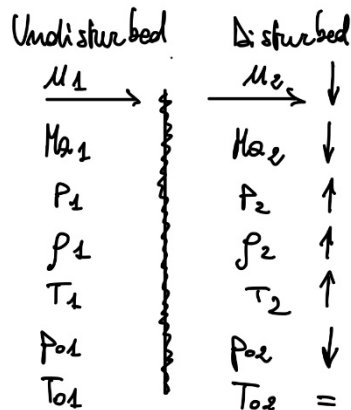


**Figure 12. Nomenclature and variation of flow quantities across a NS wave.**

### 2.2.3 Weak Waves

Consider now the case of weak, acoustic waves (*i.e.*, infinitesimal pressure disturbances) or NS waves in the limit of vanishing strength. In that case, the absolute  $\varepsilon_\alpha$  quantities are infinitesimal, differential quantities and H.O.T can be neglected. For example,  $\varepsilon_p \equiv \frac{p_2 - p_1}{p_1} \rightarrow \frac{dp}{p}$ . Therefore, linearizing our governing equations, by neglecting terms of  $\mathcal{O}(\varepsilon_\alpha^2)$  in comparison to terms of  $\mathcal{O}(\varepsilon_\alpha)$  leads to

$$\varepsilon_\rho + \varepsilon_U = 0 \text{ (continuity)} \quad (129)$$

$$\varepsilon_p + \gamma Ma_1^2 \varepsilon_U = 0 \text{ (momentum)} \quad (130)$$

$$\varepsilon_T + (\gamma - 1) Ma_1^2 \varepsilon_U = 0 \text{ (energy)} \quad (131)$$

$$\varepsilon_p - \varepsilon_\rho - \varepsilon_T = 0 \text{ (state)} \quad (132)$$

which can be rewritten in matrix form as

$$\begin{bmatrix} 1 & 0 & 0 & 1 \\ 0 & 1 & 0 & \gamma Ma_1^2 \\ 0 & 0 & 1 & (\gamma - 1) Ma_1^2 \\ -1 & 1 & -1 & 0 \end{bmatrix} \begin{bmatrix} \varepsilon_\rho \\ \varepsilon_p \\ \varepsilon_T \\ \varepsilon_U \end{bmatrix} = \begin{bmatrix} 0 \\ 0 \\ 0 \\ 0 \end{bmatrix} \quad (133)$$

This is a set of four simultaneous, linear, homogeneous, algebraic equations. The only unique solution is the trivial  $1$ ,  $\varepsilon_\rho = \varepsilon_p = \varepsilon_T = \varepsilon_U = 0$ , which we have not interested in. To find a non-trivial solution, we must reduce the rank of the coefficient matrix, *i.e.*, set the determinant of the coefficient matrix to 0 in which case the four equations are no longer independent:

$$\det \begin{bmatrix} 1 & 0 & 0 & 1 \\ 0 & 1 & 0 & \gamma Ma_1^2 \\ 0 & 0 & 1 & (\gamma - 1) Ma_1^2 \\ -1 & 1 & -1 & 0 \end{bmatrix} = 0 \quad (134)$$

Expanding the 4x4 determinant by minors on the first row:

$$\begin{aligned}
 (-1)^{1+1} \begin{vmatrix} 1 & 0 & \gamma Ma_1^2 \\ 0 & 1 & (\gamma - 1)Ma_1^2 \\ 1 & -1 & 0 \end{vmatrix} + (-1)^{1+4} \begin{vmatrix} 0 & 1 & 0 \\ 0 & 0 & 1 \\ -1 & 1 & -1 \end{vmatrix} = 0 \Rightarrow \\
 \Rightarrow (1)[(\gamma - 1)Ma_1^2 - \gamma Ma_1^2] + (-1)[-1] = 0 \Rightarrow \\
 \Rightarrow -Ma_1^2 + 1 = 0 \Rightarrow Ma_1^2 = 1 \Rightarrow Ma_1 = 1
 \end{aligned} \tag{135}$$

Also, since  $Ma_1 \equiv \frac{u_1}{a_1} = \frac{U_w - U_1}{a_1} = 1$ :

$$U_w = a_1 + U_1 \tag{136}$$

*Weak, acoustics, sound waves do indeed propagate at the speed of sound relative to the undisturbed fluid they move into, as we previously hypothesized. Also, this is why  $a$  is called the “speed of sound”.*

Now let us look at the entropy change across weak waves. Using (21):

$$\begin{aligned}
 Tds = dh - \frac{dp}{\rho} \Rightarrow ds = c_p \frac{dT}{T} - \frac{dp}{\rho T} = \left( \frac{\gamma R}{\gamma - 1} \right) \frac{dT}{T} - R \frac{dp}{p} \\
 \Rightarrow \frac{ds}{R} = \left( \frac{\gamma}{\gamma - 1} \right) \varepsilon_T - \varepsilon_p
 \end{aligned} \tag{137}$$

Using (65)-(66), (137) becomes:

$$\frac{ds}{R} = \left( \frac{\gamma}{\gamma - 1} \right) \varepsilon_T - \varepsilon_p \Rightarrow \frac{ds}{R} = \left( \frac{\gamma}{\gamma - 1} \right) [-(\gamma - 1)Ma_1^2 \varepsilon_U] + \gamma Ma_1^2 \varepsilon_U \Rightarrow \frac{ds}{R} = 0 \tag{138}$$

*Weak, acoustics, sound waves are isentropic and either weak compressions or weak expansions are possible since both satisfy the second law of thermodynamics,  $ds \geq 0$  (equality in this case). This agrees with our previous result for entropy change when  $Ma_1 = 1$ .*

### 2.3 Velocity Boundary Conditions

Solving NS problems is straightforward if  $Ma_1 = \frac{u_1}{a_1} = \frac{U_w - U_1}{a_1}$  is known. All our equations for the property variations have been developed with  $Ma_1$  as an independent variable, so if  $U_w, u_1, a_1$  are known  $Ma_1$  can be determined and the analysis proceeds easily. However, there are many situations in which this is not the case. Consider the air hammer depicted in Figure 13.

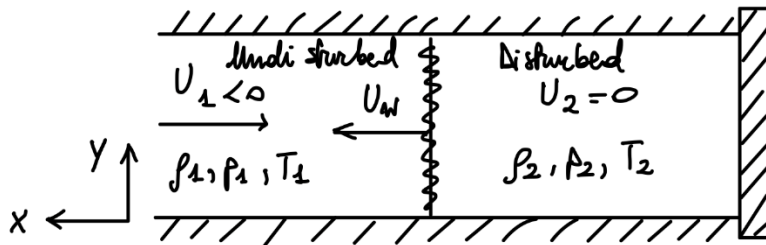
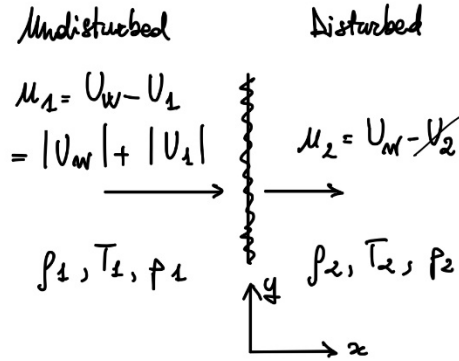


Figure 13. Schematic of air hammer setup.

Gas is flowing along a pipe at the velocity  $U_1$  relative to the walls, and we suddenly close a valve. The gas cannot penetrate the wall face, or separate from it, so the boundary condition (BC) at the valve face must be  $U_2 = 0$  in the fix coordinate system relative to the pipe. But this boundary condition must be enforced by a wave or series of waves moving back up the pipe. The first thing

we should do is determine whether the wave(s) is a finite compression NS or a series of expansion waves. Considered the coordinate system relative to the wave(s), as sketched in Figure 14.



**Figure 14. Wave-relative reference system for the air hammer problem.**

Since the velocity decreases and therefore the pressure increases across the wave,  $1 \rightarrow 2$ , in the relative coordinate system the wave must be a finite compression NS. However, in analyzing this problem,  $U_w$  is unknown, so we cannot determine  $Ma_1 = \frac{u_1}{a_1} = \frac{U_w - U_1}{a_1}$  and proceed. But we do know a boundary condition on the velocity across the wave in the fixed frame, *i.e.*,  $U_1 = \text{given}$ , and  $U_2 = 0$ . We could then imagine the following iterative solution technique:

- assume  $U_w$ ,
- calculate  $Ma_1 = \frac{U_w - U_1}{a_1}$ ,
- from NS relations (Table 1) determine  $Ma_2$  and  $T_2$ ,
- calculate  $u_2 = U_w - U_2 = U_w = Ma_2 \sqrt{\gamma RT_2}$ ;
- if the calculated value  $U_w$  matches the assumption at step (a) then we found the solutions, otherwise we assume a new value and redo the process.

Most books solve these types of problems in such iterative manner. However, there is a way to avoid iteration. Since the BC is on  $u$  across the wave, consider (97), repeated here for convenience:

$$\varepsilon_U = \frac{u_2 - u_1}{u_1} = \frac{(U_w - U_2) - (U_w - U_1)}{Ma_1 a_1} = - \left( \frac{2}{\gamma + 1} \right) \frac{Ma_1^2 - 1}{Ma_1^2} \quad (139)$$

Notice that the unknown  $U_w$  cancels out on the RHS, and one  $Ma_1$  at the denominator cancels out. We are left with a quadratic equation:

$$\frac{U_1 - U_2}{a_1} = - \left( \frac{2}{\gamma + 1} \right) \frac{Ma_1^2 - 1}{Ma_1} \Rightarrow Ma_1^2 + \left( \frac{\gamma + 1}{2} \right) \left( \frac{U_1 - U_2}{a_1} \right) Ma_1 - 1 = 0 \quad (140)$$

which can be easily solved to find  $Ma_1$ .

## 2.4 Reflection of Normal Shock Waves

### 2.4.1 Reflection from Solid Boundaries

Consider a normal shock wave moving down a tube (generated, for example, by a piston or projectile moving to the right) and impinging on the closed end of the tube (Figure 15). The disturbed fluid behind the wave is moving to the right at  $U_2 > 0$  in the fixed frame, but when the incident wave encounters the end of the tube, the fluid behind the wave cannot penetrate or separate from the solid boundary. Thus, some sort of reflected wave(s) must propagate back up to enforce the zero-velocity boundary condition. For the reflected wave, the fluid on the left

becomes the undisturbed fluid and that on the right is the disturbed one. Question: is the reflected wave a compression NS or a series of expansion waves? To answer, let us look at the steady relative reference frame, similar to what we had depicted in Figure 14. Again, since the relative velocity decreases in this frame (and pressure increases), the reflected wave must be a finite compression NS.

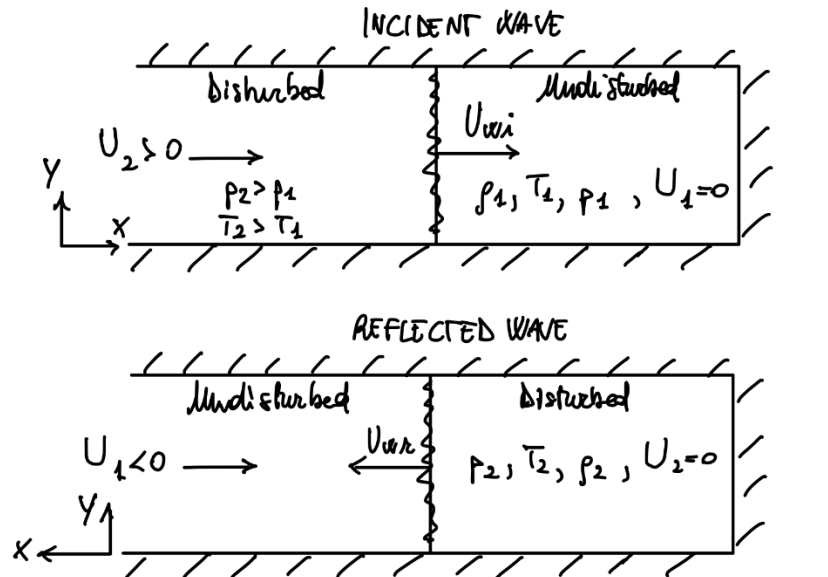


Figure 15. Incident and reflected waves from a solid boundary.

#### 2.4.2 Reflection from Constant Pressure Boundaries

Now consider the case of a NS wave moving down a tube that is open to constant pressure region such as the atmosphere,  $p = p_{atm} = \text{const.}$ , such as that shown in Figure 16. We consider only the case of subsonic inflow or outflow at the end of the tube. In this situation the static pressure of the fluid behind the incident wave is greater than that of the atmosphere, so to maintain pressure at the end of the tube, a wave or wave(s) must propagate back to the left. Question: are the reflected wave(s) a finite compression NS or a series of expansion waves?

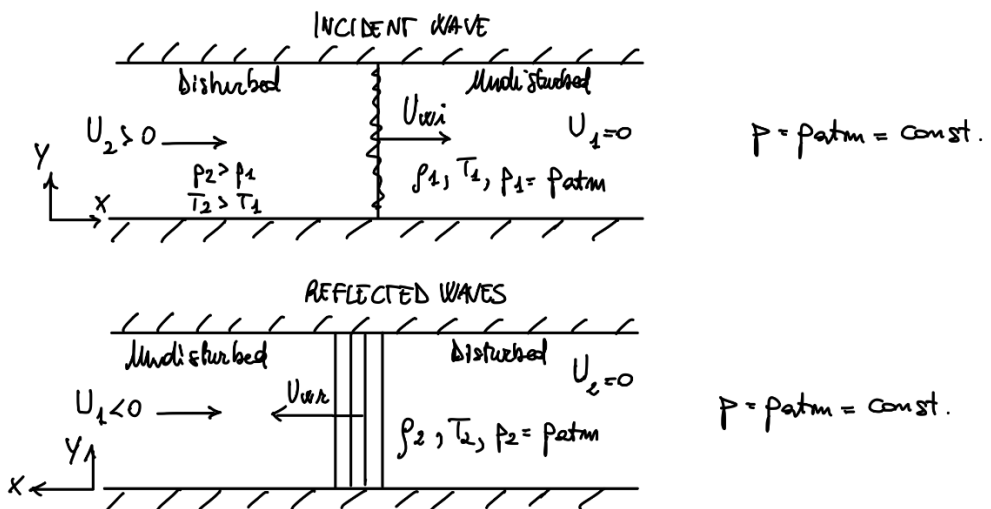


Figure 16. Incident and reflected waves from a constant pressure boundary.

In this case, since the static pressure decreases across the waves, this must be a series of expansion waves.

In conclusion, NS waves reflect from solid boundaries as NS waves and from constant pressure boundaries as a series of expansion waves.

## 2.5 Shock Tube

An important practical example of moving waves is the *shock tube*. It can be used, for example, to create a high pressure, high temperature conditions for testing materials, causing combustion, or as the source of high-pressure gas in a shock tube-driven wind tunnel. In all cases, the experiments are very transitory in nature, usually on the order of milliseconds. As shown in Figure 17 (top), the shock tube normally consists of a long tube divided into 2 sections by a diaphragm, the high pressure driven gas and the low pressure driven gas.

The gases can be different and can be at different initial temperatures. Immediately after the diaphragm is ruptured a right running NS propagates into the driven gas and a left running centered expansion propagates into the driver gas as shown in Figure 17 (middle).

As the NS moves to the right, it raises the pressure of the fluid it passes over (region ②) and induces a velocity to the right  $U_2 > 0$ . As the expansion waves travel to the left, they lower the pressure of the fluid they pass over (region ③) and induce a velocity to the right  $U_3 > 0$ . The strength of the propagated NS and centered expansion waves are determined by the boundary conditions that  $p_2 = p_3$  and  $U_2 = U_3$  across the contact surface. However, not all properties in regions ② and ③ will be the same, so they are not just a since uniform regime. As the NS moves to the right, it increases the entropy and raises the temperature of the fluid in ② compared to that in ①. The expansion waves, on the other hand, lower the temperature in ③ but leave the entropy unchanged as compared to the fluid in ④. Thus, almost assuredly, the entropies, temperatures, and densities in regions ② and ③ will be different. Thus, a contact surface separates regions ② and ③, which is defined as an imaginary interface separating two flow regions, such that the pressure and velocity on each side are the same, but the other properties may be different. In this case, the contact surface moved to the right that  $U_2 = U_3$ .

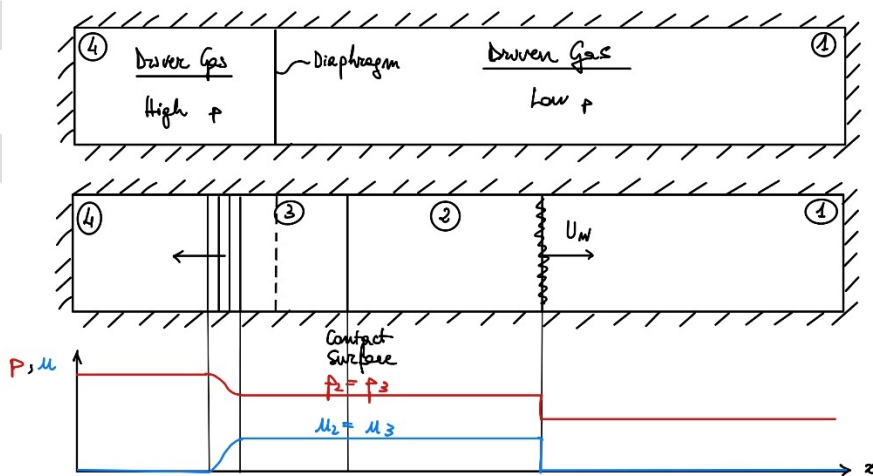


**Figure 17. Shock tube.**

Shown below is the  $x$ - $t$  or wave diagram of the initial part of the shock tube flow immediately after the diaphragm is ruptured (assuming closed ends). As previously mentioned, the shockwave propagates into the stationary driven gas ① and imparts a velocity to the right in region ②. When the shockwave impinges on the closed right end, a reflected NS must move back to the left to

enforce the boundary condition that the velocity at the end of the tube be maintained at zero. Thus region ⑤ is a stationary region of very high pressure since in essence the shockwaves have passed over this fluid. The fluid in regions ② and ③, and the contact surface all move to the right at the same velocity  $U_2 = U_3$ . When the contact surface intersects the reflected shock wave at  $g$ , a complex interaction occurs such that a transmitted shockwave penetrates the contact surface, the contact surface is transmitted to the right, and a reflected wave is generated. The reflected wave may be either a shock wave or centered expansion depending on the properties of the two sides of the contact surface and the shock before the intersection, *i.e.*, regions ②, ③, ⑤.

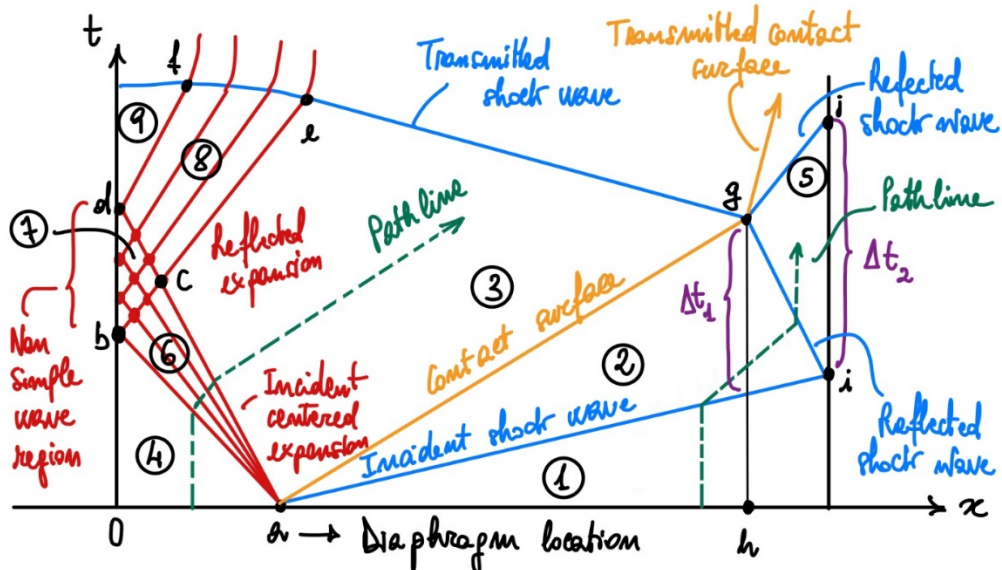


**Figure 18. Shock tube wave diagram.**

The centered expansion waves that propagate to the left immediately after the diaphragm is burst induce a velocity to the right such that  $U_3 = U_2$  and lower the pressure as they pass over the driver gas,  $p_3 = p_2$ . When these expansion waves impinge on the closest left end of the shock tube, they reflect as expansion waves, forming non simple wave region  $b-c-d$ . This enforces the zero-velocity boundary condition at the left end of the tube, forming stationary region ⑨ of very low pressure. Be reflected expansion waves intersect the reflected/transmitted NS causing it the curve in  $x$ - $t$  space such that spatially nonuniform entropy distribution is generated. The  $x$ - $t$  wave diagram can be continued in this manner for as long as it is desired.

If the shock tube is used to measure the high pressure/high temperature properties or material, or to produce combustion, behind the incident shock, we see that the object should be placed and the location  $h$  to maximize the test time,  $\Delta t_1$ . This is the maximum time interval for which the conditions will be uniform at their post-(incident) shock values. The high pressure stationary gas behind the reflected shock, *i.e.*, region ⑤, may be used as the gas source for a shock tube-driven wind tunnel. In that case, the maximum test time available  $\Delta t_2$ , is the time interval between the arrival of the incident shock wave and the arrival of the wave reflected from the complex interaction of the contact surface and the reflected shock (point  $g$  in the  $x$ - $t$  plane). Also note the two path lines sketched for particles starting in the driver and driven sections, respectively.

Let us now analyze the shock tube conditions. If we determine the shock pressure ratio  $p_2/p_1$  in terms of the initial pressure ratio across the diaphragm,  $p_4/p_1 =$  known, we can determine everything about the propagating NS and region ②. Likewise, for the propagating expansion

waves (isentropic),  $\frac{p_3}{p_4} = \frac{p_2}{p_4} = \frac{p_2}{p_1} \frac{p_1}{p_4}$ . Therefore, we are going to find  $p_2/p_1$  in terms of  $p_4/p_1$ , so that we can then define the expansion wave strength,  $p_3/p_4$ .

Note that since driver and driven gases could be different, in general  $\gamma_1 \neq \gamma_4$ . From (111) with  $\text{Ma}_1$  the relative Mach number to the wave:

$$\begin{aligned} \frac{p_2}{p_1} &= 1 + \left( \frac{2\gamma_1}{\gamma_1 + 1} \right) (\text{Ma}_1^2 - 1) \Rightarrow \text{Ma}_1^2 - 1 = \left( \frac{\gamma_1 + 1}{2\gamma_1} \right) \left( \frac{p_2}{p_1} - 1 \right) \\ &\Rightarrow \text{Ma}_1 = \left[ 1 + \left( \frac{\gamma_1 + 1}{2\gamma_1} \right) \left( \frac{p_2}{p_1} - 1 \right) \right]^{1/2} \end{aligned} \quad (141)$$

Since  $\text{Ma}_1 = \frac{U_w - U_1}{a_1} = \frac{U_w}{a_1}$ :

$$U_w = \text{Ma}_1 a_1 = a_1 \left[ 1 + \left( \frac{\gamma_1 + 1}{2\gamma_1} \right) \left( \frac{p_2}{p_1} - 1 \right) \right]^{1/2} \quad (142)$$

From the velocity BC quadratic equation (140), using the expressions for  $\text{Ma}_1^2 - 1$  and  $\text{Ma}_1$  that appear in (141) we have:

$$\frac{U_1 - U_2}{a_1} = - \left( \frac{2}{\gamma + 1} \right) \frac{\text{Ma}_1^2 - 1}{\text{Ma}_1} \Rightarrow U_2 = \frac{\frac{a_1}{\gamma_1} \left( \frac{p_2}{p_1} - 1 \right)}{\left[ 1 + \left( \frac{\gamma_1 + 1}{2\gamma_1} \right) \left( \frac{p_2}{p_1} - 1 \right) \right]^{1/2}} \quad (143)$$

We will show later, that for the isentropic expansion fan:

$$\frac{p_3}{p_4} = \left[ 1 - \frac{\gamma_4 - 1}{2} \left( \frac{U_3}{a_4} - 1 \right) \right]^{\frac{2\gamma_4}{\gamma_4 - 1}} \quad (144)$$

Solving for  $U_3$ :

$$U_3 = \frac{2a_4}{\gamma_4 - 1} \left[ 1 - \left( \frac{p_3}{p_4} \right)^{\frac{\gamma_4 - 1}{2\gamma_4}} \right] \quad (145)$$

Recalling that across the contact surface  $p_3 = p_2$  and  $U_3 = U_2$ , we can equate (143) and (145) to obtain

$$\frac{\frac{a_1}{\gamma_1} \left( \frac{p_2}{p_1} - 1 \right)}{\left[ 1 + \left( \frac{\gamma_1 + 1}{2\gamma_1} \right) \left( \frac{p_2}{p_1} - 1 \right) \right]^{1/2}} = \frac{2a_4}{\gamma_4 - 1} \left[ 1 - \left( \frac{p_2/p_1}{p_4/p_1} \right)^{\frac{\gamma_4 - 1}{2\gamma_4}} \right] \quad (146)$$

Solve for  $p_4 / p_1$ :

$$\frac{p_4}{p_1} = \frac{p_2}{p_1} \left\{ 1 - \frac{\frac{a_1}{\gamma_1} (\gamma_4 - 1) \left( \frac{p_2}{p_1} - 1 \right)}{\left\{ 2\gamma_1 \left[ (\gamma_1 + 1) \frac{p_2}{p_1} + (\gamma_1 - 1) \right] \right\}^{\frac{1}{2}}} \right\}^{\frac{2\gamma_4}{\gamma_4 - 1}} \quad (147)$$

This is the fundamental shock tube equation, giving  $p_2/p_1$  implicitly in terms of  $p_4/p_1$ . Unfortunately, obtaining  $p_2/p_1$  explicitly is not possible. Once  $p_2/p_1$  is known, all the other properties can be found using the NS relations in Table 1 and  $T_3$ ,  $\rho_3$  can be found using the isentropic relations (29) since expansion waves are isentropic.

DRAFT

### 3 Governing Equations for Generalized One-Dimensional Flow

#### 3.1 Introduction

In this section we will derive the governing equations for the situation in which three “driving potentials” or flow mechanisms are present to alter the flow: (1) area change, (2) friction, (3) stagnation temperature change (which we will find is caused by heat transfer and or work interactions). In this derivation of the governing equations, we will consider all three driving potentials simultaneously. However, in the following sections, when we solve the equations and apply them, we will consider only one effect at a time: (1) isentropic flow with area change only (section 4), (2) Fanno flow with friction only (section 5), (3) Rayleigh flow with the  $T_0$ -change only (section 6). We will then briefly discuss the case when two or all three effects are present.

It is also possible to add other driving potentials to the analysis, such as mass addition, drag on immersed objects, etc. However, we will consider just these three.

#### 3.2 Analysis

Consider the arbitrary flow passage shown in Figure 19 with control volume of length  $dx$ .

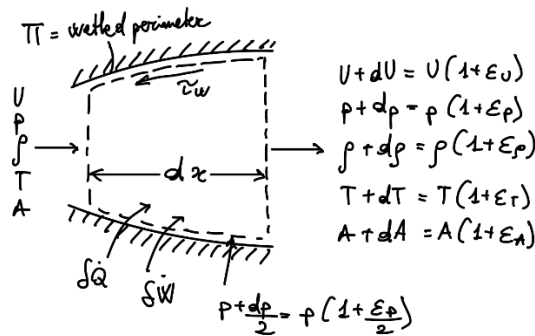


**Figure 19. Infinitesimal control volume of variable area.**

Since the control volume has a differential length, the  $\varepsilon_\alpha$  operators are differential:  $\varepsilon_\alpha = d\alpha/\alpha$  and H.O.T will be ignored.

Assumptions:

- (1) steady,
- (2) uniform, 1D flow and uniform properties at each section,
- (3) neglect body forces,
- (4) neglect gravitational potential energy,
- (5) calorically perfect gas

Objective: Given the properties at the inlet, find the properties at the exit, *i.e.*, find the  $\varepsilon_\alpha$ . Once we have the  $\varepsilon_\alpha$  for differential changes, we will integrate to find the finite flow property changes for finite values of the driving potentials.

We apply the governing equations (42), (49), and (63) to the control volume shown in Figure 19. From continuity (42) we obtain

$$\begin{aligned}
 \frac{d}{dt} \int_V \rho dV + \oint_S \rho \vec{U} \cdot \hat{n} dS &= 0 \Rightarrow \\
 \Rightarrow -\rho U A + \rho(1 + \varepsilon_P) U(1 + \varepsilon_U) A(1 + \varepsilon_A) &= 0 \Rightarrow \\
 \Rightarrow (1 + \varepsilon_P)(1 + \varepsilon_U)(1 + \varepsilon_A) &= 0 \Rightarrow
 \end{aligned} \tag{148}$$

$$\Rightarrow 1 + \varepsilon_\rho + \varepsilon_U + \varepsilon_A + \mathcal{O}(\varepsilon^2) + \mathcal{O}(\varepsilon^3) = 0$$

Neglecting higher order terms:

$$\varepsilon_\rho + \varepsilon_U + \varepsilon_A = 0 \quad (149)$$

From  $x$ -momentum conservation (49) we obtain

$$\begin{aligned} \frac{d}{dt} \int_V \rho \vec{U} dV + \oint_S \rho \vec{U} \cdot \hat{n} dS &= \int_V \rho \vec{f} dV - \oint_S p \hat{n} dS + \vec{F}_{\text{visc}} \Rightarrow \\ \frac{d}{dt} \int_V \rho U_x dV + \oint_S \rho U_x \vec{U} \cdot \hat{n} dS &= \int_V \rho f_x dV - \oint_S (pdS)_x + F_{x,\text{visc}} \Rightarrow \\ \Rightarrow pA - p(1 + \varepsilon_p)A(1 + \varepsilon_A) + p\left(1 + \frac{\varepsilon_p}{2}\right)A\varepsilon_A - \tau_w \Pi dx \\ &= -\rho U^2 A + \rho(1 + \varepsilon_\rho)U^2(1 + \varepsilon_U)^2 A(1 + \varepsilon_A) \end{aligned} \quad (150)$$

where  $p + \frac{dp}{2} = p\left(1 + \frac{\varepsilon_p}{2}\right)$  is the pressure force of the inner walls of the domain, and  $F_{x,\text{visc}} = -\tau_w \Pi dx$ , with  $\tau_w$  being the wall shear stress, and  $\Pi$  the wetter perimeter.

Since  $(1 + \varepsilon_\rho)(1 + \varepsilon_p)(1 + \varepsilon_A) = 1$  from continuity, then (82) gives

$$\begin{aligned} pA\left(1 - 1 - \varepsilon_p - \varepsilon_A - \varepsilon_p\varepsilon_A + \varepsilon_A + \frac{\varepsilon_p\varepsilon_A}{2}\right) - \tau_w \Pi dx &= \rho U^2 A(-1 + 1 + \varepsilon_U) \Rightarrow \\ \Rightarrow -\varepsilon_p - \frac{\tau_w \Pi}{p A} dx &= \frac{\rho}{p} U^2 \varepsilon_U \end{aligned} \quad (151)$$

We introduce the hydraulic diameter, defined by:

$$D_h \equiv \frac{4A}{\Pi} \Rightarrow \frac{\Pi}{A} = \frac{4}{D_h} \quad (152)$$

and a Moody or Darcy friction factor, defined by

$$f \equiv \frac{4\tau_w}{\frac{1}{2}\rho U^2} \Rightarrow \frac{\tau_w}{p} = \frac{1}{2} \frac{\rho U^2 f}{4p} \quad (153)$$

Substituting (152) and (153) into (151):

$$\begin{aligned} -\varepsilon_p - \frac{1}{2} \frac{\rho U^2 f}{4p} \frac{4}{D_h} dx &= \frac{\rho}{p} U^2 \varepsilon_U \Rightarrow -\varepsilon_p - \frac{\rho U^2}{p} \frac{f}{2D_h} dx = \frac{\rho}{p} U^2 \varepsilon_U \\ \Rightarrow -\varepsilon_p - \gamma Ma^2 \frac{f dx}{2D_h} &= \gamma Ma^2 \varepsilon_U \end{aligned} \quad (154)$$

Defining the differential effect of friction over  $dx$

$$\varepsilon_f \equiv \frac{f dx}{D_h} \neq \frac{df}{f} \quad (155)$$

equation (154) becomes:

$$\varepsilon_p + \gamma Ma^2 \frac{\varepsilon_f}{2} + \gamma Ma^2 \varepsilon_U = 0 \quad (156)$$

From *energy* conservation (63), for infinitesimal amounts of heat transfer and work:

$$\begin{aligned} \frac{d}{dt} \int_V \rho \left( e + \frac{U^2}{2} + gz \right) dV + \oint_S \rho \left( e + \frac{U^2}{2} + gz \right) \vec{U} \cdot \hat{n} dS \\ = \delta \dot{Q} + \delta \dot{W}_{\text{visc}} - \oint_S p \vec{U} \cdot \hat{n} dS \end{aligned} \quad (157)$$

Note that for convenience we have not developed the different components of the transfer rate  $\dot{Q}$ . Putting together the two surface integrals and using (2) and (71) we rewrite (157) as

$$\oint_S \rho h_0 \vec{U} \cdot \hat{n} dS = \delta \dot{Q} + \delta \dot{W}_{\text{visc}} \quad (158)$$

or since we assumed calorically perfect gas:

$$\oint_S \rho c_p T_0 \vec{U} \cdot \hat{n} dS = \oint_S \rho \left( c_p T + \frac{U^2}{2} \right) \vec{U} \cdot \hat{n} dS = \delta \dot{Q} + \delta \dot{W}_{\text{visc}} \quad (159)$$

Evaluating (159) for our control volume:

$$\begin{aligned} \delta \dot{Q} + \delta \dot{W}_{\text{visc}} &= c_p T_0 (-\rho U A) + c_p T_0 (1 + \varepsilon_{T_0}) [\rho (1 + \varepsilon_\rho) U (1 + \varepsilon_U) A (1 + \varepsilon_A)] = \\ &= \left( c_p T + \frac{U^2}{2} \right) (-\rho U A) \\ &\quad + \left[ c_p T (1 + \varepsilon_T) + \frac{U^2 (1 + \varepsilon_U)^2}{2} \right] [\rho (1 + \varepsilon_\rho) U (1 + \varepsilon_U) A (1 + \varepsilon_A)] \end{aligned} \quad (160)$$

Using continuity, dividing everything by  $c_p \rho U A = c_p [\rho (1 + \varepsilon_\rho) U (1 + \varepsilon_U) A (1 + \varepsilon_A)] = c_p \dot{m}$ , and neglecting the  $\mathcal{O}(\varepsilon_U^2)$  we obtain

$$\frac{\delta \dot{Q} + \delta \dot{W}_{\text{visc}}}{c_p \dot{m}} = -T_0 + T_0 (1 + \varepsilon_{T_0}) = T_0 \varepsilon_{T_0} = T \varepsilon_T + \frac{U^2}{c_p} \varepsilon_U \quad (161)$$

Consider first the left-hand equality:

$$\frac{\delta \dot{Q} + \delta \dot{W}_{\text{visc}}}{c_p \dot{m}} = T_0 \varepsilon_{T_0} = T_0 \frac{dT_0}{T_0} = dT_0 \quad (162)$$

We see immediately that:

$$\delta \dot{Q} + \delta \dot{W}_{\text{visc}} = \dot{m} c_p dT_0 \quad (163)$$

which tells us that heat transfer and work interactions directly cause (and are essentially equivalent to) stagnation temperature changes in the flow. For finite interactions, this can be integrated to:

$$\dot{Q} + \dot{W}_{\text{visc}} = \dot{m} c_p (T_{02} - T_{01}) \quad (164)$$

Given the equivalency between heat transfer and work rate with the stagnation temperature it is convenient to just use the right-hand equivalency of (161). Dividing by  $T$ :

$$\frac{T_0}{T} \varepsilon_{T_0} = \varepsilon_T + \frac{U^2}{c_p T} \varepsilon_U \quad (165)$$

Using (8) and (76), and rearranging:

$$\varepsilon_T + (\gamma - 1) \left( \frac{U^2}{\gamma RT} \right) \varepsilon_U - \left( 1 + \frac{\gamma - 1}{2} Ma^2 \right) \varepsilon_{T_0} = 0 \quad (166)$$

or

$$\varepsilon_T + (\gamma - 1) Ma^2 \varepsilon_U - \left( 1 + \frac{\gamma - 1}{2} Ma^2 \right) \varepsilon_{T_0} = 0 \quad (167)$$

Using the equation of state (1) for the undisturbed flow:

$$p = \rho RT \quad (168)$$

while for the disturbed flow:

$$p(1 + \varepsilon_p) = \rho(1 + \varepsilon_\rho)RT(1 + \varepsilon_T) \quad (169)$$

Dividing (169) by (168):

$$\varepsilon_p - \varepsilon_\rho - \varepsilon_T = 0 \quad (170)$$

With (149), (156), (167), (170) we can construct a system of 4 algebraic equations. However, we have 7 unknowns  $\varepsilon_\rho$ ,  $\varepsilon_U$ ,  $\varepsilon_A$ ,  $\varepsilon_p$ ,  $\varepsilon_f$ ,  $\varepsilon_T$ ,  $\varepsilon_{T_0}$  with  $Ma$  and  $\gamma$  as known independent variables. The procedure is to treat three of the  $\varepsilon_\alpha$  as known independent variables and solve for the others in terms of those three and  $Ma$  and  $\gamma$ . In particular, we will treat the three driving potentials,  $\varepsilon_A$  (area change),  $\varepsilon_f$  (friction),  $\varepsilon_{T_0}$  (stagnation temperature change) as independent, known variables, and solve for  $\varepsilon_\rho$ ,  $\varepsilon_U$ ,  $\varepsilon_p$ ,  $\varepsilon_T$  as functions of  $(\varepsilon_A, \varepsilon_f, \varepsilon_{T_0}, \gamma, Ma)$ . In inspecting our governing equations, we have a set of 4 linear, inhomogeneous, algebraic equations, that can be solved using several standard techniques. A particularly straightforward one is to solve continuity for  $\varepsilon_\rho$ , momentum for  $\varepsilon_p$ , energy for  $\varepsilon_T$  in terms of  $\varepsilon_U$  and the other independent variables, substitute into the equation of state and solve for  $\varepsilon_U$ . Then back-substitute to find  $\varepsilon_\rho$ ,  $\varepsilon_p$ ,  $\varepsilon_T$ . In the following we omit all the details of the algebra that leads to the solution.

From the equation of state (170):

$$\begin{aligned} \varepsilon_p - \varepsilon_\rho - \varepsilon_T &= 0 \Rightarrow \\ \Rightarrow - \left( \gamma Ma^2 \frac{\varepsilon_f}{2} + \gamma Ma^2 \varepsilon_U \right) + (\varepsilon_U + \varepsilon_A) + \left[ (\gamma - 1) Ma^2 \varepsilon_U - \left( 1 + \frac{\gamma - 1}{2} Ma^2 \right) \varepsilon_{T_0} \right] &= \end{aligned} \quad (171)$$

Solving for  $\varepsilon_U$ :

$$\varepsilon_U = \left( \frac{-1}{1 - Ma^2} \right) \varepsilon_A + \left[ \frac{\gamma Ma^2}{2(1 - Ma^2)} \right] \varepsilon_f + \left( \frac{1 + \frac{\gamma - 1}{2} Ma^2}{1 - Ma^2} \right) \varepsilon_{T_0} \quad (172)$$

Back-substituting (172) in the continuity equation (149):

$$\varepsilon_p = \left( \frac{Ma^2}{1 - Ma^2} \right) \varepsilon_A - \left[ \frac{\gamma Ma^2}{2(1 - Ma^2)} \right] \varepsilon_f - \left( \frac{1 + \frac{\gamma - 1}{2} Ma^2}{1 - Ma^2} \right) \varepsilon_{T_0} \quad (173)$$

Back-substituting (172) in the momentum equation (156):

$$\varepsilon_p = \left( \frac{\gamma Ma^2}{1 - Ma^2} \right) \varepsilon_A - \left\{ \frac{\gamma Ma^2 [1 + (\gamma - 1) Ma^2]}{2(1 - Ma^2)} \right\} \varepsilon_f - \left[ \frac{\gamma Ma^2 \left( 1 + \frac{\gamma - 1}{2} Ma^2 \right)}{1 - Ma^2} \right] \varepsilon_{T_0} \quad (174)$$

Back-substituting (172) in the energy equation (167):

$$\varepsilon_T = \left[ \frac{(\gamma - 1) Ma^2}{1 - Ma^2} \right] \varepsilon_A - \left[ \frac{\gamma(\gamma - 1) Ma^4}{2(1 - Ma^2)} \right] \varepsilon_f + \left[ \frac{(1 - \gamma Ma^2) \left( 1 + \frac{\gamma - 1}{2} Ma^2 \right)}{1 - Ma^2} \right] \varepsilon_{T_0} \quad (175)$$

At this point, it is also very useful to derive expressions for other dependent variables  $\varepsilon_{Ma^2} = dMa^2/Ma^2$ ,  $\varepsilon_{p_0} = dp_0/p_0$ ,  $\varepsilon_s = ds/c_p \neq ds/s$  and a function of the same variables ( $\varepsilon_A, \varepsilon_f, \varepsilon_{T_0}, \gamma, Ma$ ).

From (34):

$$\ln Ma^2 = \ln U^2 - \ln \gamma R - \ln T = 2 \ln U - \ln \gamma R - \ln T \quad (176)$$

Differentiating:

$$\varepsilon_{Ma^2} = \frac{dMa^2}{Ma^2} = 2 \frac{dU}{U} - \frac{dT}{T} = 2\varepsilon_U - \varepsilon_T \quad (177)$$

Using (172) and (175) in (177):

$$\begin{aligned} \varepsilon_{Ma^2} = & - \left[ \frac{2 \left( 1 + \frac{\gamma - 1}{2} Ma^2 \right)}{1 - Ma^2} \right] \varepsilon_A + \left[ \frac{\gamma Ma^2 \left( 1 + \frac{\gamma - 1}{2} Ma^2 \right)}{1 - Ma^2} \right] \varepsilon_f \\ & + \left[ \frac{(1 + \gamma Ma^2) \left( 1 + \frac{\gamma - 1}{2} Ma^2 \right)}{1 - Ma^2} \right] \varepsilon_{T_0} \end{aligned} \quad (178)$$

From (77):

$$\ln p_0 = \ln p + \left( \frac{\gamma}{\gamma - 1} \right) \ln \left( 1 + \frac{\gamma - 1}{2} Ma^2 \right) \quad (179)$$

Differentiating:

$$\varepsilon_{p_0} = \frac{dp_0}{p_0} = \frac{dp}{p} + \left( \frac{\gamma}{\gamma - 1} \right) \frac{\frac{\gamma - 1}{2} Ma^2 \frac{dMa^2}{Ma^2}}{1 + \frac{\gamma - 1}{2} Ma^2} = \varepsilon_p + \frac{\frac{\gamma Ma^2}{2} \varepsilon_{Ma^2}}{1 + \frac{\gamma - 1}{2} Ma^2} \quad (180)$$

Using (174) and (178) in (180):

$$\varepsilon_{p_0} = -\left(\frac{\gamma Ma^2}{2}\right)\varepsilon_f - \left(\frac{\gamma Ma^2}{2}\right)\varepsilon_{T_0} \quad (181)$$

From (21):

$$Tds = dh - \frac{dp}{\rho} \Rightarrow ds = c_p \frac{dT}{T} - \frac{dp}{\rho T} = c_p \frac{dT}{T} - R \frac{dp}{p} \Rightarrow \varepsilon_s = \frac{ds}{c_p} = \varepsilon_T - \frac{\gamma - 1}{\gamma} \varepsilon_p \quad (182)$$

Using (174) and (175) in (182):

$$\varepsilon_s = \left[\frac{(\gamma - 1)Ma^2}{2}\right]\varepsilon_f + \left(1 + \frac{\gamma - 1}{2}Ma^2\right)\varepsilon_{T_0} \quad (183)$$

All these equations are conveniently tabulated in Table 3. Each entry in the table is the coefficient of the driving potential listed at the top, which when added to the other coefficient-driving potential products along a given line gives the dependent  $\varepsilon_\alpha$  quantity listed at the left.

**Table 3. Table of influence coefficients**

	$\varepsilon_A = \frac{dA}{A}$	$\varepsilon_f = \frac{fdx}{D_h}$	$\varepsilon_{T_0} = \frac{dT_0}{T_0}$
$\varepsilon_{Ma^2} = \frac{dMa^2}{Ma^2}$	$\frac{-2\left(1 + \frac{\gamma - 1}{2}Ma^2\right)}{1 - Ma^2}$	$\frac{\gamma Ma^2\left(1 + \frac{\gamma - 1}{2}Ma^2\right)}{1 - Ma^2}$	$\frac{\left(1 + \gamma Ma^2\right)\left(1 + \frac{\gamma - 1}{2}Ma^2\right)}{1 - Ma^2}$
$\varepsilon_U = \frac{dU}{U}$	$\frac{-1}{1 - Ma^2}$	$\frac{\gamma Ma^2}{2(1 - Ma^2)}$	$\frac{1 + \frac{\gamma - 1}{2}Ma^2}{1 - Ma^2}$
$\varepsilon_\rho = \frac{d\rho}{\rho}$	$\frac{Ma^2}{1 - Ma^2}$	$\frac{-\gamma Ma^2}{2(1 - Ma^2)}$	$\frac{-\left(1 + \frac{\gamma - 1}{2}Ma^2\right)}{1 - Ma^2}$
$\varepsilon_p = \frac{dp}{p}$	$\frac{\gamma Ma^2}{1 - Ma^2}$	$\frac{-\gamma Ma^2[1 + (\gamma - 1)Ma^2]}{2(1 - Ma^2)}$	$\frac{-\gamma Ma^2\left(1 + \frac{\gamma - 1}{2}Ma^2\right)}{1 - Ma^2}$
$\varepsilon_T = \frac{dT}{T}$	$\frac{(\gamma - 1)Ma^2}{1 - Ma^2}$	$\frac{-\gamma(\gamma - 1)Ma^4}{2(1 - Ma^2)}$	$\frac{\left(1 - \gamma Ma^2\right)\left(1 + \frac{\gamma - 1}{2}Ma^2\right)}{1 - Ma^2}$
$\varepsilon_{p_0} = \frac{dp_0}{p_0}$	0	$\frac{-\gamma Ma^2}{2}$	$\frac{-\gamma Ma^2}{2}$
$\varepsilon_s = \frac{ds}{c_p}$	0	$\frac{(\gamma - 1)Ma^2}{2}$	$1 + \frac{\gamma - 1}{2}Ma^2$

The coefficients are usually called *influence coefficients* since they determine the “influence” of each driving potential on the change in each dependent variable. Also, the influence coefficients are the partial derivatives of each dependent variable with respect to each driving potential. For example, for isentropic flow with area change and  $\varepsilon_f = \varepsilon_{T_0} = 0$ , from (172) we have

$$\varepsilon_U = \left( \frac{-1}{1 - Ma^2} \right) \varepsilon_A \Rightarrow \frac{dU}{U} = \left( \frac{-1}{1 - Ma^2} \right) \frac{dA}{A} \quad (184)$$

namely, the influence coefficient is

$$\text{influence coefficient} = \left( \frac{-1}{1 - Ma^2} \right) = \frac{dU/U}{dA/A} \quad (185)$$

giving the fractional change in velocity per unit fraction change in area at any Mach number, *i.e.*, the influence of area change  $A$  on the flow velocity  $U$ .

Also note that the factor  $1 - Ma^2$  occurs in the denominator of many of the influence coefficients, meaning the dependent variables change in opposite direction in subsonic and supersonic flow. Also, the condition  $Ma = 1$  would appear to be a problem. This is further discussed in the next several sections.

## 4 Isentropic Flows with Area Change

### 4.1 Introduction

In this section we analyze compressible flow with area change, in the absence of friction, and  $T_0$ -change (caused by work/heat transfer). This flow is generally valid for “short” nozzles, ducts, diffusers for which frictional effects are small and no deliberate attempts at heat transfer/work have been made. We will be able to analyze a number of important practical flows, such as nozzles and diffusers, using these results.

### 4.2 Analysis

Consider again the schematic shown earlier in Figure 19 and the 5 assumptions made in section 3.2 to which we add the following assumptions:

- (6) frictionless (i.e.,  $\tau_w = 0$ )
- (7) adiabatic (i.e.,  $\delta\dot{Q} = 0$ )
- (8) no viscous work (i.e.,  $\delta\dot{W}_{\text{visc}} = 0$ )

From (6)  $f = 0 \Rightarrow \varepsilon_f = f dx/D_h = 0$ , whereas from (7) and (8)  $\frac{\delta\dot{Q} + \delta\dot{W}_{\text{visc}}}{c_p m T_0} = \varepsilon_{T_0} = 0$ . Because  $\varepsilon_f = \varepsilon_{T_0} = 0$ , we can ignore the second and third columns in Table 3 from our generalized, 1D analysis, and we can write immediately:

$$\begin{aligned}
 \varepsilon_{\text{Ma}^2} &= \frac{d\text{Ma}^2}{\text{Ma}^2} = \frac{-2 \left(1 + \frac{\gamma - 1}{2} \text{Ma}^2\right) dA}{1 - \text{Ma}^2} \frac{dA}{A} \\
 \varepsilon_U &= \frac{dU}{U} = \frac{-1}{1 - \text{Ma}^2} \frac{dA}{A} \\
 \varepsilon_\rho &= \frac{dp}{\rho} = \frac{\text{Ma}^2}{1 - \text{Ma}^2} \frac{dA}{A} \\
 \varepsilon_p &= \frac{dp}{p} = \frac{\gamma \text{Ma}^2}{1 - \text{Ma}^2} \frac{dA}{A} \\
 \varepsilon_T &= \frac{dT}{T} = \frac{(\gamma - 1) \text{Ma}^2}{1 - \text{Ma}^2} \frac{dA}{A}
 \end{aligned} \tag{186}$$

Also, since  $\varepsilon_s = \frac{ds}{c_p} = 0$ , the flow is isentropic under these assumptions, which is not surprising

since it is both adiabatic and frictionless. In addition, since  $\varepsilon_{p_0} = \frac{dp_0}{p_0}$  and  $\varepsilon_{T_0} = \frac{dT_0}{T_0}$ , the stagnation pressure and temperature (and density) are all constant in such isentropic flow with area change.

Constancy of the stagnation properties is important because the flow often originates from a large reservoir or tank where the velocity is negligible. The pressure and temperature measured in the tank are the local stagnation and static properties for the tank, and in an isentropic flow, these are the stagnation properties throughout the flow.

Before integrating the differential equations to find the flow property variations for finite area variations, return to the expressions for  $\varepsilon_\rho$ ,  $\varepsilon_U$ ,  $\varepsilon_p$ ,  $\varepsilon_T$  as functions of  $(\varepsilon_A, \gamma, \text{Ma})$  and look at the directions of change of these properties for subsonic and supersonic flows, illustrated in Table 4. Note that the direction of change of each of these expressions switches at unit Mach number, so the effects of area change on subsonic and supersonic flows are opposite. The supersonic results are also generally opposite to our incompressible intuition. Also, it looks like to accelerate a subsonic flow to supersonic conditions, or decelerate a supersonic flow to subsonic conditions, both isentropically, we must attach a subsonic nozzle or diffuser to a supersonic nozzle or diffuser,

respectively, i.e., we must pass through an area minimum where  $\text{Ma} = 1$ . We can also see this mathematically, e.g., looking at  $\varepsilon_p$ :

$$\varepsilon_p = \frac{\gamma \text{Ma}^2}{1 - \text{Ma}^2} \frac{dA}{A} \rightarrow \frac{0}{0} \quad \text{as} \quad \text{Ma} \rightarrow 1 \quad (187)$$

As the Mach number tends to 1, in order to keep  $\varepsilon_p$  bounded we must go to the indeterminate form 0/0, i.e.,  $\varepsilon_p = dA/A \rightarrow 0$ , so we must have either an area minimum or maximum. Looking at the table, we know it must be a minimum.

**Table 4. Property trends in isentropic flow**

	Diverging section ( $\varepsilon_A > 0$ )		Converging section ( $\varepsilon_A < 0$ )	
	Subsonic diffuser ( $\text{Ma} < 1$ )	Supersonic nozzle ( $\text{Ma} > 1$ )	Subsonic nozzle ( $\text{Ma} < 1$ )	Supersonic diffuser ( $\text{Ma} > 1$ )
$\varepsilon_U = \frac{-1}{1 - \text{Ma}^2} \frac{dA}{A}$	–	+	+	–
$\varepsilon_\rho = \frac{\text{Ma}^2}{1 - \text{Ma}^2} \frac{dA}{A}$	+	–	–	+
$\varepsilon_p = \frac{\gamma \text{Ma}^2}{1 - \text{Ma}^2} \frac{dA}{A}$	+	–	–	+
$\varepsilon_T = \frac{(\gamma - 1)\text{Ma}^2}{1 - \text{Ma}^2} \frac{dA}{A}$	+	–	–	+

Now integrate the differential equations to find the property variations (for finite area change) in isentropic flow. Starting from the first line of the Table 3:

$$\frac{d\text{Ma}^2}{\text{Ma}^2} = \frac{-2 \left(1 + \frac{\gamma - 1}{2} \text{Ma}^2\right) dA}{1 - \text{Ma}^2} \quad (188)$$

Separating and integrating from  $\text{Ma}^2 = 1, A = A^*$  to a state where  $\text{Ma}^2 = \text{Ma}^2, A = A$ , we obtain

$$\int_{A^*}^A \frac{dA}{A} = - \int_1^{\text{Ma}^2} \frac{1 - \text{Ma}^2}{2 \left(1 + \frac{\gamma - 1}{2} \text{Ma}^2\right)} \frac{d\text{Ma}^2}{\text{Ma}^2} \quad (189)$$

Using  $\text{Ma}^2$  and the integration variable, the RHS integral in (189) can be carried out using partial fractions, leading to:

$$\frac{A}{A^*} = \frac{1}{\text{Ma}} \left[ \frac{2}{\gamma + 1} \left(1 + \frac{\gamma - 1}{2} \text{Ma}^2\right) \right]^{\frac{\gamma + 1}{2(\gamma - 1)}} \quad (190)$$

This is the key function in isentropic flows with area change because it relates the area variation, i.e., the driving potential, to the Mach number variation.

Likewise, we can find the static pressure, temperature, and density variations in an isentropic flow by integrating relations of Table 3. For example, for the static pressure  $p$ :

$$\frac{dp}{p} = \left( \frac{\gamma Ma^2}{1 - Ma^2} \right) \frac{dA}{A} = \left( \frac{\gamma Ma^2}{1 - Ma^2} \right) \left[ \frac{-(1 - Ma^2)}{2 \left( 1 + \frac{\gamma - 1}{2} Ma^2 \right)} \frac{dMa^2}{Ma^2} \right] \quad (191)$$

Integrating from  $p = p_0$ ,  $Ma^2 = 0$  to  $p = p$ ,  $Ma^2 = Ma^2$ , we obtain

$$\int_{p_0}^p \frac{dp}{p} = -\frac{\gamma}{2} \int_0^{Ma^2} \frac{1}{\left( 1 + \frac{\gamma - 1}{2} Ma^2 \right)} dMa^2 \quad (192)$$

In summary, for static pressure, temperature, and density we get:

$$\frac{p}{p_0} = \left( 1 + \frac{\gamma - 1}{2} Ma^2 \right)^{-\frac{\gamma}{\gamma-1}} \quad (193)$$

$$\frac{\rho}{\rho_0} = \left( 1 + \frac{\gamma - 1}{2} Ma^2 \right)^{-\frac{1}{\gamma-1}} \quad (194)$$

$$\frac{T}{T_0} = \left( 1 + \frac{\gamma - 1}{2} Ma^2 \right)^{-1} \quad (195)$$

Thus, we simply recover the isentropic relations between the static and stagnation states that we derived in section 1.3. The relations for  $A/A^*$ ,  $p/p_0$ ,  $\rho/\rho_0$ ,  $T/T_0$  are tabulated as a function of  $Ma$ , for  $\gamma = 1.4$  in Isentropic Flow Tables.<sup>3</sup> These are useful to void evaluating the functions respectively, especially in exams situations with limited time and where approximate solutions are acceptable. For more accurate solution, software is available, such as `vucalc` from NASA-Glenn.<sup>4</sup> The tables and software are especially useful in inverse situations, when, for example  $p/p_0$  or  $A/A^*$  is given and  $Ma$  and other properties are desired, given that some of these functions such as (190) are not explicitly invertible for  $Ma$ .

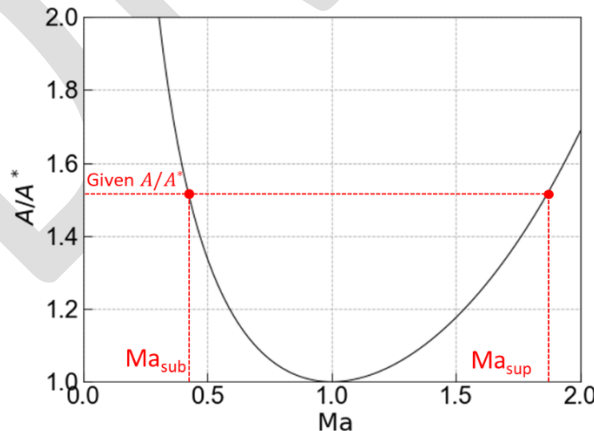


**Figure 20.** For a given area ratio  $A/A^*$ , we have two solutions, subsonic and supersonic.

<sup>3</sup> <https://www.grc.nasa.gov/www/BGH/Images/naca1135.pdf>

<sup>4</sup> <https://www.pdas.com/vucalc.html>

There is another complication with  $A/A^*$  that can be seen by plotting (190) as a function of Ma for a given value of the adiabatic coefficient  $\gamma$  (see example in Figure 20 for  $\gamma = 1.4$ ), i.e., it has both a subsonic and a supersonic branch. These two different values of the Mach number can lead to very different values of pressure, temperature and density, so we must be very careful that we choose the right ones. This depends on the boundary conditions of the flow. We do see from the plot in Figure 20, however, that to accelerate a flow isentropically from subsonic to supersonic conditions, we must pass through an area minimum at sonic conditions, Ma=1, as we discussed previously.

**Table 5. Isentropic Flow Functions**

$$\frac{A}{A^*} = \frac{1}{Ma} \left[ \frac{2}{\gamma + 1} \left( 1 + \frac{\gamma - 1}{2} Ma^2 \right) \right]^{\frac{\gamma+1}{2(\gamma-1)}} \quad (196)$$

$$\frac{p}{p_0} = \left( 1 + \frac{\gamma - 1}{2} Ma^2 \right)^{-\frac{\gamma}{\gamma-1}} \quad (197)$$

$$\frac{\rho}{\rho_0} = \left( 1 + \frac{\gamma - 1}{2} Ma^2 \right)^{-\frac{1}{\gamma-1}} \quad (198)$$

$$\frac{T}{T_0} = \left( 1 + \frac{\gamma - 1}{2} Ma^2 \right)^{-1} \quad (199)$$

$$\frac{pA}{p_0 A^*} = \frac{\left( \frac{2}{\gamma + 1} \right)^{\frac{\gamma+1}{2(\gamma-1)}}}{Ma \left( 1 + \frac{\gamma - 1}{2} Ma^2 \right)^{1/2}} \quad (200)$$

### 4.3 Mass Flow Functions

The standard expression for mass flow rate is  $\dot{m} = \rho U A$ . In compressible flow, however  $\rho$  is not constant and is not as easily measurable as  $p$  and  $T$ . Also, in our 1D analyses, the Mach number is the velocity parameter that is used most often, rather than the velocity  $U$ . Therefore, it is convenient to recast the expression for  $\dot{m}$  in terms of  $p$ ,  $T$ , and Ma. Using the equation of state (1), and (33)-(34) for the speed of sound and the Mach number we can write

$$\dot{m} = \rho U A = \frac{p}{RT} Ma(\gamma RT)^{1/2} A = p A Ma \left( \frac{\gamma}{RT} \right)^{1/2} \quad (201)$$

In dimensionless form we can recast (201) as

$$(p, T) : \frac{\dot{m}(RT)^{1/2}}{pA} = Ma(\gamma)^{1/2} \quad (202)$$

We can also trivially rewrite (202) in various other forms by eliminating  $p$  and/or  $T$ , in favor of  $p_0$ ,  $T_0$  using the isentropic adiabatic relations (193)-(195):

$$(p_0, T): \frac{\dot{m}(RT)^{1/2}}{p_0 A} = \frac{\text{Ma}(\gamma)^{1/2}}{\left(1 + \frac{\gamma-1}{2} \text{Ma}^2\right)^{\frac{\gamma}{\gamma-1}}} \quad (203)$$

$$(p, T_0): \frac{\dot{m}(RT_0)^{1/2}}{p A} = \text{Ma} \left[ \gamma \left(1 + \frac{\gamma-1}{2} \text{Ma}^2\right) \right]^{1/2} \quad (204)$$

$$(p_0, T_0): \frac{\dot{m}(RT_0)^{1/2}}{p_0 A} = \text{Ma}(\gamma)^{1/2} \left(1 + \frac{\gamma-1}{2} \text{Ma}^2\right)^{\frac{-(\gamma+1)}{2(\gamma-1)}} \quad (205)$$

A particularly convenient location to evaluate  $\dot{m}$  in the form of (205) is at the sonic locations (for example, the throat of a choked convergent-divergent nozzle), where  $\text{Ma} = 1$  and  $A = A^*$ :

$$\frac{\dot{m}(RT_0)^{1/2}}{p_0 A^*} = (\gamma)^{1/2} \left(\frac{\gamma+1}{2}\right)^{\frac{-(\gamma+1)}{2(\gamma-1)}} = \text{const.} = \mathbb{C} \quad (206)$$

We note that only  $\gamma$  appears in the RHS of (206), therefore, for a calorically perfect gas ( $\gamma = \text{const.}$ ) the quantity  $\frac{\dot{m}(RT_0)^{1/2}}{p_0 A^*}$  is constant. For calorically perfect air gas ( $\gamma = 1.4$ ),  $\mathbb{C} = 0.6847$  in (206), and for  $R = 287 \text{ m}^2/(\text{s}^2\text{K}) = 1716 \text{ ft}^2/(\text{s}^2\text{R})$ :

$$\frac{\dot{m}(T_0)^{1/2}}{p_0 A^*} = 0.04042 \frac{[\text{kg}/\text{s}][\text{K}^{1/2}]}{[\text{Pa}][\text{m}^2]} \quad (207)$$

$$\frac{\dot{m}(T_0)^{1/2}}{p_0 A^*} = 0.5318 \frac{[\text{lbm}/\text{s}][\text{^{\circ}R}^{1/2}]}{[\text{lbm}/\text{in}^2][\text{in}^2]} \quad (208)$$

The choked-flow expression (206)-(208) for the mass flow rate are called Fliegner's formulae.

**Table 6. Mass Flow Functions**

$$\frac{\dot{m}(RT)^{1/2}}{p A} = \text{Ma}(\gamma)^{1/2} \quad (209)$$

$$\frac{\dot{m}(RT)^{1/2}}{p_0 A} = \frac{\text{Ma}(\gamma)^{1/2}}{\left(1 + \frac{\gamma-1}{2} \text{Ma}^2\right)^{\frac{\gamma}{\gamma-1}}} \quad (210)$$

$$\frac{\dot{m}(RT_0)^{1/2}}{p A} = \text{Ma} \left[ \gamma \left(1 + \frac{\gamma-1}{2} \text{Ma}^2\right) \right]^{1/2} \quad (211)$$

$$\frac{\dot{m}(RT_0)^{1/2}}{p_0 A} = \text{Ma}(\gamma)^{1/2} \left(1 + \frac{\gamma-1}{2} \text{Ma}^2\right)^{\frac{-(\gamma+1)}{2(\gamma-1)}} \quad (212)$$

$$\frac{\dot{m}(RT_0)^{1/2}}{p_0 A^*} = (\gamma)^{1/2} \left(\frac{\gamma+1}{2}\right)^{\frac{-(\gamma+1)}{2(\gamma-1)}} = \text{const.} = \mathbb{C} \quad (213)$$

#### 4.4 Relationship between $p_0$ and $A^*$ across a Normal Shock Wave

Consider now a NS in the steady, relative frame shown in Figure 21.

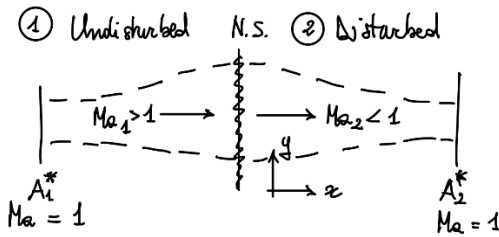


Figure 21. Sonic flow upstream and downstream of a NS wave.

Applying the mass flow function at the (imaginary) sonic locations ( $Ma = 1$ ) on the undisturbed and disturbed sides of the NS in the form (213) we get

$$\dot{m}_1 = \dot{m}_2 \Rightarrow \frac{\mathbb{C}p_{01}A_1^*}{(RT_{01})^{1/2}} = \frac{\mathbb{C}p_{02}A_2^*}{(RT_{02})^{1/2}} \quad (214)$$

Since for adiabatic processes the stagnation temperature is conserved  $T_{01} = T_{02}$  we have

$$p_{01}A_1^* = p_{02}A_2^* \quad (215)$$

Also note that for isentropic flow  $p_0 = \text{const.}$ , therefore  $A^*$  is constant in isentropic flow. We know for irreversible, adiabatic shock processes that the entropy increases across the shock is equivalent to a loss in stagnation pressure. From this relation we see that the sonic area  $A^*$  must increase across the shock (to swallow the flow behind the shock).

#### 4.5 Applications of Isentropic Flow and Normal Shock Waves

##### 4.5.1 Converging Nozzle

Earlier we found that to accelerate a subsonic flow to supersonic velocities, the flow must pass through an area minimum in a converging-diverging (CD) passage. Thus, if we have a simple converging passage, the flow will never attain supersonic velocities no matter how much we contract the passage or how large a pressure difference we impose across it. *The best we can ever achieve is  $Ma = 1$  at the exit* (Figure 22)

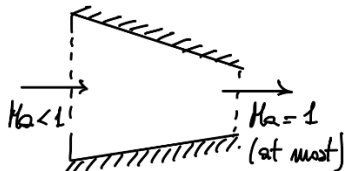


Figure 22. Schematic of a converging nozzle.

Consider the situation sketched in Figure 23, where a converging nozzle is supplied from a large plenum at constant stagnation pressure  $p_0$  and temperature  $T_0$ , and exhaust to another downstream plenum<sup>5</sup> where we can control the back pressure  $p_b$  with a valve. Assuming isentropic flow through the nozzle,  $p_0$  and  $T_0$  are constant throughout and are fixed at the plenum values. We will investigate the flow in the converging nozzle as the valve is opened and back pressure  $p_b$  is lowered.

<sup>5</sup> A chamber or reservoir where gas pressure is maintained at a certain level.

Start with the valve closed (1) and consider the four diagrams sketched in the figure. There is no flow through the nozzle  $\dot{m} = 0$ , and the pressure distribution is uniform at  $p(x)/p_b = 1$ ,  $p_e/p_0 = p_b/p_0 = 1$ .

As the valve is opened and the back pressure is lowered slightly, the flow throughout the nozzle is subsonic, so the velocity increases continuously, and the back pressure decreases continuously in the streamwise direction as shown by (2). Mass flow is now induced through the nozzle and the exit Mach number is smaller than unit ( $\text{Ma}_e < 1$ ). Also, since the flow is exiting subsonically, information about the back pressure change, which propagates at the speed of sound relative to the fluid it moves into, is able to propagate all the way upstream, so that the flow exits with  $p_e = p_b$  (which sets  $\dot{m}$  and  $\text{Ma}_e$ ).

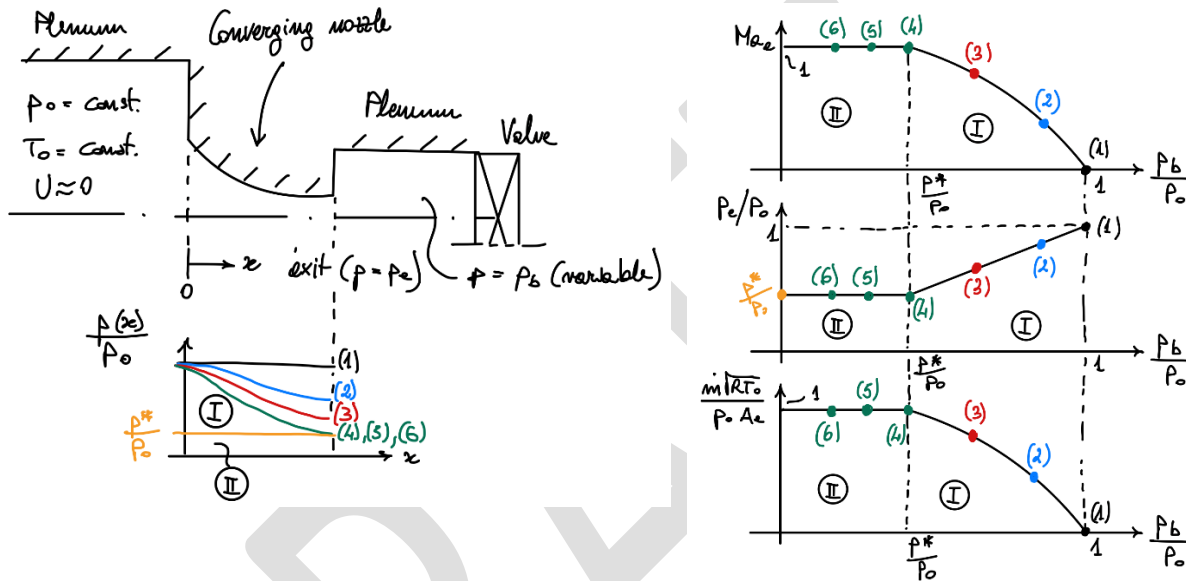


**Figure 23. Mach number, pressure ratio and mass flow for a converging nozzle with variable backpressure.**

The situation is qualitatively the same for condition (3), for which  $p_b$  is lower, but the flow still exits subsonically. The acceleration in the nozzle is just stronger and  $\dot{m}$  and  $\text{Ma}_e$  are larger (but still subsonic), and  $p_e = p_b$ .

Consider now the case (4) in which the back pressure is lowered just to the value to produce  $\text{Ma}_e = 1$  at the exit. From our isentropic relations, we know that this value is given by

$$\frac{p_e}{p_0} = \frac{p_b}{p_0} = \frac{p^*}{p_0} = \left(1 + \frac{\gamma - 1}{2} \text{Ma}^2\right)^{\frac{-\gamma}{\gamma-1}} = \left(\frac{\gamma + 1}{2}\right)^{\frac{-\gamma}{\gamma-1}} \quad (216)$$

This value is given the symbol  $p^*/p_0$  to signify conditions at unit Mach number and is called the *critical pressure ratio*. At condition (4), where we lowered  $p_b$  just enough to produce  $\text{Ma}_e = 1$ , the flow still exits uniformly and one-dimensionally with  $p_e = p_b = p^*$  and more mass flow is induced through the nozzle compared to condition (3).

Now consider the condition for which the back pressure is lowered to values less than  $p^*$  at condition (4). The information about this additional opening of the valve and lowering of back pressure propagates by means of weak, acoustic waves and the speed of sound relative to the fluid they move into. but at the exit of the nozzle, they immediately encounter sonic flow moving downstream. Therefore, this information about the back pressure change cannot cross this sonic

location, and the pressure distribution upstream of the exit. Here,  $\dot{m}$  and  $\text{Ma}_e = 1$  are the same for all cases with  $p_b < p^*$  as they are for case (4) (see cases (5) and (6)).

For the latter two cases, the exit plane pressure is greater than the back pressure ( $p_e = p^* > p_b$ ), which is called *underexpanded*. From the flow's perspective, it has not been expanded enough to meet the low back pressure. The adjustment to the back pressure boundary condition occurs outside the nozzle in the form of reversible, Prandtl-Meyer expansion waves (Figure 24) which are farther analyzed later in the course.

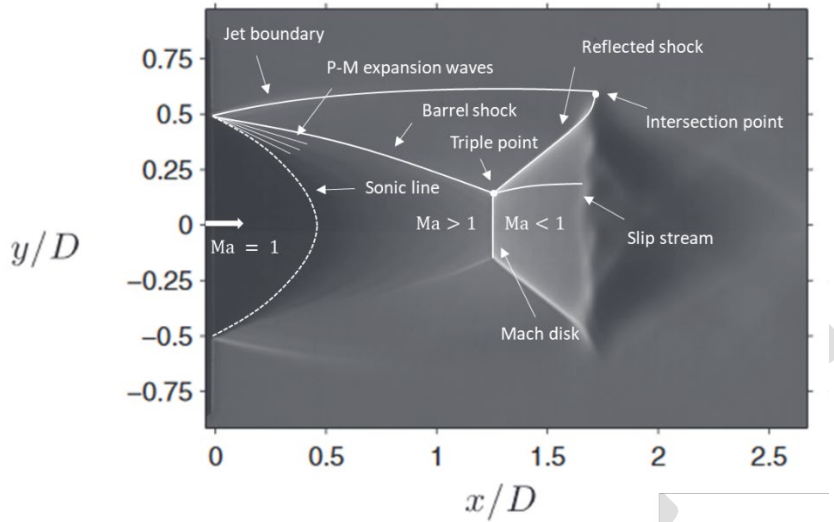


**Figure 24. Flow features in a converging underexpanded jet.**<sup>6</sup>

So, again, for all cases with  $p_b/p_0 \leq p^*/p_0 \Rightarrow \text{Ma}_e = 1$ ,  $\dot{m}$  is constant, and  $p_e = p^* \geq p_b$  and the pressure distribution in the nozzle is constant. This result about  $\dot{m}$  is rather surprising since it says that no matter how much  $p_b$  is lowered below  $p^*$  (thus increasing  $\Delta p$  across the nozzle),  $\dot{m}$  will remain constant. The nozzle is said to be *choked* under these conditions.

This nozzle has very important applications in flow-metering, and for propulsion at lower nozzle pressure ratios (NPRs)  $p_0/p_b$ .

In summary, for converging nozzle operation we have two regimes which are summarized in Table 7.

**Table 7. Regimes for convergent nozzle operation**

Regime I	$\frac{p_b}{p_0} > \frac{p^*}{p_0}$	$p_e = p_b$	$\text{Ma}_e < 1$	$\dot{m}$ dependent on $p_b$ (unchoked)
Regime II	$\frac{p_b}{p_0} \leq \frac{p^*}{p_0}$	$p_e = p^* \geq p_b$	$\text{Ma}_e = 1$	$\dot{m}$ independent of $p_b$ (choked)

#### 4.5.2 Pitot Probe

If we want to measure the stagnation pressure of a flow, we need some kind of device that will isentropically decelerate the flow to zero velocity. What is commonly used is a Pitot tube.

<sup>6</sup> Schlieren picture adapted from Edgington-Mitchell, Daniel, Damon R. Honnery, and Julio Soria. "The underexpanded jet Mach disk and its associated shear layer." *Physics of Fluids* 26.9 (2014): 1578.

In a subsonic flow, the flow can adjust in a continuous manner to the probe since information can be communicated upstream. The flow enters the Pitot probe, stagnates essentially isentropically, so the pressure measured is  $p_{01}$ . In wind tunnels there is often a static pressure tap present that is drilled carefully normal to the wall and is connected to a pressure measurement device. Note that since the static pressure tap is normal to the velocity vector at the wall, no deceleration occurs, so that the pressure measured is indeed the static pressure.

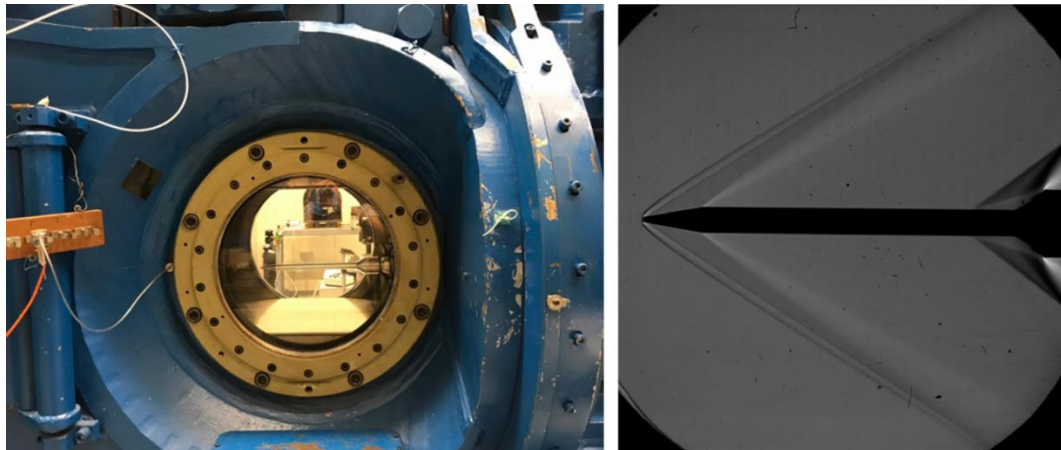


**Figure 25. Pitot tube probe in the TU Delft Supersonic Wind Tunnel<sup>7</sup>**

Given these two pressure measurements, the Mach number of the flow can be determined using isentropic relations. From (197):

$$Ma_1^2 = \left( \frac{2}{\gamma - 1} \right) \left[ \left( \frac{p_1}{p_{01}} \right)^{\frac{\gamma-1}{\gamma}} - 1 \right] \quad (217)$$

If the flow is supersonic, the probe does not isentropically decelerate to the flow because the supersonic flow cannot adjust continuously to the presence of the probe as in the subsonic case, but rather does so discontinuously by means of a shock wave (a bow shock in this case). That is, a shock wave is generated in supersonic flow in order to enforce the boundary condition that the velocity at the entrance to the probe is zero.

Away from the probe, the shock curves away from the flow (*i.e.*, is oblique to the flow), but along the stagnation streamline, which is the location we are actually interested in, the shock must be normal to the flow by symmetry.

Since the probe isentropically decelerates the subsonic flow behind the shock, what it actually measures is  $p_{02}$  (disturbed). If we have the same static pressure tap available as before, we see that it measures  $p_1$  (for the undisturbed flow). From (197) (isentropic flow) and (114) (NS), we have:

$$\frac{p_1}{p_{02}} = \frac{(p_1/p_{01})_{IF}}{(p_{02}/p_{01})_{NS}} = \frac{\left( 1 + \frac{\gamma-1}{2} Ma_1^2 \right)^{\frac{-\gamma}{\gamma-1}}}{\left( \frac{\gamma+1}{2} Ma_1^2 \right)^{\frac{\gamma}{\gamma-1}} \left( \frac{2\gamma}{\gamma+1} Ma_1^2 - \frac{\gamma-1}{\gamma+1} \right)^{\frac{-1}{\gamma-1}}} = f(Ma_1, \gamma) \quad (218)$$

<sup>7</sup> <https://dare.tudelft.nl/2019/01/supersonic-speed-estimation/>

This is called the *Rayleigh-Pitot formula*. With  $p_1$  and  $p_{02}$  known we can determine  $Ma_1$ , known  $\gamma$ . However, it cannot be explicitly inverted for  $Ma_1$ , so we must use a numerical root-finding strategy. For quick, approximate estimations (205) is tabulated in the NS tables for  $\gamma = 1.4$ .

Note, finally, that with  $p$  and  $p_0$  available, we can determine the approach Mach number for either subsonic or supersonic flow, but with only the two pressures measurements available, we may not know if the flow is subsonic or supersonic beforehand. To find whether the flow is subsonic or supersonic, one may compare  $p/p_0$  to  $p^*/p_0$ :

$$\begin{aligned} \text{If } 1 \geq \frac{p}{p_0} > \frac{p^*}{p_0} = \left(\frac{\gamma+1}{2}\right)^{\frac{1}{\gamma-1}} \Rightarrow \text{subsonic (use IF } p/p_0 \text{ relation (197) to get } Ma_1) \\ \text{If } 0 \leq \frac{p}{p_0} \leq \frac{p^*}{p_0} = \left(\frac{\gamma+1}{2}\right)^{\frac{1}{\gamma-1}} \Rightarrow \text{supersonic (use IF } p/p_0 \text{ relation (197) and NS} \\ &\text{NS } p_{02}/p_{01} \text{ relation (114) to get } Ma_1) \end{aligned} \quad (219)$$

#### 4.5.3 Converging-Diverging Nozzle

In this section we analyzed converging-diverging (CD) nozzles, which are extremely important in propulsion application in the higher  $NPR \equiv p_0/p_b$  range.

Consider the same situation analyzed in section 4.5.1 for the converging nozzle, where the CD nozzle is supplied from a large plenum at constant stagnation pressure conditions,  $p_{01}$  and  $T_{01}$ , and it exhausts to a second downstream plenum where we control the back pressure  $p_b$ . Consider the three plots in Figure 26 that illustrate the operation of the CD nozzle.

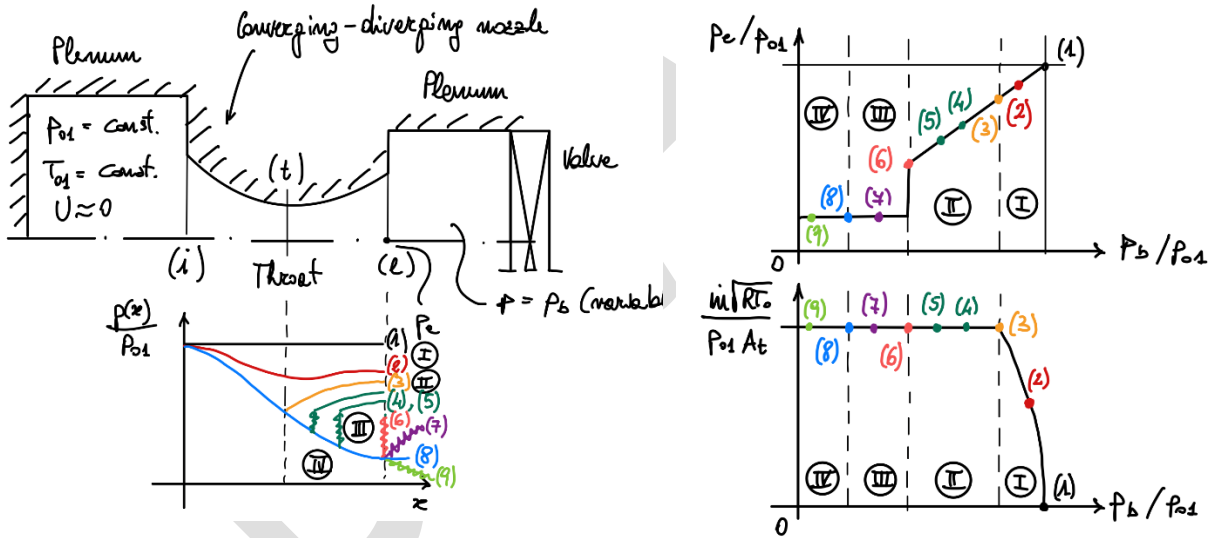


**Figure 26. Pressure ratio and mass flow for a converging-diverging nozzle with variable backpressure.**

For (1), the back pressure is shut, there is no flow through the CD nozzle,  $\dot{m} = 0$ , and the pressure distribution is uniform at  $p(x)/p_b = 1 \Rightarrow p_e/p_{01} = p_b/p_{01} = 1$ .

As the back pressure is lowered slightly to (2), subsonic flow exits throughout the nozzle, and the static pressure falls until the throat, and the rises in the diverging section to meet the back pressure  $p_e/p_{01} = p_b/p_{01}$ . Mass flow is now induced through the nozzle. A whole family of these nozzle flows exists.

When the back pressure is lowered just sufficiently to produce  $Ma_t = 1$  at the throat (3) no further changes in the mass flow can occur by lowering  $p_b$ , nor will the static pressure distribution

upstream of the throat change. This is the *choking point* or *subsonic design point* determined by the relation:

$$\frac{A_e}{A_t} = \frac{A_e}{A^*} = \frac{1}{\text{Ma}_e} \left[ \frac{2}{\gamma + 1} \left( 1 + \frac{\gamma - 1}{2} \text{Ma}_e^2 \right) \right]^{\frac{\gamma+1}{2(\gamma-1)}} \quad (220)$$

At these conditions, the flow still exits uniformly and one-dimensionally with  $p_e/p_{01} = p_b/p_{01}$ .

There is also another isentropic one-dimensional solution to  $A_e/A_t = A_e/A^*$  for  $\text{Ma}_t = 1$  at the throat, a supersonic solution, giving  $\text{Ma}_e > 1$ , called the *supersonic design point*. In this case, the flow again exits uniformly and one-dimensionally with  $p_e/p_{01} = p_b/p_{01}$  and the same  $\dot{m}$  as case (3), but the flow past the throat in this case continues accelerating to low values of  $p_e/p_{01} = p_b/p_{01}$  (depending on the area ratio  $A_e/A_t$ ). We call this case (8).

The question now is, what happens between the operating points (3) and (8), namely between the choking point and the supersonic design point? As the back pressure is lowered below that at (3), a NS stands in the diverging part of the nozzle (4), and the subsonic flow behind the shock diffuses to the back pressure such that  $p_e = p_b$  (exits subsonically). Also, there is a pressure jump across the NS. As the back pressure is lowered further, the NS moves toward the duct exit and becomes stronger (5), until the limit (6), where it stands just at the duct exit. For all these cases with a NS in the duct  $p_e = p_b$  since the flow exits subsonically.

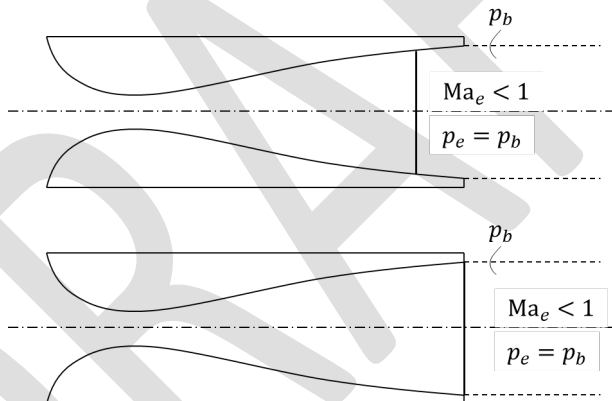


**Figure 27. Flow at the exit of the CD nozzle with  $p_e = p_b$ . Top: condition (5), bottom: condition (6).**

For back pressures between those at (6) (NS at exit) and (8) (supersonic design point), the NS is expelled from the nozzle and an oblique shock (OS) is attached to the exit lip (7), as shown in Figure 28.

Since the shock wave has been expelled for condition (7), the flow everywhere inside the nozzle is identical to that at the supersonic design point. The adjustment to the back pressure boundary conditions occurs outside the nozzle via the OS. Since  $p_e < p_b$ , this is called an *overexpanded condition* and the jet boundary streamline converges toward the centerline.

As the back pressure is lower further, eventually the supersonic design point (8) is reached for which the flow exits uniformly and one-dimensionally with  $p_e = p_b$ .

For back pressures below the supersonic design point, such as at (9), the adjustment to the low back pressure boundary condition again occurs outside the nozzle by means of a centered Prandtl-Meyer expansion fan at the nozzle exit lip.

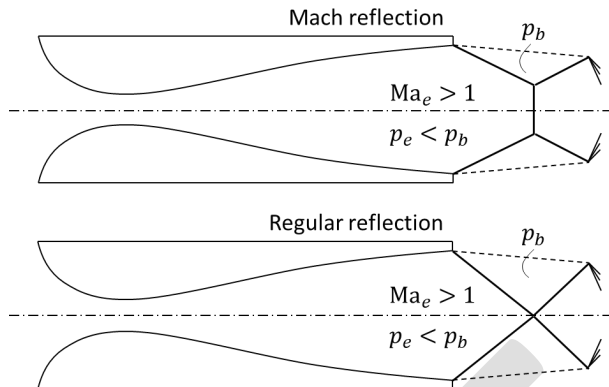


**Figure 28. Flow at the exit of the overexpanded CD nozzle (regime III). Mach reflection (closer to (6)) and regular reflection (closer to 8)).**

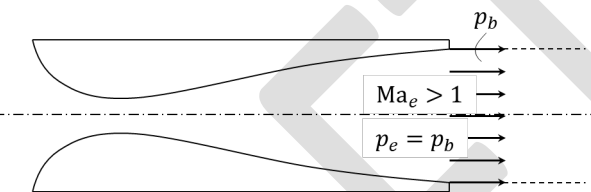


**Figure 29. Flow at the exit of the CD nozzle with  $p_e = p_b$  (condition (8)).**

Since the adjustment to the back pressure boundary condition occurs outside the nozzle, the flow inside the nozzle is again identical to that at the supersonic design point. Since  $p_e > p_b$ , this is called an *underexpanded condition*.



**Figure 30. Flow at the exit of the underexpanded CD nozzle (regime IV).**

It is important to note that for all back pressure below that at which a NS stands at the nozzle exit, the flow in the nozzle is identical to that at the supersonic design point.

In summary, for CD nozzle operation we have two regimes which are summarized in Table 8. The critical points or *breakoff points* between the four regimes are the choking point (3), the NS at the exit point (6), and the supersonic design point (8). In a given CD nozzle problem, it is usually a good idea to find these points first if possible (need  $A_e/A_t$ ), and then to determine which regime the nozzle is operating in (need  $p_b/p_{01}$ ). Note that the critical pressure ratio  $p^*/p_{01} = 0.5282$  for  $\gamma = 1.4$  has nothing to do with determining the regime or choked operation of a CD nozzle.

**Table 8. Regimes for CD nozzle operation**

Regime I (1-2-3)	Subsonic flow throughout	$p_e = p_b$	$\text{Ma}_e < 1$	$\dot{m}$ dependent on $p_b$ (unchoked)
Regime II (3-4-5-6)	NS in nozzle	$p_e = p_b$	$\text{Ma}_e < 1$	$\dot{m}$ independent of $p_b$ (choked)

Regime III (6-7-8)	OS at exit	$p_e \leq p_b$ (overexpanded)	$\text{Ma}_{e,\text{sup}}$	$\dot{m}$ independent of $p_b$ (choked)
Regime IV (8-9)	PM expansion at exit	$p_e \geq p_b$ (underexpanded)	$\text{Ma}_{e,\text{sup}}$	$\dot{m}$ independent of $p_b$ (choked)

#### 4.5.4 Supersonic Wind Tunnel Diffuser

In this section we will concentrate our discussion on open-loop type supersonic wind tunnels that exhaust to the ambient, although similar conclusions apply to closed-loop tunnels.

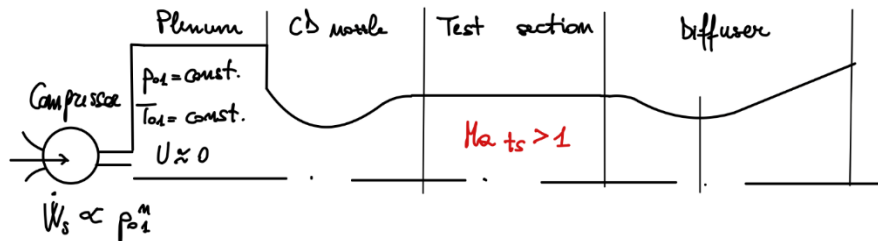


Figure 31. Schematic of supersonic wind tunnel.

Consider the sketch in Figure 31, where we use a compressor work is  $\dot{W}_s \propto p_{01}^n$  with  $n > 1$  to establish a uniform supersonic flow in the test section with minimum compressor power (i.e., minimum  $p_{01}$ ). We will now investigate the design of the nozzle/test-section/diffuser to achieve this goal.

As one option, consider the achievement of a uniform, supersonic jet flow with no diffuser exiting to the atmosphere. To achieve uniform supersonic flow at the exit plane with no OS or PM expansion waves requires attainment of the supersonic design pressure ratio  $\frac{p_b}{p_{01}} = \left(\frac{p_e}{p_{01}}\right)_{\text{Ma}_{e,\text{sup},\text{des}}}$ .

For example, if we aim at achieving Mach 2 flow at the exit with a back pressure of 100 kPa, we would need to supply  $p_{01} = \frac{p_b}{\left(\frac{p_e}{p_{01}}\right)_{\text{Ma}_{e,\text{sup},\text{des}}}} = \frac{100 \text{ kPa}}{0.1278} = 782.5 \text{ kPa}$ , about 113.5 psia. This a pretty high pressure.

One way we could reduce the required supply pressure would be to utilize a second-throat supersonic diffuser with a throat area equal to the nozzle throat area  $A_{t2} = A_{t1}$ . If the area at the exit of the subsonic diffuser is large  $A_e \rightarrow \infty$ , to that  $\text{Ma}_e \approx 0$  and the exit static and station pressures are essentially equal, we have in the ideal isentropic limit  $p_e = p_b = p_{01}$ . Of course, frictional effects will be present so that the compressor must be used to overcome there. In this case, the supersonic diffuser is essentially a reversed CD nozzle.

However, there is a problem with this design that occurs during startup of the system. Thinking back to our CD nozzle discussion, we know that as we raise  $p_{01}$ , which is equivalent to lowering  $p_b$ , we first have the family of unchoked, subsonic flows in the CD nozzle. As  $p_{01}$  is raised further the nozzle eventually chokes, and a further increase in  $p_{01}$  will cause a NS to stand in the diverging portion of the nozzle. It is this NS that causes the problem in the second-throat diffuser system. From continuity across a NS:  $p_{01}A_1^* = p_{02}A_2^*$  or  $\frac{p_{02}}{p_{01}} = \frac{A_1^*}{A_2^*} < 1$ . We see that in order for the diffuser to swallow the flow after the shock, the downstream choking area (diffuser throat)  $A_2^*$  must be larger than the upstream choking area (nozzle throat)  $A_1^*$ . The most extreme condition occurs when the supply pressure is raised such that the shock reaches the test section because this shock

is the strongest, thus incurring the largest stagnation pressure loss and the largest required increase in  $A^*$  (diffuser throat area) to swallow the flow after the shock.

At the ideal isentropic limit, we must therefore have:

$$\frac{A_{t2}}{A_{t1}} = \left( \frac{A_2^*}{A_1^*} \right)_{\text{Ma}_{\text{des}}} = \frac{1}{\left( \frac{p_{02}}{p_{01}} \right)_{\text{Ma}_{\text{des}}}} \quad (221)$$

What happens when  $A_{t2}$  is smaller than this requirement is that the system chokes only at the second throat and not the first and supersonic flow conditions are never established in the test section.

Thus, the ideal, fixed geometry, supersonic, second throat diffuser and operating characteristics are those shown in Figure 32.

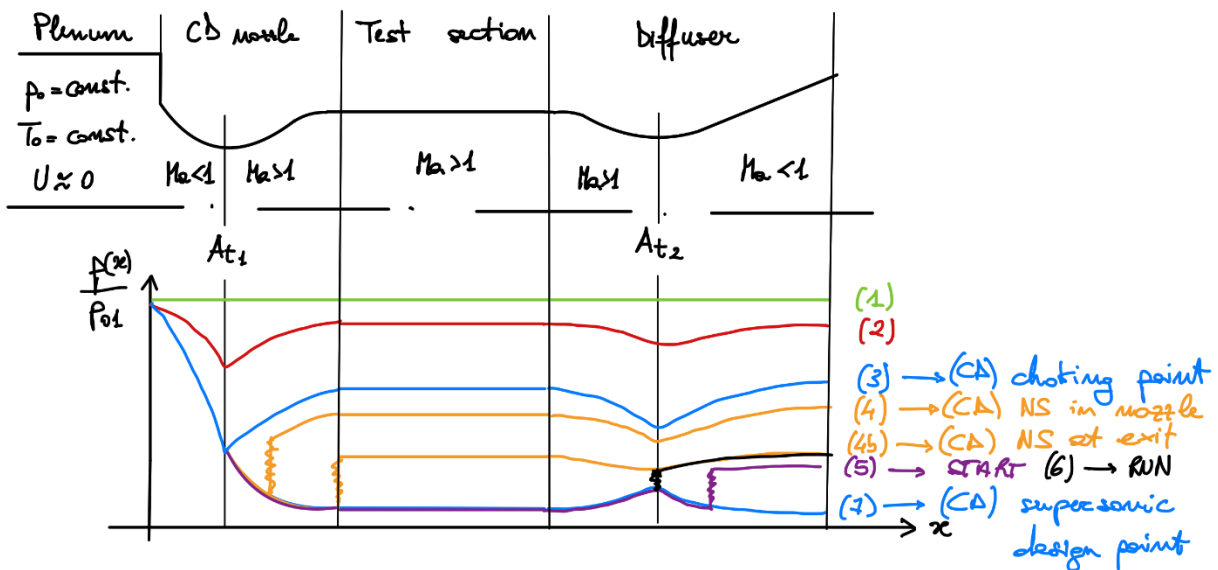


Figure 32. Pressure evolution in supersonic wind tunnel.

When  $p_b = p_{01}$ , there is no flow through the system (1). As the back pressure is lowered slightly (or  $p_{01}$  raised), subsonic flow (2) exits throughout the system with the pressure at the second throat greater than that at the first since the area ratio is larger. As the back pressure is lowered further, we eventually reach the condition at which sonic flow is achieved at the first throat, and the system is choked (3). Further reductions in the back pressure will induce no more flow through the system nor change the pressure distribution upstream of the first throat. At this condition, the Mach number at the second throat is still subsonic, again because of its larger area ratio.

An isentropic, 1D solution also exists for entirely supersonic flow from the first throat on (like supersonic design point for CD nozzle), such that the flow exits uniformly and one-dimensionally with  $p_e = p_b$ . But this occurs for very high values of  $p_{01}$  and is of no interest here (7).

As the back pressure is lowered from the choking value (3) a NS will stand in the diverging part of the nozzle. The stagnation pressure loss associated with the shock is equivalent to a required increase in the choking area  $A^*$ , so the flow at the second throat is approaching sonic conditions (4). When the NS reaches the test section, we have the maximum loss in  $p_0$  and the maximum required increase in  $A^*$  (5). If the diffuser has been designed to the ideal limit such that (221) is satisfied the flow at the second throat will just be reaccelerated to sonic conditions. The shock is

neutrally stable in the constant-area test section (unstable in converging sections; stable in diverging sections). A slight increase in supply pressure or decreasing back pressure will cause the shock to move through the test section to a location in the diverging part of the diffuser where the area is equal to that in the test section. The wind tunnel is now started.

The supply pressure increase may now be lowered, or the back pressure raised to locate the shock at the second throat of the diffuser. This is the minimum supply pressure or maximum back pressure at which we will have started, supersonic design conditions in the test section (6). That slight lowering of the supply pressure or raising of the back pressure from (6) will cause the shock to jump back into the diverging part of the CD nozzle, thus *unstarting* the test section. At the diffuser throat, the shock is the weakest possible, with supersonic flow in the test section, thus entailing the smallest loss in stagnation pressure and minimum compressor power requirement.

In summary, to start a fixed-geometry, supersonic diffuser, the geometrical requirement is:

$$\frac{A_{t2}}{A_{t1}} \geq \left( \frac{A_2^*}{A_1^*} \right)_{Ma_{des}} = \frac{1}{\left( \frac{p_{02}}{p_{01}} \right)_{Ma_{des}}} \quad (222)$$

Rather than designing at the ideal limit, which would not start in real life, more conservatively the second throat is made larger than the ideal limit  $\frac{A_{t2}}{A_{t1}} = \left( \frac{A_2^*}{A_1^*} \right)_{Ma_{des}}$  by some percentage, say 10%.

Then, at the round condition the shock is not located right at the second throat but at some slightly larger area in the diverging diffuser. This will compensate for non-ideal conditions and the fact that if the shock is located right at the throat, just a slight increase in back pressure or decrease in  $p_{01}$  will cause the shock to jump back into the nozzle, thus unstarting the test section. The shock is neutrally stable when located right at the second throat.

Many large, sophisticated wind tunnels utilize variable area second throat diffusers, where for starting, the diffuser configuration and pressure ratio must be as above for the fixed-geometry case. But once the shock has been moved out of the test section into the diffuser second-throat area can be reduced and back pressure increased or supply pressure reduced so that a very weak shock is located near diffuser throat. In the ideal limit  $A_{t2} = A_{t1}$  so that  $Ma_{t2} = 1$ , and the supersonic diffuser is essentially a reversed CD nozzle (which would never work in practice). Also, conservative versions of this where for starting  $\frac{A_{t2}}{A_{t1}} \geq \left( \frac{A_2^*}{A_1^*} \right)_{Ma_{des}}$  and for running  $A_{t2} > A_{t1}$  and the shock is located at an area larger than  $A_{t2}$ .

## 5 Flow with Friction (Fanno Flow)

### 5.1 Introduction

In this section we analyze compressible flow with friction, in the absence of friction, and  $T_0$ -change. This flow is often referred to as Fanno flow. Obviously, wall friction is always present in any internal flow, but it is particularly important for long ducts where the effects of friction cannot be ignored. Thus, the primary application of this section is compressible gas flow in pipelines/piping systems.

### 5.2 Analysis

Consider the schematic shown earlier in Figure 19 and the 5 assumptions made in section 3.2 to which we add the following assumptions:

- (6) Constant area duct (*i.e.*,  $\varepsilon_A = \frac{dA}{A} = 0$ )
- (7) adiabatic (*i.e.*,  $\delta\dot{Q} = 0$ )
- (8) no viscous work (*i.e.*,  $\delta\dot{W}_{\text{visc}} = 0$ )

From (7) and (8)  $\frac{\delta\dot{Q} + \delta\dot{W}_{\text{visc}}}{c_p m T_0} = \varepsilon_{T_0} = 0$ . Because  $\varepsilon_A = \varepsilon_{T_0} = 0$ , we can ignore the first and third columns in Table 3 from our generalized, 1D analysis, and we can write immediately:

$$\begin{aligned}
 \varepsilon_{\text{Ma}^2} &= \frac{d\text{Ma}^2}{\text{Ma}^2} = \frac{\gamma \text{Ma}^2 \left(1 + \frac{\gamma - 1}{2} \text{Ma}^2\right) f dx}{1 - \text{Ma}^2} \frac{f dx}{D_h} \\
 \varepsilon_U &= \frac{dU}{U} = \frac{\gamma \text{Ma}^2}{2(1 - \text{Ma}^2)} \frac{f dx}{D_h} = -\varepsilon_p \\
 \varepsilon_p &= \frac{dp}{\rho} = \frac{-\gamma \text{Ma}^2}{2(1 - \text{Ma}^2)} \frac{f dx}{D_h} = -\varepsilon_U \\
 \varepsilon_p &= \frac{dp}{p} = \frac{-\gamma \text{Ma}^2 [1 + (\gamma - 1) \text{Ma}^2]}{2(1 - \text{Ma}^2)} \frac{f dx}{D_h} \\
 \varepsilon_T &= \frac{dT}{T} = \frac{-\gamma(\gamma - 1) \text{Ma}^4}{2(1 - \text{Ma}^2)} \frac{f dx}{D_h} \\
 \varepsilon_{p_0} &= \frac{dp_0}{p_0} = \frac{-\gamma \text{Ma}^2}{2} \frac{f dx}{D_h} \\
 \varepsilon_s &= \frac{ds}{c_p} = \frac{(\gamma - 1) \text{Ma}^2}{2} \frac{f dx}{D_h}
 \end{aligned} \tag{223}$$

Applying the second law of thermodynamics (cf. section 1.1.4), with the specified assumptions, we have:

$$\begin{aligned}
 \frac{d}{dt} \int_V \rho s dV + \oint_S \rho s \vec{U} \cdot \hat{n} dS - \oint_S \frac{\dot{q}''}{T} dS &\geq 0 \Rightarrow \\
 \Rightarrow s(-\rho U A) + s(1 + \varepsilon_s) [\rho(1 + \varepsilon_p) U(1 + \varepsilon_U) A(1 + \varepsilon_A)] &\geq 0
 \end{aligned} \tag{224}$$

which using continuity becomes:

$$-s + s(1 + \varepsilon_s) \geq 0 \tag{225}$$

In this case, since we have friction (an irreversibility), it is the inequality ( $> 0$ ) that applies and we conclude that:

$$\varepsilon_s = \frac{ds}{c_p} > 0 \Rightarrow \frac{(\gamma - 1)Ma^2}{2} \frac{fdx}{D_h} > 0 \quad (226)$$

Also, since  $\frac{(\gamma - 1)Ma^2}{2} > 0$  always, we can conclude that:

$$\varepsilon_f = \frac{fdx}{D_h} > 0 \quad (227)$$

Equation (227) tells us that  $f > 0$  or  $\tau_w > 0$ , i.e., we chose the correct direction for  $\tau_w$  in our original control volume momentum analysis for generalized 1D flow (cf. section 3.2). Knowing that  $\varepsilon_f > 0$  we can now choose the signs of  $\varepsilon_{Ma^2}, \varepsilon_U, \varepsilon_\rho, \dots$  in both subsonic and supersonic flow, i.e., the directions of change of  $Ma^2, U, \rho, \dots$  in both cases. These are shown in Table 9. Notice that  $\varepsilon_{Ma^2}, \varepsilon_U, \varepsilon_\rho, \varepsilon_p, \varepsilon_T$  change sign at  $Ma = 1$  because of the  $1 - Ma^2$  factor in the denominator of each. Thus, the effect of friction on these parameters is opposite in subsonic and supersonic flow.

**Table 9. Property trends in Fanno flow**

	Ma < 1	Ma > 1
$\varepsilon_{Ma^2} = \frac{dMa^2}{Ma^2} = \frac{\gamma Ma^2 \left(1 + \frac{\gamma - 1}{2} Ma^2\right)}{1 - Ma^2} \frac{fdx}{D_h}$	+	-
$\varepsilon_U = \frac{dU}{U} = \frac{\gamma Ma^2}{2(1 - Ma^2)} \frac{fdx}{D_h} = -\varepsilon_\rho$	+	-
$\varepsilon_\rho = \frac{d\rho}{\rho} = \frac{-\gamma Ma^2}{2(1 - Ma^2)} \frac{fdx}{D_h} = -\varepsilon_U$	-	+
$\varepsilon_p = \frac{dp}{p} = \frac{-\gamma Ma^2 [1 + (\gamma - 1)Ma^2]}{2(1 - Ma^2)} \frac{fdx}{D_h}$	-	+
$\varepsilon_T = \frac{dT}{T} = \frac{-\gamma(\gamma - 1)Ma^4}{2(1 - Ma^2)} \frac{fdx}{D_h}$	-	+
$\varepsilon_{p_0} = \frac{dp_0}{p_0} = \frac{-\gamma Ma^2}{2} \frac{fdx}{D_h}$	-	-
$\varepsilon_s = \frac{ds}{c_p} = \frac{(\gamma - 1)Ma^2}{2} \frac{fdx}{D_h}$	+	+

In summary:

- (1) In subsonic Fanno flow (constant-area duct flow with friction), the Mach number and the velocity increase, but the static pressure, temperature, and density all decrease with  $x$ .
- (2) In supersonic Fanno flow, the Mach number and the velocity decrease, but the static pressure, temperature, and density all increase with  $x$ .

- (3) In both subsonic and supersonic Fanno flow, the stagnation pressure always decreases, the entropy always increases, and the stagnation temperature is constant.

Thus, we have the strange-looking results that friction accelerates a subsonic flow but does so at the expense of a loss in stagnation pressure (increase in entropy), i.e., irreversibly.

We can also see that friction cannot be used to continuously accelerate a subsonic flow to supersonic conditions or to continuously decelerate a supersonic flow to subsonic conditions. Subsonic flow can at most be accelerated by friction to  $Ma = 1$ . Supersonic flows are decelerated by friction, also at most to  $Ma = 1$ .

Now let us integrate our differential equations to find the property variations for finite amounts of friction (i.e., finite duct lengths) instead of differential. Starting from the relation in the first line of Table 3:

$$\varepsilon_{Ma^2} = \frac{dMa^2}{Ma^2} = \frac{\gamma Ma^2 \left(1 + \frac{\gamma-1}{2} Ma^2\right) f dx}{1 - Ma^2} \frac{D_h}{D_h} \quad (228)$$

Separating and integrating from an arbitrary location where  $x = 0$ ,  $Ma^2 = Ma^2$  to the sonic location where  $x = L_{\max}$ ,  $Ma^2 = 1$  (the maximum possible length for the given inlet conditions without readjustment):

$$\begin{aligned} \int_0^{L_{\max}} \frac{f dx}{D_h} &= \int_{Ma^2}^1 \frac{1 - Ma^2}{\gamma Ma^4 \left(1 + \frac{\gamma-1}{2} Ma^2\right)} dMa^2 \Rightarrow \\ &\Rightarrow \frac{L_{\max}}{D_h} \frac{1}{L_{\max}} \int_0^{L_{\max}} f dx = \int_{Ma^2}^1 \frac{1 - Ma^2}{\gamma Ma^4 \left(1 + \frac{\gamma-1}{2} Ma^2\right)} dMa^2 \end{aligned} \quad (229)$$

We define an average friction coefficient as:

$$\bar{f} = \frac{1}{L_{\max}} \int_0^{L_{\max}} f dx \quad (230)$$

which appears on the LHS of (229). Then, carrying out the integral in (229):

$$\frac{\bar{f} L_{\max}}{D_h} = \frac{1 - Ma^2}{\gamma Ma^2} + \left(\frac{\gamma+1}{2\gamma}\right) \ln \left[ \frac{(\gamma+1)Ma^2}{2 \left(1 + \frac{\gamma-1}{2} Ma^2\right)} \right] \quad (231)$$

Note that the friction factor  $f$  is the Darcy or Moody friction, which is 4 times the Fanning skin friction coefficient  $f = f_D = f_M = 4f_F$ , so that the function  $\frac{\bar{f} L_{\max}}{D_h}$  is identical to the  $\frac{4f L^*}{D}$  seen in many other books (including Anderson's compressible flow book) and software. This  $\frac{\bar{f} L_{\max}}{D_h}$  is the "key" gas dynamic function in Fanno flow because it related the driving potential (friction) to the Mach number.

Likewise, we can find the  $U, \rho, p, T, p_0$  variations in Fanno flow by integrating succeeding lines in T of IC's (Table 3). For example, for the velocity (using the integrand in (229)):

$$\begin{aligned}\varepsilon_U &= \frac{dU}{U} = \frac{\gamma Ma^2}{2(1 - Ma^2)} \frac{fdx}{D_h} = \frac{\gamma Ma^2}{2(1 - Ma^2)} \frac{1 - Ma^2}{\gamma Ma^4 \left(1 + \frac{\gamma - 1}{2} Ma^2\right)} \\ &= \frac{1}{2Ma^2 \left(1 + \frac{\gamma - 1}{2} Ma^2\right)} dMa^2\end{aligned}\quad (232)$$

Integrating from  $U$  to  $U^*$ ,  $\rho$  to  $\rho^*$ ,  $Ma^2$  to  $Ma^2 = 1$ :

$$\begin{aligned}\int_U^{U^*} \frac{dU}{U} &= - \int_{\rho}^{\rho^*} \frac{d\rho}{\rho} = \int_{Ma^2}^1 \frac{1}{2Ma^2 \left(1 + \frac{\gamma - 1}{2} Ma^2\right)} dMa^2 \Rightarrow \\ \Rightarrow \frac{U}{U^*} &= \frac{\rho^*}{\rho} = Ma \left[ \frac{(\gamma + 1)/2}{\left(1 + \frac{\gamma - 1}{2} Ma^2\right)} \right]^{\frac{1}{2}}\end{aligned}\quad (233)$$

And, similarly, for the other properties as listed in Table 10. These properties are tabulated as a function of  $Ma$  in the Fanno flow tables and can be evaluated for any  $\gamma$  using any compressible flow calculator such as `vucalc`. Note that not all functions are explicitly invertible for  $Ma$ , which make the tables and software especially useful.

**Table 10. Fanno Flow Functions**

$$\frac{\bar{f}L_{\max}}{D_h} = \frac{1 - Ma^2}{\gamma Ma^2} + \left(\frac{\gamma + 1}{2\gamma}\right) \ln \left[ \frac{\frac{(\gamma + 1)}{2} Ma^2}{\left(1 + \frac{\gamma - 1}{2} Ma^2\right)} \right] \quad (234)$$

$$\frac{U}{U^*} = \frac{\rho^*}{\rho} = Ma \left[ \frac{\frac{(\gamma + 1)}{2}}{\left(1 + \frac{\gamma - 1}{2} Ma^2\right)} \right]^{\frac{1}{2}} \quad (235)$$

$$\frac{p}{p^*} = \frac{1}{Ma} \left[ \frac{\frac{(\gamma + 1)}{2}}{\left(1 + \frac{\gamma - 1}{2} Ma^2\right)} \right]^{\frac{1}{2}} \quad (236)$$

$$\frac{T}{T^*} = \frac{\frac{(\gamma + 1)}{2}}{\left(1 + \frac{\gamma - 1}{2} Ma^2\right)} \quad (237)$$

$$\frac{p_0}{p_0^*} = \frac{1}{Ma} \left[ \frac{\left(1 + \frac{\gamma - 1}{2} Ma^2\right)}{\frac{(\gamma + 1)}{2}} \right]^{\frac{\gamma + 1}{2(\gamma - 1)}} = \left( \frac{A}{A^*} \right)_{\text{IF}} \quad (238)$$

Note that  $\frac{\bar{f}L_{\max}}{D_h}$  is a double-valued function of the Mach number with both a subsonic and supersonic branch (see Figure 33), so the correct solution needs to evaluate properly depending

on the boundary conditions for the problem. The function  $\frac{p}{p_0^*}$  is also double-valued since it is identical to the isentropic  $\frac{A}{A^*}$  function. In the limit of very high Mach numbers  $\frac{\bar{f}L_{\max}}{D_h}$  tends to the asymptotic value  $\lim_{\text{Ma} \rightarrow \infty} \frac{\bar{f}L_{\max}}{D_h} = -\frac{1}{\gamma} + \left(\frac{\gamma+1}{2\gamma}\right) \ln\left(\frac{\gamma+1}{\gamma-1}\right)$  which is equal to 0.82153 for  $\gamma = 1.4$ .

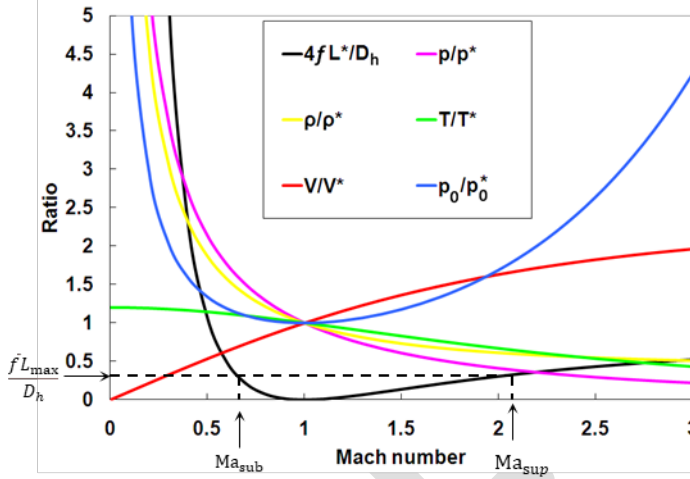


Figure 33. Fanno flow ratios as a function of Mach number.

### 5.3 Fanno Line

A useful graphical representation of Fanno flows is to present them on a  $(T, s)$  diagram. Under our assumptions, we can write continuity, energy and state equations as:

$$\text{Continuity: } \rho U = \text{const. } (A \text{ is constant}) \quad (239)$$

$$\text{Energy: } h + \frac{U^2}{2} = h_0 = \text{const. } (\text{steady, adiabatic, no work, and no grav. pot. en.}) \quad (240)$$

$$\text{State: } p = \rho RT \quad (241)$$

Recall equation (23) for the entropy changes of a calorically perfect gas. Using continuity, it becomes:

$$\begin{aligned} s - s_1 &= c_v \ln\left(\frac{T}{T_1}\right) - R \ln\left(\frac{\rho}{\rho_1}\right) \Rightarrow \\ &\Rightarrow s - s_1 = c_v \ln\left(\frac{T}{T_1}\right) - R \ln\left(\frac{U_1}{U}\right) \Rightarrow \end{aligned} \quad (242)$$

Here “1” is an arbitrary reference state. Using energy,  $U = 2(h_0 - h)^{1/2} = [2c_p(T_0 - T)]^{1/2}$ :

$$\begin{aligned} s - s_1 &= c_v \ln\left(\frac{T}{T_1}\right) - R \ln\left[\frac{2c_p(T_0 - T_1)}{2c_p(T_0 - T)}\right]^{1/2} \Rightarrow \\ &\Rightarrow s - s_1 = c_v \ln\left(\frac{T}{T_1}\right) - \frac{1}{2} R \ln\frac{(T_0 - T_1)}{(T_0 - T)} \Rightarrow \\ &\Rightarrow \frac{s - s_1}{c_v} = \ln\left(\frac{T}{T_1}\right) + \frac{1}{2} \frac{R}{c_v} \ln\frac{(T_0 - T)}{(T_0 - T_1)} \Rightarrow \end{aligned} \quad (243)$$

Using (9) and taking the reference condition “1” and the sonic (Ma = 1) condition “\*”:

$$\frac{s - s^*}{c_v} = \ln\left(\frac{T}{T^*}\right) + \frac{\gamma - 1}{2} \ln\left(\frac{T_0 - T}{T_0 - T^*}\right) \Rightarrow \quad (244)$$

Figure 34 shows a plot of this equation, known as the Fanno curve, on a  $(T, s)$  diagram in which is essentially identical to a  $(h, s)$  diagram (or Mollier diagram) for a calorically perfect gas.

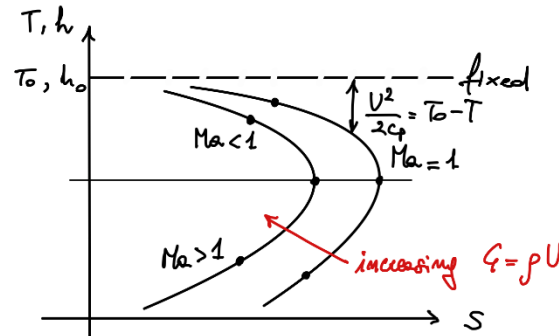


**Figure 34. Fanno curves.**

The governing equations of continuity for a constant-area duct, adiabatic energy, and state are satisfied along each Fanno line in Figure 34. Note that the momentum equation has not been used in the above derivation. To move from point to point along a given Fanno line corresponds to moving from down the duct with differing amounts of friction, which is the momentum equation. For a given stagnation temperature  $T_0$ , each different Fanno line involved a different value of the mass flux  $G = \rho V$ , with  $G$  increasing inward.

Let us now examine the maximum  $s(T)$  location on a given Fanno line by differentiating (244)  $\frac{d}{dT}\left(\frac{s - s^*}{c_v}\right)$  and equating to zero:

$$\frac{d}{dT}\left(\frac{s - s^*}{c_v}\right) = 0 \Rightarrow \frac{1}{T} - \frac{\gamma - 1}{2} \frac{1}{T_0 - T} = 0 \quad (245)$$

Because by energy  $T_0 - T = \frac{U^2}{2c_p}$ , substituting in (245) gives:

$$\frac{1}{T} = \frac{\gamma - 1}{2} \frac{2c_p}{U^2} = \frac{\gamma - 1}{U^2} \frac{\gamma R}{\gamma - 1} \Rightarrow \frac{\gamma R T}{U^2} = 1 \Rightarrow \text{Ma}^2 = 1 \quad (246)$$

Therefore, the maximum entropy point on each Fanno line is the sonic condition. Since the distance between  $T_0$  and  $T$  on each line is  $T_0 - T = \frac{U^2}{2c_p}$ , points above the sonic point correspond to subsonic flow. The sonic conditions at the “knee” of a Fanno line are denoted by \*, such as  $p^*$ ,  $T^*$ , etc. However, the \* in this case applies to the Fanno process under consideration and is not the same as the “\*\*” (sonic) condition for isentropic flow, for example.

From the second law of thermodynamics for this adiabatic steady flow, we know that the entropy must increase, i.e., it must move to the right. Thus, we see again graphically that subsonic Fanno flows are accelerated towards Ma = 1, but do so at the expense of a loss of stagnation pressure. Likewise, supersonic flows are decelerated towards Ma = 1, again with a loss in stagnation pressure. It is also again apparent that continuous transitions from subsonic to supersonic flow

or vice versa are not possible purely with Fanno flow since this would involve an entropy decrease, hence a violation of the second law.

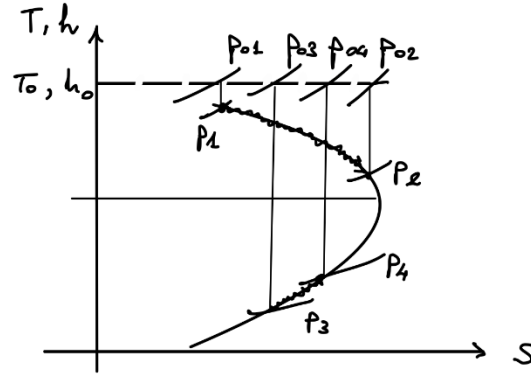


Figure 35. Fanno ( $T, s$ ) diagram.

#### 5.4 Readjustments

If we have a subsonic flow with given inlet conditions entering a frictional duct of just sufficient length to reach Mach 1,  $x = L_{\max}$ , and then add an additional length of duct, the flow readjusts by lowering its mass flow rate (jumping to an outer Fanno line of smaller  $\dot{m}$ ), such that  $Ma = 1$  is maintained at the new exit. The duct is choked by friction; since for a subsonic inflow we can never have supersonic outflow,  $Ma = 1$  at the new exit is the best we can do. The new length of the duct is the new value of  $L_{\max}$  and  $Ma_{\text{inlet}}$  drops accordingly.

For supersonic inflow into a frictional duct of just sufficient length to reach Mach 1, and we then add more duct length, the flow unable to sense that the duct is “too long” and readjusts itself by means of a normal shock whose position is dependent on the length of the duct and the backpressure boundary condition to which the flow exhausts.

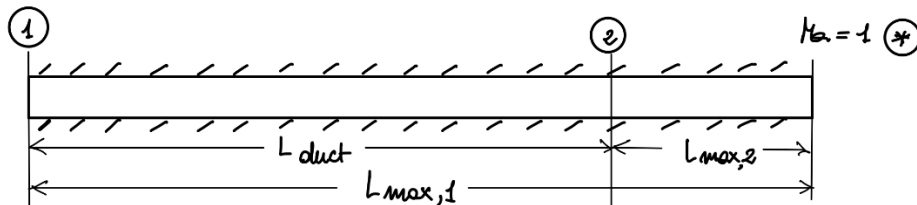


Figure 36. Readjusted duct.

Finally, consider a situation of a given duct inlet condition (subsonic or supersonic) with  $L_{\text{duct}} < L_{\max}$  for the given  $Ma_1$ . How do we determine  $Ma_2$ ? Just geometrically we see that

$$L_{\max,2} = L_{\max,1} - L_{\text{duct}} \quad (247)$$

Multiplying by  $\frac{\bar{f}}{D_h}$ :

$$\left( \frac{\bar{f} L_{\max}}{D_h} \right)_{Ma_2} = \left( \frac{\bar{f} L_{\max}}{D_h} \right)_{Ma_1} - \frac{\bar{f} L_{\text{duct}}}{D_h} \quad (248)$$

Here the term on the LHS can be inverted to get  $Ma_2$ , while the two terms in the RHS are known from  $Ma_1$  and from  $(\bar{f}, L_{\text{duct}}, D_h)$ , respectively. Equation (248) is the key relation in Fanno flow

allowing one to move from station to station. More fundamentally, this is an integrated form of the first line of the Table of Influence Coefficients.

### 5.5 Converging Nozzle Feeding a Constant Area Duct with Friction

Consider a similar situation to that examined in section 4.5.1, but this time with the converging nozzle discharging into a constant area duct. The system is fed by a large plenum at constant  $p_0$ ,  $T_0$  and exits to a second downstream plenum where the backpressure  $p_b$  is controlled by a valve. We will consider the converging nozzle to be isentropic, which is generally a good assumption, with friction in the constant area duct only.

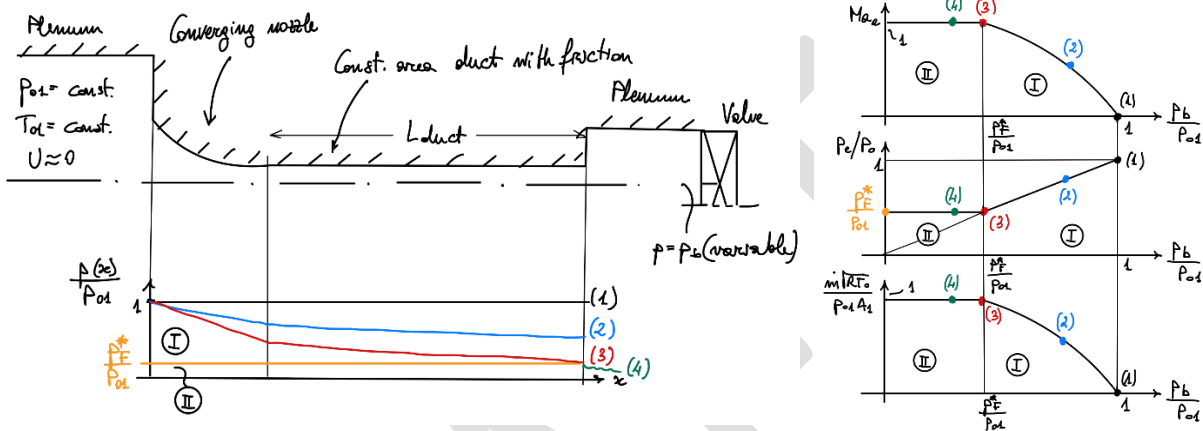


**Figure 37. Mach number, pressure ratio and mass flow for a converging nozzle-duct with friction configuration for variable backpressure.**

As the back pressure is lowered and subsonic flow is induced through the system, the flow is accelerated by both the converging nozzle and the frictional duct. So sonic conditions are reached first at the duct exit, and the system chokes there at a back pressure ratio of  $\frac{p_F^*}{p_{01}} = g\left(\frac{\bar{f}L_{\text{duct}}}{D_h}\right) < \frac{p_F^*}{p_{01}}$ .

For all back pressure ratios at or below  $\frac{p_F^*}{p_{01}}$ , the nozzle-duct combination is choked ( $\text{Ma}_e = 1$ ), the mass flow  $\dot{m}$  is at its maximum value,  $p_e = p_F^* \geq p_b$ , and the pressure distribution upstream of the exit is fixed. There are just two regimes of operation, qualitatively identical to the simple converging nozzle. These are summarized in Table 11.

**Table 11. Regimes of operation for convergent nozzle-duct configuration**

Regime I	$\frac{p_b}{p_0} > \frac{p_F^*}{p_0}$	$p_e = p_b$	$\text{Ma}_e < 1$	$\dot{m}$ dependent on $p_b$ (unchoked)
Regime II	$\frac{p_b}{p_0} \leq \frac{p_F^*}{p_0}$	$p_e = p_F^* \geq p_b$	$\text{Ma}_e = 1$	$\dot{m}$ independent of $p_b$ (choked)

## 6 Flow with Heat Transfer (Rayleigh Flow)

### 6.1 Introduction

We now come to our last “simple flow” (i.e., flow with just a single driving potential): the flow with  $T_0$  change (which we know is equivalent to heat transfer and/or work interactions) in the absence of area change and friction. We take  $\varepsilon_{T_0} = \frac{dT_0}{T_0} = \frac{\delta\dot{Q} + \delta\dot{W}_{visc}}{c_p \dot{m} T_0}$  as the driving potential in this case. Since heat transfer effects are much more common in applications than work interactions, we will generally state our simple  $T_0$ -change results in terms of *heat transfer*. As usual, frictional effects always occur in internal flows, but frictionless Rayleigh assumption is valid if large amounts of energy are exchanged in relatively short ducts, for example in combustors. This assumption is less appropriate for heat exchanger since frictional effects tend to be large in those systems.

### 6.2 Analysis

Consider the schematic shown earlier in Figure 19 and the 5 assumptions made in section 3.2 to which we add the following assumptions:

$$(6) \text{ Constant area duct (i.e., } \varepsilon_A = \frac{dA}{A} = 0\text{)}$$

$$(7) \text{ frictionless (i.e., } \tau_w = 0\text{)}$$

Because  $\varepsilon_A = \varepsilon_f = 0$ , we can ignore the first and second columns in Table 3 from our generalized, 1D analysis, and we can write immediately:

$$\begin{aligned} \varepsilon_{Ma^2} &= \frac{dMa^2}{Ma^2} = \frac{(1 + \gamma Ma^2) \left(1 + \frac{\gamma - 1}{2} Ma^2\right) dT_0}{1 - Ma^2} \frac{dT_0}{T_0} \\ \varepsilon_U &= \frac{dU}{U} = \frac{1 + \frac{\gamma - 1}{2} Ma^2}{1 - Ma^2} \frac{dT_0}{T_0} \\ \varepsilon_p &= \frac{dp}{\rho} = \frac{-\left(1 + \frac{\gamma - 1}{2} Ma^2\right) dT_0}{1 - Ma^2} \frac{dT_0}{T_0} \\ \varepsilon_p &= \frac{dp}{p} = \frac{-\gamma Ma^2 \left(1 + \frac{\gamma - 1}{2} Ma^2\right) dT_0}{1 - Ma^2} \frac{dT_0}{T_0} \\ \varepsilon_T &= \frac{dT}{T} = \frac{(1 - \gamma Ma^2) \left(1 + \frac{\gamma - 1}{2} Ma^2\right) dT_0}{1 - Ma^2} \frac{dT_0}{T_0} \\ \varepsilon_{p_0} &= \frac{dp_0}{p_0} = \frac{-\gamma Ma^2}{2} \frac{dT_0}{T_0} \\ \varepsilon_s &= \frac{ds}{c_p} = \left(1 + \frac{\gamma - 1}{2} Ma^2\right) \frac{dT_0}{T_0} \end{aligned} \tag{249}$$

In section 3.2, from the energy equation we had derived (164):

$$\dot{Q} + \cancel{\dot{W}_{visc}} = \dot{m} c_p (T_{02} - T_{01}) \tag{250}$$

which relates heat additions or subtractions to changes in stagnation temperature. As previously stated, we neglect work contributions and focus on heat. We see that *heating* ( $\dot{Q} > 0$ ) corresponds to increases in  $T_0$ , while *cooling* ( $\dot{Q} < 0$ ) corresponds to decreases in  $T_0$ .

Applying the second law of thermodynamics (cf. section 1.1.4), with the specified assumptions, we have:

$$\begin{aligned} \frac{d}{dt} \int_V \rho s dV + \oint_S \rho s \vec{U} \cdot \hat{n} dS - \oint_S \frac{\dot{q}''}{T} dS &\geq 0 \Rightarrow \\ \Rightarrow s(-\rho U A) + s(1 + \varepsilon_s) [\rho(1 + \varepsilon_\rho) U(1 + \varepsilon_U) A(1 + \varepsilon_A)] &\geq \oint_S \frac{\dot{q}''}{T} dS \end{aligned} \quad (251)$$

which using continuity becomes:

$$\begin{aligned} -s + s(1 + \varepsilon_s) &\geq \frac{1}{m} \oint_S \frac{\dot{q}''}{T} dS \Rightarrow s\varepsilon_s \geq \frac{1}{m} \oint_S \frac{\dot{q}''}{T} dS \Rightarrow s \frac{ds}{s} \geq \frac{1}{m} \oint_S \frac{\dot{q}''}{T} dS \Rightarrow \\ &\Rightarrow ds \geq \frac{1}{m} \oint_S \frac{\dot{q}''}{T} dS \end{aligned} \quad (252)$$

If the heat transfer is reversible, the equality holds and for

$$\left. \begin{array}{l} \text{heat added: } \dot{q}'' > 0 \Rightarrow ds > 0 \\ \text{heat rejected: } \dot{q}'' < 0 \Rightarrow ds < 0 \end{array} \right\} \text{Directions on Reyleigh lines} \quad (253)$$

Table 12 give the direction of change (*i.e.*, the sign) for the various properties for *heating*  $\varepsilon_{T_0} = dT_0/T_0 > 0$ . For cooling the directions of change are opposite. Note that that  $\varepsilon_{Ma^2}$ ,  $\varepsilon_U$ ,  $\varepsilon_\rho$ ,  $\varepsilon_p$ ,  $\varepsilon_T$  change sign at  $Ma = 1$  because of the  $1 - Ma^2$  factor in their denominators, indicating that the effect of heating on these parameters is opposite in subsonic and supersonic flow. In addition,  $\varepsilon_T$  changes sign at  $Ma = 1/\sqrt{\gamma}$  because of the  $1 - \gamma Ma^2$  factor in its numerator.

In summary:

- (1) For subsonic Rayleigh flow with heating, the Mach number and the velocity increase, while the static pressure and density decrease. For  $0 < Ma < 1/\sqrt{\gamma}$ , temperature increases, while for  $1/\sqrt{\gamma} < Ma < 1$ , temperature decreases.
- (2) For supersonic Rayleigh flow with heating, the Mach number and the velocity decreases, while the static pressure, density and temperature increase with heating.
- (3) In both subsonic and supersonic Rayleigh flow with heating, the stagnation pressure always decreases, the entropy always increases, and the stagnation temperature is constant.

The directions of change for cooling are just the opposite. Since heating drives both subsonic and supersonic flow toward  $Ma = 1$ , heating alone cannot be used to continuously accelerate a subsonic flow to supersonic conditions (or vice versa), although heating a subsonic flow to  $Ma = 1$  followed by cooling above  $Ma = 1$  could theoretically be done (not achieved in practice).

Now let us integrate our differential equations to find the property variations for finite (instead of differential) amounts of  $T_0$  change in Rayleigh flow. Starting from the relation in the first line of Table 3 (Table of Influence Coefficients):

$$\varepsilon_{Ma^2} = \frac{dMa^2}{Ma^2} = \frac{(1 + \gamma Ma^2) \left(1 + \frac{\gamma - 1}{2} Ma^2\right) dT_0}{1 - Ma^2} \quad (254)$$

**Table 12. Property trends in Rayleigh flow for heating ( $\varepsilon_{T_0} = \frac{dT_0}{T_0} > 0$ ).**

	Ma < 1	Ma > 1
$\varepsilon_{Ma^2} = \frac{dMa^2}{Ma^2}$	+	-
$= \frac{(1 + \gamma Ma^2) \left(1 + \frac{\gamma - 1}{2} Ma^2\right) dT_0}{1 - Ma^2} \frac{1}{T_0}$		
$\varepsilon_U = \frac{dU}{U} = \frac{1 + \frac{\gamma - 1}{2} Ma^2}{1 - Ma^2} \frac{dT_0}{T_0}$	+	-
$\varepsilon_\rho = \frac{d\rho}{\rho} = \frac{-(1 + \frac{\gamma - 1}{2} Ma^2) dT_0}{1 - Ma^2} \frac{1}{T_0}$	-	+
$\varepsilon_p = \frac{dp}{p} = \frac{-\gamma Ma^2 \left(1 + \frac{\gamma - 1}{2} Ma^2\right) dT_0}{1 - Ma^2} \frac{1}{T_0}$	-	+
$\varepsilon_T = \frac{dT}{T} = \frac{(1 - \gamma Ma^2) \left(1 + \frac{\gamma - 1}{2} Ma^2\right) dT_0}{1 - Ma^2} \frac{1}{T_0}$	$0 < Ma < 1/\sqrt{\gamma}$	$1/\sqrt{\gamma} < Ma < 1$
$\varepsilon_{p_0} = \frac{dp_0}{p_0} = \frac{-\gamma Ma^2 dT_0}{2} \frac{1}{T_0}$	-	-
$\varepsilon_s = \frac{ds}{c_p} = \left(1 + \frac{\gamma - 1}{2} Ma^2\right) \frac{dT_0}{T_0}$	+	+

Separating and integrating from an arbitrary location where  $T_0 = T_0$ ,  $Ma^2 = Ma^2$  to the sonic location where  $T_0 = T_0^*$ ,  $Ma^2 = 1$  (which defines the maximum amount of heat that can be transferred to the duct before “thermal choking” occurs):

$$\int_{T_0}^{T_0^*} \frac{dT_0}{T_0} = \int_{Ma^2}^1 \frac{1 - Ma^2}{(1 + \gamma Ma^2) \left(1 + \frac{\gamma - 1}{2} Ma^2\right) Ma^2} dMa^2 \quad (255)$$

which leads to:

$$\frac{T_0}{T_0^*} = \frac{2(\gamma + 1)Ma^2 \left(1 + \frac{\gamma - 1}{2} Ma^2\right)}{(1 + \gamma Ma^2)^2} \quad (256)$$

This is the “key” gas dynamic function in Rayleigh flow because it relates the driving potential ( $T_0$  change) to the Mach number variation.

Likewise, we can find the  $U, \rho, p, T, p_0$  variations in Rayleigh flow, by integrating succeeding lines in T of IC's (Table 3). These are summarized in Table 13, which provides the Rayleigh flow functions. These function are tabulated as a function of Ma and  $\gamma = 1.4$  in the Raileigh flow tables

and can be evaluated for any  $\gamma$  using any compressible flow calculator, such as `vucalc`. Note that not all functions are explicitly invertible for  $Ma$ , which make the tables and software especially useful.

**Table 13. Rayleigh Flow Functions**

$$\frac{T_0}{T_0^*} = \frac{2(\gamma + 1)Ma^2 \left(1 + \frac{\gamma - 1}{2}Ma^2\right)}{(1 + \gamma Ma^2)^2} \quad (257)$$

$$\frac{U}{U^*} = \frac{\rho^*}{\rho} = \frac{(\gamma + 1)Ma^2}{1 + \gamma Ma^2} \quad (258)$$

$$\frac{p}{p^*} = \frac{\gamma + 1}{1 + \gamma Ma^2} \quad (259)$$

$$\frac{T}{T^*} = \frac{(\gamma + 1)^2 Ma^2}{1 + \gamma Ma^2} \quad (260)$$

$$\frac{p_0}{p_0^*} = \frac{\gamma + 1}{1 + \gamma Ma^2} \left[ \frac{2 \left(1 + \frac{\gamma - 1}{2} Ma^2\right)}{\gamma + 1} \right]^{\frac{\gamma}{\gamma - 1}} \quad (261)$$

When plotting the Rayleigh flow functions versus  $Ma$ , we notice that three functions are double-valued function of the Mach number with both a subsonic and supersonic branch (see Figure 38):  $\frac{p}{p^*}$ ,  $\frac{T}{T^*}$ , and  $\frac{T_0}{T_0^*}$ . Thus, we must be sure to obtain the correct root  $Ma$  when performing calculations.

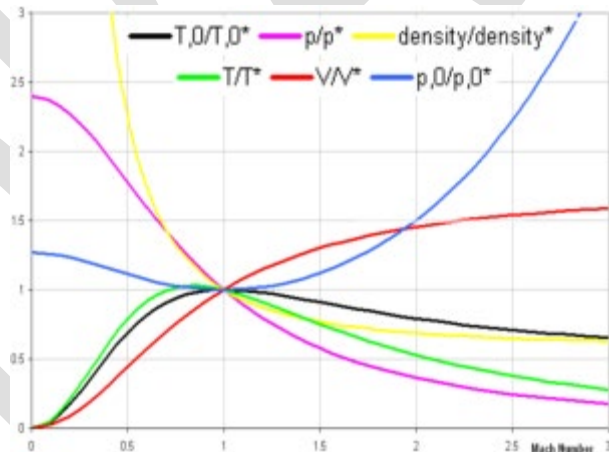


**Figure 38. Fanno flow ratios as a function of Mach number.**

### 6.3 Rayleigh Line

Similar to what we did for the Fanno flows, it is useful to present a graphical representation of Rayleigh flows on a  $(T, s)$  diagram. Here, we start from continuity, momentum and state equations:

$$\text{Continuity: } \rho U = \rho^* U^* \quad (262)$$

$$\text{Momentum: } p + \rho U^2 = p^* + \rho^* U^{*2} \quad (263)$$

$$\text{State: } p = \rho RT \quad (264)$$

Without going through the details using equation (23), together with (263)-(265), leads to:

$$\frac{s - s^*}{c_v} = \ln\left(\frac{T}{T^*}\right) - \frac{\gamma - 1}{\gamma} \ln \frac{(\gamma + 1) \pm [(\gamma + 1)^2 - 4\gamma(T/T^*)]^{1/2}}{2} \quad (265)$$

Figure 34 shows a plot of this equation, known as the Rayleigh line.

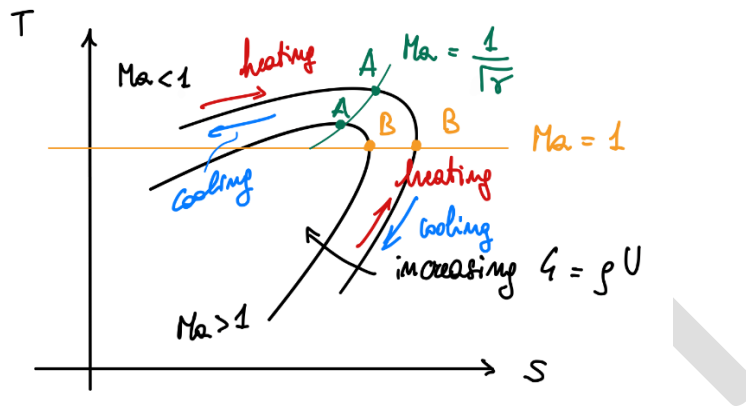


*Figure 39. Rayleigh line.*

Same as for Fanno, each different Rayleigh line corresponds to a fixed value of the mass flux  $G = \rho V$ , with  $G$  increasing inward, and has a maximum  $T(s)$  (point B) corresponding to sonic “\*” conditions. Remember that these are Rayleigh sonic conditions, and not isentropic flow, nor Fanno flow sonic conditions. Rayleigh line points above and below point B correspond to subsonic and supersonic flow, respectively. Point A, the maximum of the Raileigh line, is obtained by differentiating the Rayleigh temperature function (260)  $\frac{d}{d\text{Ma}} \left( \frac{T}{T^*} \right)$  and equating to zero which leads to

$$Ma = \frac{1}{\sqrt{\gamma}} \quad (266)$$

which is  $\text{Ma} = 0.845 \dots$  for  $\gamma = 1.4$ . Back-substituting in (260), we find:

$$\left(\frac{T}{T^*}\right)_{\max} = \frac{(\gamma + 1)^2}{4\gamma} \quad (267)$$

which is  $\left(\frac{T}{T^*}\right)_{\max} = 1.02857 \dots$  for  $\gamma = 1.4$ .

We notice that points A and B, that is max temperature and max entropy points, respectively, are close together in the  $(T, s)$  diagram.

From our Second Law results for reversible heat transfer, we know that heating corresponds to increasing  $s$ , while cooling corresponds to decreasing  $s$ . Therefore, heating processes move to the right along the Rayleigh line and cooling to the left. Heating is much like friction, it drives both subsonic and supersonic flows towards  $Ma = 1$ , while colling drives both away from  $Ma = 1$ . It is also apparent from the  $(T, s)$  diagram/Rayleigh line, that continuous transition from subsonic to supersonic flow or vice versa are not possible with heating alone since they would involve a decrease in entropy in violation of the Second Law.

the preceding results for points A and B also imply that heating the subsonic flow between these points decreases the static temperature, while cooling increases it! These results can be verified, for example, by inspection of the Rayleigh Tables.

Note that for the Rayleigh line we have satisfied continuity for a constant area duct, frictionless momentum, and state and have said nothing about energy. In order to change states in Rayleigh flow and thus move along the Rayleigh line requires varying amounts of energy exchange (i.e.,  $T_0$  change), which is in the energy equation.

#### 6.4 Readjustments

If we have a subsonic flow entering a frictional duct with just sufficient heating to reach  $\text{Ma} = 1$  at its exit, and then additional energy is transferred in, the flow readjusts by lowering its mass flow rate (jumping to an outer Rayleigh line of smaller  $G$ ), and the inlet Mach number readjusts to a new lower value. The new, higher value of  $T_0$  at the exit becomes the new  $T_0^*$  with  $\text{Ma} = 1$  maintained at the exit, and all conditions upstream must adjust accordingly. The duct is *thermally choked*.

For supersonic inflow, the flow readjusts by means of a NS wave. However, the NS occurs in the CD nozzle supplying the duct and not in the duct itself. Because the shock is adiabatic, it cannot relieve the overheating, so the shock occurs in the nozzle supplying the duct, this *unstarting* the duct.

#### 6.5 Rayleigh Line – Fanno Line Intersections

From our previous discussions of the Fanno and Rayleigh lines, we know that the analyses in each case apply to constant area ducts and the following equations are satisfied in each case:

##### Fanno Line

- 1) Continuity
- 2) Adiabatic Energy
- 3) State

##### Rayleigh Line

- 1) Continuity
- 2) Frictionless Momentum
- 3) State

On a Mollier diagram the Fanno and Rayleigh lines for the same mass flux  $G = \rho U = \dot{m}/A$  exhibit the behavior shown in Figure 40. At the intersection points, the flow must satisfy the four equations: continuity for a constant area duct, frictionless momentum, adiabatic energy, and state. These are exactly the four governing questions satisfied by the NS wave. State ① is on the supersonic, upstream side of the shock while state ② is on the corresponding subsonic downstream side. Note that the entropy must decrease for this irreversible, adiabatic process and that the wavy line  $\textcircled{1} \rightarrow \textcircled{2}$  does not represent the series of states the fluid passes inside the shock (where indeed nonequilibrium processes occur that we model as a discontinuing), but rather only the initial and final states ① and ②.

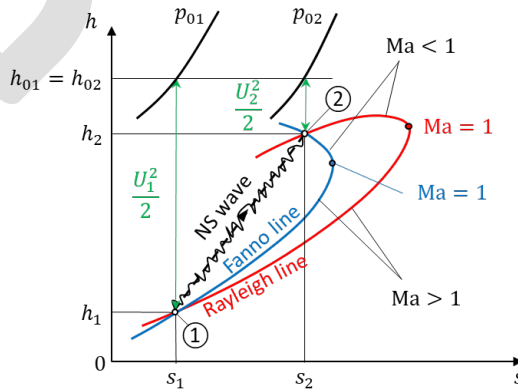


Figure 40. Rayleigh Line – Fanno Line Intersections.

## 6.6 Problem Solution Technique

In a given Rayleigh flow problem, we might typically have the inlet conditions given by  $U, p, T$ , for example, and the heat transfer rate,  $\dot{Q}$ , or a specific heat transfer,  $q \equiv \dot{Q}/\dot{m}$  known. Or alternatively, in a combustion scenario with the same inlet conditions, we may be given the heating values of the fuel  $HV_f$  and the fuel-area ratio  $FA = \dot{m}_f/\dot{m}_a$ . We want then to find block conditions after the energy addition, i.e., state ② in the two cases.

For the first situation, we use the fundamental energy equation (250), which leads to:

$$T_{02} = T_{01} + \frac{\dot{Q}}{\dot{m}c_p} = T_{01} + \frac{q}{c_p} \quad (268)$$

We have enough information to calculate everything possible at ① and from (268) we can compute  $T_{02}$ . Then we move to location ② by:

$$\frac{T_{02}}{T_0^*} = \left( \frac{T_{02}}{T_{01}} \right) \left( \frac{T_{01}}{T_0^*} \right)_{Ma_1} \quad (269)$$

From this we can determine  $Ma_2$  and all other quantities of interest at ②.

In the combustion case, the energy balance states that the total energy release rate from the fuel goes to heat the air, that is:

$$\dot{Q} = \dot{m}_f HV_f = \dot{m}_a c_{p,a} (T_{02} - T_{01}) \quad (270)$$

or

$$T_{02} = T_{01} + \frac{\dot{m}_f HV_f}{\dot{m}_a c_{p,a}} = T_{01} + \frac{FA \cdot HV_f}{c_{p,a}} \quad (271)$$

From this we can then apply (269) to determine  $Ma_2$  and all other quantities of interest at ②.

## 6.7 Converging Nozzle Feeding a Constant Area Heated Duct

Consider a converging nozzle feeding a heated duct. The situation is very similar to that analyzed in section 5.5, but this time with heating instead of friction. We conveniently assume the heating to be uniform along the duct. Since heating accelerates the flow, the system will once again choke at its exit with  $\frac{p_R^*}{p_{01}} = g \left( \frac{T_{02}}{T_{01}} \right) < \frac{p_I^*}{p_{01}}$ . There are only two regimes of operation, an unchoked one and a choked on, which are summarized in Table 14.

**Table 14. Regimes of operation for convergent nozzle-duct configuration**

Regime I	$\frac{p_b}{p_0} > \frac{p_R^*}{p_0}$	$p_e = p_b$	$Ma_e < 1$	$\dot{m}$ dependent on $p_b$ (unchoked)
Regime II	$\frac{p_b}{p_0} \leq \frac{p_R^*}{p_0}$	$p_e = p_R^* \geq p_b$	$Ma_e = 1$	$\dot{m}$ independent of $p_b$ (choked)

Note that in simple Rayleigh flows the length of the duct over which the addition occurs does not enter the analysis at all. Thus, the energy may be added in a concentrated region, such as the flame front in a combustor, or over a distributed region such as the tubes of a heat exchanger.

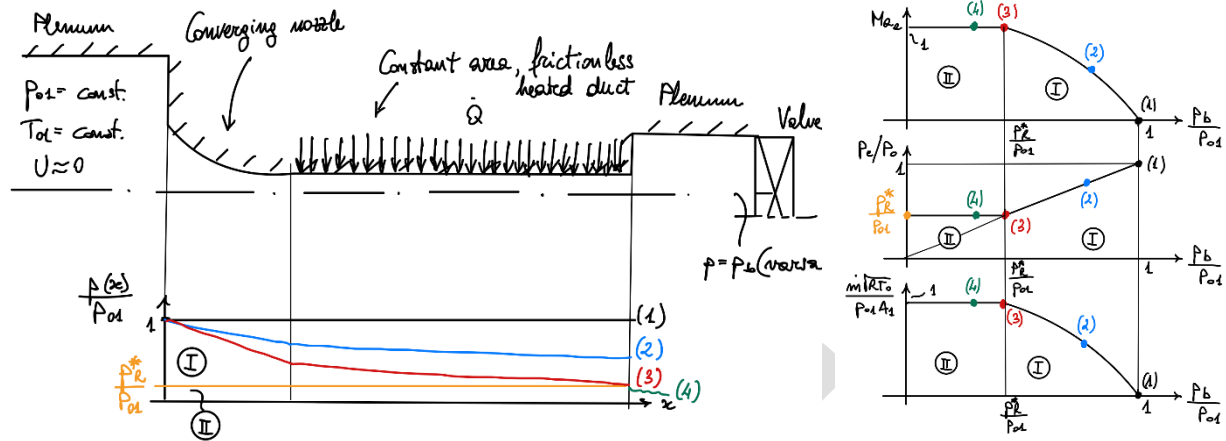


Figure 41. Mach number, pressure ratio and mass flow for a converging nozzle- heated duct configuration for variable backpressure.

## 7 Oblique Shock Waves

### 7.1 Introduction

In section 2 we spent a great deal of time analyzing normal shock waves, i.e., shock discontinuities that are normal to the flow direction. We found that only compression NS's satisfy the Second Law of Thermodynamics, and across them occur decreases in Mach number, velocity, and stagnation pressure, and increases in static pressure, temperature, density, and entropy. Stagnation temperature remains unchanged.

However, there is another important family of shocks discontinuity release, of which the NS is just a special case: the oblique shock (OS) wave. in this case the shock wave is inclined (oblique) the direction of flow and, in general, may be curved. However, for tomorrow we will focus on the straight, planar oblique shock immersed in a uniform, supersonic flow. In this case, the flow upstream and downstream of the OS is uniform and may be treated by 1D methods (as opposed to the axisymmetric, conical shock that we will discuss later).

There are several examples of planar, 2D, OS. See a few flow visualizations in Figure 43.

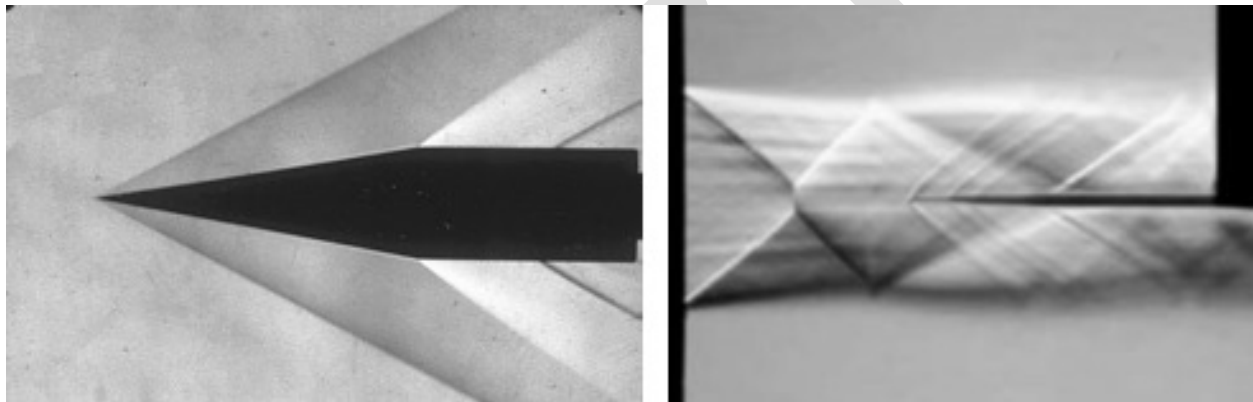


**Figure 42.** Schlieren visualizations of OS. Left: axisymmetric cone at Mach 3. Right: overexpanded nozzle.

Consider the two typical cases sketched in Figure 43. In the first case (wedge), the supersonic flow must adjust discontinuously to a change in flow direction into the presence of the wedge. In the second case (overexpanded nozzle) the supersonic flow at the exit of the nozzle must adjust to the back pressure boundary condition,  $p_b > p_e$ . In both cases, the adjustment is by means of an OS.

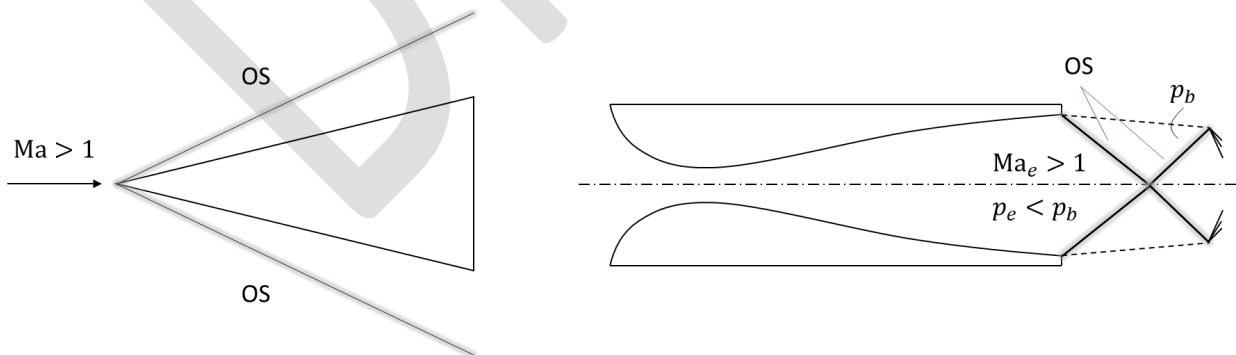


**Figure 43.** Oblique shock configurations.

### 7.2 Steady, Two-Dimensional Mach Waves

Now consider a point source of the sound that moves the velocity  $U$  less than the speed of sound,  $U < a$ . It emits sound waves at equal time intervals  $t = 0, \Delta t, 2\Delta t, 3\Delta t, \dots$ . Take a snapshot of the sound waves and point source at time  $t = 3\Delta t$ . Scenes in any time increment the points words

does not move as far as the sound waves, the fluid ahead of the point source is forewarned of its approach. The asymmetry of the wave pattern in this subsonic case is an illustration of the Doppler effect. Now consider the point source moving faster than the speed of sound  $U > a$  (supersonic case) and perform the same experiment. In this case, since the point source is moving faster than the speed of sound, fluid ahead of the point source is unaware of its approach. In fact, only fluid aware of the passage of the point source is that inside the lines drawn tangent to the spherical sound waves with the point source at the apex. These lines are called Mach lines or Mach waves, and the 3D surface generated by them is called the Mach cone. The region inside the Mach cone that is aware of the passage of the point source is called the *Zone of Action*, while undisturbed region outside the Mach cone is called the *Zone of Silence*.

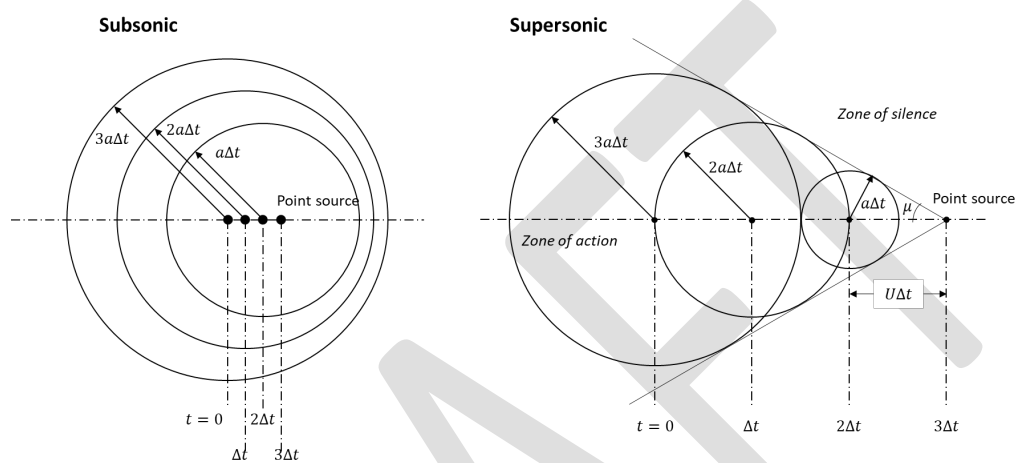


**Figure 44. Point source of sound moving at subsonic (left) and supersonic (right) speeds.**

The half angle  $\mu$  of the Mach cone, which is the angle at which the Mach waves are generated, is called the Mach angle. From trigonometry:

$$\sin \mu = \frac{a\Delta t}{U\Delta t} = \frac{a}{U} = \frac{1}{Ma}$$

or

$$\mu = \sin^{-1} \left( \frac{1}{Ma} \right) \quad (272)$$

For  $Ma < 1$ ,  $\mu$  is undefined; for  $Ma = 1$ ,  $\mu = \pi/2$ ; for  $Ma > 1$ ,  $0 \leq \mu \leq \pi/2$ .

Also consider the case in which the disturbance is stationary and immersed in a supersonic flow. The Mach angle is the angle at which infinitesimal disturbances are propagated into a supersonic flow (downstream only).

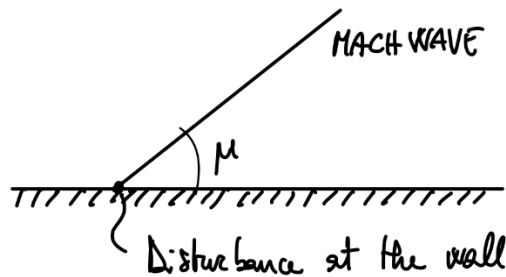


**Figure 45. Mach waves are generated by wall disturbances at a Mach angle  $\mu$ .**

### 7.3 Analysis

Consider the oblique shock shown in Figure 46. Assume the shock to have negligible thickness, i.e., modelled as a discontinuity. Take the control volume across the shock with unit cross-sectional area, and defining a normal-tangential  $n-t$  coordinate system normal and tangential to the OS.

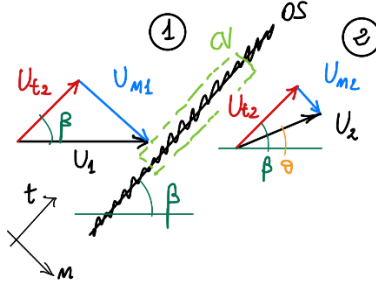


**Figure 46. Reference frame and velocity triangles for OS analysis.**

With reference to Figure 46 we use the following nomenclature:

- (1) = upstream side of the OS,
- (2) = downstream side of the OS,
- $\beta$  = angle between the shock and the approach flow velocity  $\vec{U}_1$ , also called *shock angle*,
- $\theta$  = angle through which the flow is turned, i.e., the angle between  $\vec{U}_1$  and  $\vec{U}_2$ , also called *turning angle* or *streamline deflection angle*.

In this case, we must use finite  $\varepsilon_\alpha$  operators, i.e.  $\varepsilon_\alpha = (\alpha_2 - \alpha_1)/\alpha_1$ .

Assumptions:

- (1) steady,
- (2) uniform flow and uniform properties at (1) and (2),
- (3) neglect friction,
- (4) neglect body forces,
- (5) neglect gravitational potential energy,
- (6) adiabatic,
- (7) no viscous work,
- (8) OS of infinitesimal thickness; control volume of unit cross sectional area,
- (9) calorically perfect gas.

Objective: Given the properties at (1), find the properties at (2), i.e., find the  $\varepsilon_\alpha$ .

We apply the governing equations (42), (49), and (63) to the control volume shown in Figure 46. From continuity (42) we obtain

$$\begin{aligned} \frac{d}{dt} \int_V \rho dV + \oint_S \rho \vec{U} \cdot \hat{n} dS &= 0 \Rightarrow \\ \Rightarrow -\rho U_{n1} \cdot 1 + \rho(1 + \varepsilon_\rho) U_{n1} (1 + \varepsilon_{U_n}) \cdot 1 &= 0 \Rightarrow \\ \Rightarrow -1 + 1 + \varepsilon_\rho + \varepsilon_{U_n} + \varepsilon_\rho \varepsilon_{U_n} &= 0 \end{aligned} \tag{273}$$

or

$$\varepsilon_\rho + \varepsilon_{U_n} + \varepsilon_\rho \varepsilon_{U_n} = 0 \tag{274}$$

From momentum conservation (65) in the normal direction we obtain:

$$\begin{aligned} \frac{d}{dt} \int_V \rho \vec{U} dV + \oint_S \rho \vec{U} \vec{U} \cdot \hat{n} dS &= \int_V \rho \vec{f} dV - \oint_S p \hat{n} dS = \sum F_n = F_{\text{surf},n} + F_{\text{body},n} \Rightarrow \\ \Rightarrow p_1 \cdot 1 - p_1(1 + \varepsilon_p) \cdot 1 &= U_{n1}(-\rho_1 U_{n1} \cdot 1) + U_{n1}(1 + \varepsilon_{U_n})[\rho_1(1 + \varepsilon_p) U_{n1}(1 + \varepsilon_{U_n}) \cdot 1] \end{aligned} \quad (275)$$

Since  $(1 + \varepsilon_p)(1 + \varepsilon_{U_n}) = 1$  from continuity, then

$$-p_1(1 - 1 - \varepsilon_p) = \rho_1 U_{n1}^2 [-1 + 1 + \varepsilon_{U_n}] \Rightarrow \varepsilon_p + \frac{\rho_1 U_{n1}^2}{p_1} \varepsilon_{U_n} = 0 \quad (276)$$

or

$$\varepsilon_p + \gamma Ma_{n1}^2 \varepsilon_{U_n} = 0 \quad (277)$$

In the tangential direction instead:

$$\begin{aligned} \frac{d}{dt} \int_V \rho \vec{U} dV + \oint_S \rho \vec{U} \vec{U} \cdot \hat{n} dS &= \int_V \rho \vec{f} dV - \oint_S p \hat{n} dS = \sum F_t = F_{\text{surf},t} + F_{\text{body},t} \Rightarrow \\ \Rightarrow U_{t1}(-\rho_1 U_{t1} \cdot 1) + U_{t1}(1 + \varepsilon_{U_t})[\rho_1(1 + \varepsilon_p) U_{n1}(1 + \varepsilon_{U_n}) \cdot 1] & \end{aligned} \quad (278)$$

Since  $(1 + \varepsilon_p)(1 + \varepsilon_{U_n}) = 1$  from continuity, then

$$\rho_1 U_{t1}^2 [-1 + 1 + \varepsilon_{U_n}] = 0 \quad (279)$$

or

$$\varepsilon_{U_t} = 0 \text{ or } U_{t1} = U_{t2} \quad (280)$$

Thus, *there is no mechanism for changing the tangential velocity component across a shock*. From *energy* conservation (66):

$$\begin{aligned} \frac{d}{dt} \int_V \left( e + \frac{|\vec{U}|^2}{2} \right) dV + \oint_S \rho \left( e + \frac{|\vec{U}|^2}{2} \right) \vec{U} \cdot \hat{n} dS &= \int_V \rho \vec{q} dV + \int_V \rho \vec{f} \cdot \vec{U} dV - \oint_S p \vec{U} \cdot \hat{n} dS \\ \Rightarrow \oint_S \rho \left( h + \frac{|\vec{U}|^2}{2} \right) \vec{U} \cdot \hat{n} dS &= 0 \Rightarrow \\ \Rightarrow \oint_S \rho \left( c_p T + \frac{|\vec{U}|^2}{2} \right) \vec{U} \cdot \hat{n} dS &= 0 \end{aligned} \quad (281)$$

$$\Rightarrow -\rho_1 \left( c_p T_1 + \frac{U_{n1}^2 + U_{t1}^2}{2} \right) U_{n1} + \rho_1 (1 + \varepsilon_\rho) \left[ c_p T_1 (1 + \varepsilon_T) + \frac{U_{n2}^2 + U_{t2}^2}{2} \right] U_{n1} (1 + \varepsilon_{U_n}) = 0$$

Since  $(1 + \varepsilon_\rho)(1 + \varepsilon_{U_n}) = 1$  from continuity, then (281) gives

$$\begin{aligned} -\rho_1 U_{n1} \left( T_1 + \frac{U_{n1}^2 + U_{t1}^2}{2c_p} \right) + \rho_1 U_{n1} \left[ T_1 (1 + \varepsilon_T) + \frac{U_{n2}^2 + U_{t2}^2}{2c_p} \right] &= 0 \Rightarrow \\ \Rightarrow T_1 (-1 + 1 + \varepsilon_T) + \left[ \frac{(U_{n2}^2 + U_{t2}^2) - (U_{n1}^2 + U_{t1}^2)}{2c_p} \right] &= 0 \Rightarrow \\ \Rightarrow T_1 \varepsilon_T + \left[ \frac{U_{n1}^2 (1 + \varepsilon_{U_n})^2 + U_{t2}^2 (1 + \varepsilon_{U_t})^2 - U_{n1}^2 - U_{t1}^2}{2c_p} \right] &= 0 \end{aligned} \quad (282)$$

Since  $\varepsilon_{U_t} = 0$  and from (280)  $U_{t1} = U_{t2}$ , we have

$$T_1 \varepsilon_T + \left[ \frac{U_{n1}^2 (1 + \varepsilon_{U_n})^2 - U_{n1}^2}{2c_p} \right] = 0 \Rightarrow T_1 \varepsilon_T + \left[ \frac{U_{n1}^2 (1 + 2\varepsilon_{U_n} + \varepsilon_{U_n}^2) - U_{n1}^2}{2c_p} \right] = 0 \quad (283)$$

Dividing by  $T_1$  and using (8):

$$\varepsilon_T + \left( \frac{\gamma - 1}{2} \right) \frac{U_{n1}^2}{\gamma R T_1} (2\varepsilon_{U_n} + \varepsilon_{U_n}^2) = 0 \quad (284)$$

or

$$\varepsilon_T + \left( \frac{\gamma - 1}{2} \right) \text{Ma}_{n1}^2 (2\varepsilon_{U_n} + \varepsilon_{U_n}^2) = 0 \quad (285)$$

Using the equation of state (1) for the undisturbed flow:

$$p_1 = \rho_1 R T_1 \quad (286)$$

while for the disturbed flow:

$$p_1 (1 + \varepsilon_p) = \rho_1 (1 + \varepsilon_\rho) R T_1 (1 + \varepsilon_T) \quad (287)$$

Dividing (90) by (89):

$$\varepsilon_p - \varepsilon_\rho - \varepsilon_T - \varepsilon_\rho \varepsilon_T = 0 \quad (288)$$

Looking at continuity (274),  $n$ -momentum (277), energy (285) and state (288), we see that they involve only the static thermodynamic properties and the normal velocity components/normal Mach number. In fact, if we refer back to our NS analysis, we see that these four equations are identical to the continuity, momentum, energy, and state equations for the NS with  $\varepsilon_{U_n}$  substituted for  $\varepsilon_U$  and  $\text{Ma}_{n1}$  substituted for  $\text{Ma}_1$ , and with 1 and 2 corresponding to the undisturbed and disturbed flow for the NS. Thus, we do not even need to solve equations (274), (277), (285), (288) because we have already done so in section 2.2 for the NS.

Therefore, *oblique shock waves can be analyzed by using the normal components of Mach number and velocity in conjunction with the NS relations (Table 1)*.

Notice that an observer moving along an OS at  $U_{t1} = U_{t2}$  observed a NS with Mach numbers  $\text{Ma}_{n1}$  and  $\text{Ma}_{n2}$ . Static thermodynamic properties are independent of the reference frame. Also, we will consider OS problems only in coordinates relative to the wave. Moving OS problems are quite unusual.

Note that the Mach number behind an OS can be supersonic. The normal components of Ma must behave like a NS, i.e.,  $\text{Ma}_{n1} > 1$  and  $\text{Ma}_{n2} < 1$ , but since the tangential velocity component is conserved, we (usually) have  $\text{Ma}_2 > 1$  for oblique shocks.

Also, observe that *because the normal velocity component decreases across the wave, but in general component is unchanged, the OS turns the flow towards the wave and away from the normal.*

### 7.3.1 Oblique Shock Wave Solution Parameters

For normal shock waves (1D problem), we found that specification of two parameters,  $\gamma$  and  $\text{Ma}_1$ , was sufficient to completely solve the problem. All our equations for the NS were written in terms of  $\gamma$  and  $\text{Ma}_1$ .

For oblique shocks, however, there is an extra degree of freedom which we can interpret as the shock angle, making this a two-dimensional problem. This also results in the OS wave being a three-parameter problem. We will take the two parameters to be  $\gamma$  and  $\text{Ma}_1$ . For the third we might choose  $\beta$ ,  $\theta$  or  $p_2/p_1$ . With  $\beta$  the OS system is straightforward to solve. However, usually  $\beta$  is unknown, and one rather knows  $\theta$  such as in the wedge case shown in Figure 43 (left) or  $p_2/p_1$  such as in the overexpanded nozzle case in Figure 43 (right), where  $\frac{p_2}{p_1} = \frac{p_b}{p_e}$ .

Therefore, our third parameter is chosen from  $\theta$  and  $p_2/p_1$ . Choosing  $\theta$ , we know can set ourselves the objective to express properties such as  $\beta$ ,  $\text{Ma}_2$ ,  $p_2/p_1$ ,  $T_2/T_1$ , etc. as a function of  $(\gamma, \text{Ma}_1, \theta)$ , knowing that once those are obtained, we can easily use  $\text{Ma}_{n1} = \text{Ma}_1 \sin \beta$  and the apply the NS relations to get  $\text{Ma}_{n2}$ ,  $p_2/p_1$ ,  $T_2/T_1$ , etc.

From the velocity triangles we know that:

$$U_{n1} = U_1 \sin \beta \quad (289)$$

$$U_{t1} = U_1 \cos \beta \quad (290)$$

$$U_{n2} = U_2 \sin(\beta - \theta) \quad (291)$$

$$U_{n2} = U_2 \cos(\beta - \theta) \quad (292)$$

Dividing (289) by (290), and (291) by (292):

$$\frac{U_{n1}}{U_{t1}} = \tan \beta \quad (293)$$

$$\frac{U_{n2}}{U_{t2}} = \tan(\beta - \theta) \quad (294)$$

Dividing (293) by (294), and using continuity, we have:

$$\frac{\tan(\beta - \theta)}{\tan \beta} = \frac{U_{n1}/U_{t1}}{U_{n2}/U_{t2}} = \frac{U_{n1}}{U_{n2}} = \frac{U_{n1}(1 + \varepsilon_{U_n})}{U_{n1}} = (1 + \varepsilon_{\rho})^{-1} = \frac{\rho_1}{\rho_2} \quad (295)$$

From the NS relations then:

$$\frac{\tan(\beta - \theta)}{\tan \beta} = \frac{\rho_1}{\rho_2} = 1 - \left( \frac{2}{\gamma + 1} \right) \frac{Ma_{n1}^2 - 1}{Ma_{n1}^2} \quad (296)$$

or

$$\frac{\tan(\beta - \theta)}{\tan \beta} = 1 - \left( \frac{2}{\gamma + 1} \right) \frac{Ma_1^2 \sin^2 \beta - 1}{Ma_1^2 \sin^2 \beta} \quad (297)$$

Equation (297) is an implicit, transcendental, algebraic equation for  $\beta = \beta(\gamma, Ma_1, \theta)$ . After a lengthy algebraic rearrangement and application of trigonometry identities, it can be written as:

$$(\sin^2 \beta)^3 + b(\sin^2 \beta)^2 + c(\sin^2 \beta) + d \quad (298)$$

with

$$b = -\frac{Ma_1^2 + 2}{Ma_1^2} - \gamma \sin^2 \theta \quad (299)$$

$$c = \frac{2Ma_1^2 + 1}{Ma_1^4} + \left[ \frac{(\gamma + 1)^2}{4} + \frac{(\gamma - 1)}{Ma_1^2} \right] \sin^2 \theta \quad (300)$$

$$d = -\frac{\cos^2 \theta}{Ma_1^4} \quad (301)$$

This cubic equation for  $\sin^2 \beta$  tells us that there are three possible solutions for  $\beta = \beta(\gamma, Ma_1, \theta)$ . Positive and negative roots for  $\sin \beta$  just tell us that the shock wave can be inclined up or down. One of the three solutions of (298), the smallest must be discarded as a violation of the Second Law of Thermodynamics. The other two solutions however are completely valid; the middle solution is called the *weak solution* and the largest solution is called the *strong solution*, which one occurs in a given application is dependent on the backpressure boundary condition to which the flow exhausts, as follows.

For internal flow in a duct, if the back pressure is low enough, the weak solution will occur at a *compression corner*, while the strong solution will occur when a large back pressure is imposed on the flow. The weak OS occurs at a smaller shock angle and  $Ma_2$  is usually supersonic, while  $Ma_2$  for the strong OS is always subsonic and  $\beta$  is larger (Figure 47).

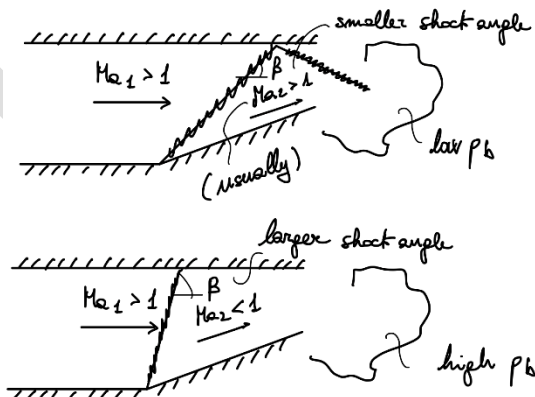


Figure 47. Weak (top) and strong (bottom) OS.

For external flow, for example supersonic flow over the sharp, wedge-shaped LE of a wing in the atmosphere, only the weave OS is found to occur, since there is no mechanism to support a large pressure difference across the OS.

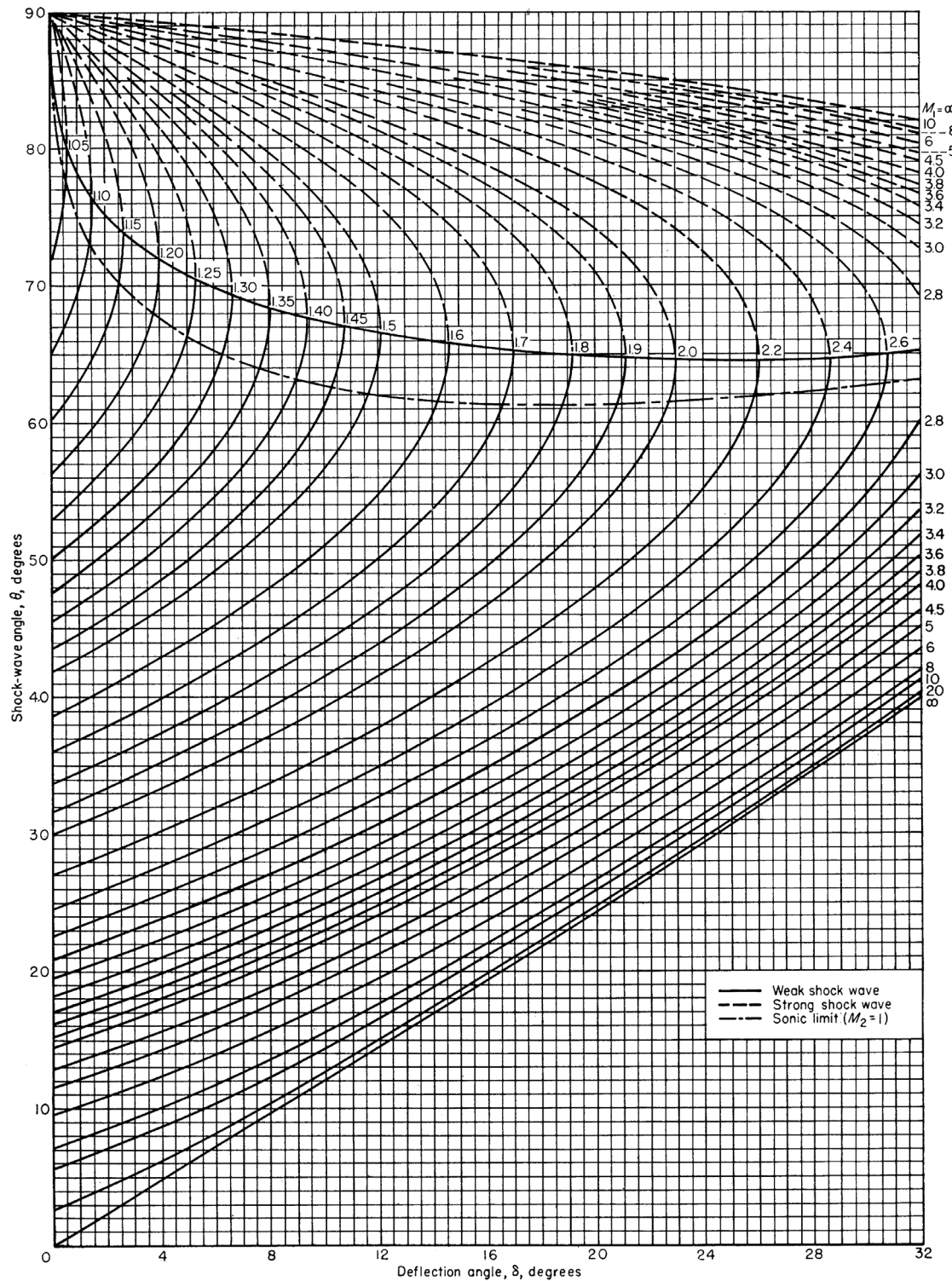


CHART 2.—Variation of shock-wave angle with flow-deflection angle for various upstream Mach numbers. Perfect gas,  $\gamma = 1.4$ .

**Figure 48. Chart 2 of NACA 1135.**

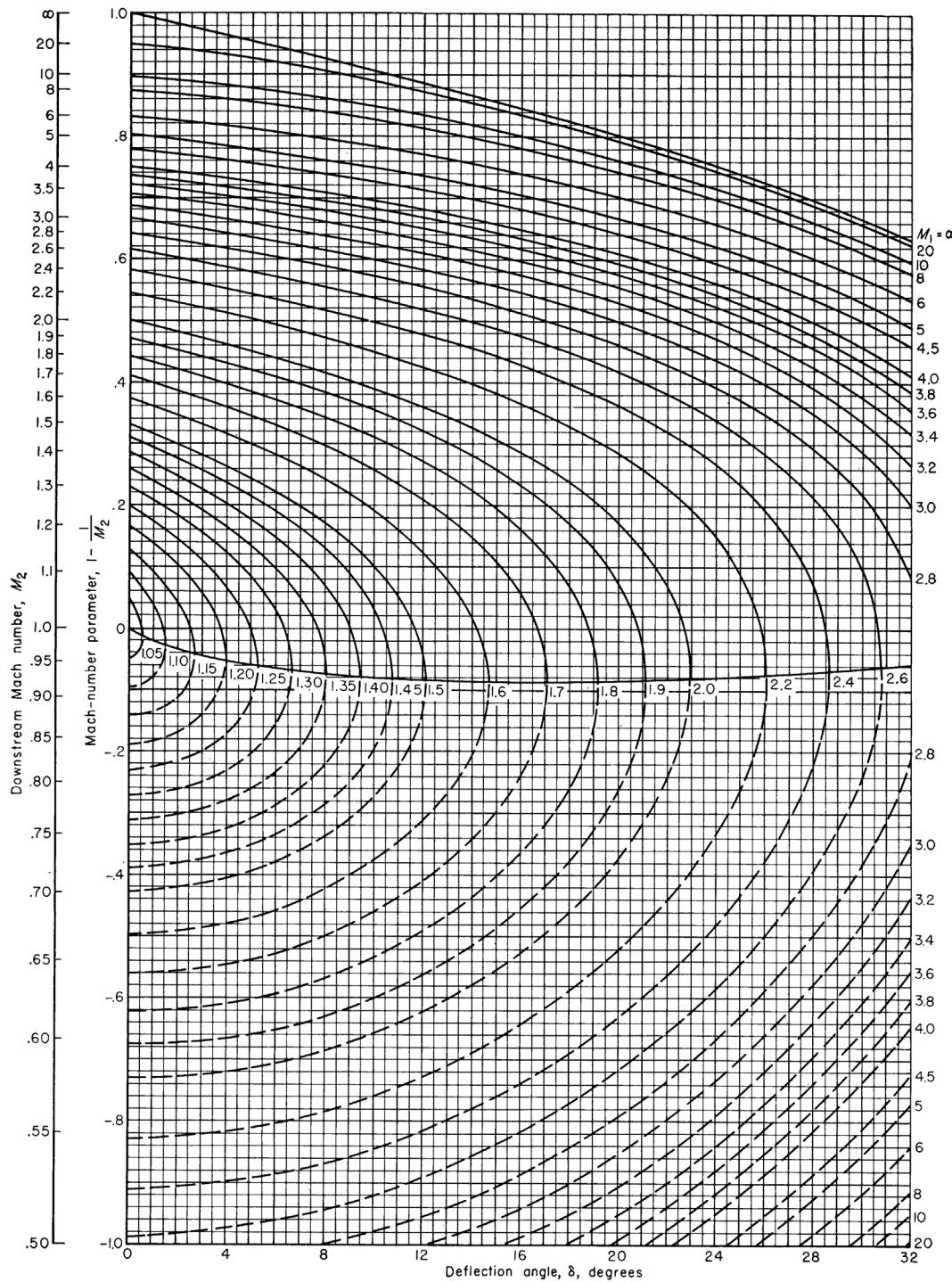


CHART 4.—Variation of Mach number downstream of a shock wave with flow-deflection angle for various upstream Mach numbers. Perfect gas,  $\gamma = 1.4$ .

**Figure 49. Chart 4 of NACA 1135.**

Now let us a look at the solution of (298). Because we have three parameters, OS solutions are usually represented graphically, rather than in a tabular form. Using graphs usually leads to approximations but software such as *vucalc* can be used to obtain accurate, quantitative answers. However, the solution graphs provide interesting information. An example solution of (298) for

$\gamma = 1.4$  can be found in Chart 2 of the NACA 1135<sup>8</sup> report (Figure 48). Note that those charts use a different nomenclature. Our streamline deflection angle  $\theta$  is  $\delta$ , while our shock angle  $\beta$  is  $\theta$  in NACA 1135.

For a given Mach number  $Ma_1$  and  $\theta$ , the solution with the larger  $\beta$  the strong solution and the solution with the smaller  $\beta$  is the weak solution. The strong solution limit at  $\theta = 0^\circ$  is the normal shock wave,  $\beta = 90^\circ$ , which implies  $Ma_2 < 1$ . The weak solution at  $\theta = 0^\circ$  is the Mach wave, such that  $Ma_1^2 \sin^2 \beta = 1$ , or  $\beta = \mu = \sin^{-1} \left( \frac{1}{Ma_1} \right)$ , where  $\mu$  is the Mach angle. Note that  $Ma_1^2 \sin^2 \beta = 1$  implies  $Ma_{1n} = 1$ , so that the pre-shock flow in weak shocks is asymptotically sonic.

Note the

Given  $Ma_1$  and  $\beta$  we can calculate  $Ma_2$  as  $Ma_2 = \sqrt{Ma_{n2}^2 + Ma_{t2}^2}$ , or alternatively  $Ma_2 = Ma_{n2}/\sin(\beta - \theta)$ . The results are plotted in Chart 4 from the NACA 1135 report. Note that there is a small range for which  $Ma_2$  for the weak solution is subsonic. Generally, however, it is supersonic.  $Ma_2$  for the strong solution instead is always subsonic. The weak solution limit  $\beta = 0^\circ$  is the Mach wave  $Ma_2 = Ma_1$ . The strong solution at  $\beta = 90^\circ$  is the normal shock at  $Ma_2 = (Ma_2)_{NS}$ .

The static and stagnation thermodynamic properties can be obtained from the NS relations (Table 1) and the IF relations (Table 5), respectively. These are summarized in Table 15 for convenience. Note that the normal component of the Mach number  $Ma_{n1} = Ma_1 \sin \beta$  must be used to obtain the static properties. Remember that stagnation properties depend on the reference frame in which they are viewed, but here we are always interested in stationary OS's (i.e., the frame relative to the wave) so we can use the IF relations in Table 5.

**Table 15. OS functions.**

$$\frac{\tan(\beta - \theta)}{\tan \beta} = 1 - \left( \frac{2}{\gamma + 1} \right) \frac{Ma_1^2 \sin^2 \beta - 1}{Ma_1^2 \sin^2 \beta} \quad (302)$$

$$p_2 = \left( \frac{p_2}{p_1} \right)_{NS, Ma_{n1}} \quad p_1 = p_1 \left[ 1 + \left( \frac{2\gamma}{\gamma + 1} \right) (Ma_1^2 \sin^2 \beta - 1) \right] \quad (303)$$

$$T_2 = \left( \frac{T_2}{T_1} \right)_{NS, Ma_{n1}} \quad T_1 = T_1 \left\{ 1 + \left[ \frac{2(\gamma - 1)}{(\gamma + 1)^2} \right] \left( \frac{Ma_1^2 \sin^2 \beta - 1}{Ma_1^2 \sin^2 \beta} \right) (\gamma Ma_1^2 \sin^2 \beta + 1) \right\} \quad (304)$$

$$p_{01} = \frac{p_1}{(p_1/p_{01})_{Ma_1}} = p_1 \left( 1 + \frac{\gamma - 1}{2} Ma_1^2 \right)^{\frac{\gamma}{\gamma - 1}} \quad (305)$$

$$T_{01} = \frac{T_1}{(T_1/T_{01})_{Ma_1}} = T_1 \left( 1 + \frac{\gamma - 1}{2} Ma_1^2 \right) \quad (306)$$

$$p_{02} = \frac{p_2}{(p_2/p_{02})_{Ma_2}} = p_2 \left( 1 + \frac{\gamma - 1}{2} Ma_2^2 \right)^{\frac{\gamma}{\gamma - 1}} \quad (307)$$

<sup>8</sup> <https://www.grc.nasa.gov/www/BGH/Images/naca1135.pdf>

$$T_{02} = \frac{T_2}{(T_2/T_{02})_{\text{Ma}_2}} = T_2 \left( 1 + \frac{\gamma - 1}{2} \text{Ma}_2^2 \right) \quad (308)$$

$$T_{02} = T_{01} \quad (309)$$

$$p_{02} = \left( \frac{p_{02}}{p_{01}} \right)_{\text{NS, Ma}_{n1}} p_{01} \quad (310)$$

Also note that here, since the flow is assumed to be steady and adiabatic, we have  $T_{02} = T_{01}$ .

Interestingly, even though it seems that it does not properly account for the conserved tangential velocity component  $p_{02}$  can be determined using equation (310), which can be argued noting that:

$$\frac{p_{02}}{p_{01}} = \frac{p_{02}/p_2}{p_{01}/p_1} \cdot \frac{p_2}{p_1} = \left( \frac{T_{02}/T_2}{T_{01}/T_1} \right)^{\frac{\gamma}{\gamma-1}} \frac{p_2}{p_1} = \frac{p_2/p_1}{(T_2/T_1)^{\frac{\gamma}{\gamma-1}}} \quad (311)$$

Since the static properties are independent of the reference frame and can be calculated from the NS relations at  $\text{Ma}_{n1}$ ,  $p_{02}/p_{01}$  can too.

Note that in each of the solution graphs, Chart 2 (Figure 48) and Chart 4 (Figure 49), in addition to the possibility of two solutions for weak and strong waves, there is the possibility of *no solutions*, for  $\theta > \theta_{\max}$ . That is, for a given value of  $\text{Ma}_1$ , there is a maximum value of the turning angle  $\theta$ , that can be accommodated. Conversely, this may be interpreted that for a given value of  $\theta$ , that is a minimum initial Mach number,  $\text{Ma}_1$ , that is possible. The line in Charts 2 and 4 separating the weak and strong solutions is the locus of these  $\theta_{\max}$ 's (or  $\text{Ma}_{\min}$ 's). For  $\gamma = 1.4$ ,  $\theta_{\max} = 45.6^\circ$ .

For turning angles  $\theta > \theta_{\max}$  the shock becomes detached (Figure 50). For detached OS, the wave is normal along the stagnation line and it curved away to become a Mach wave far from the body. Near the tip, where the shock is strong, the flow behind the shock is subsonic while it is supersonic further back along with the body. This renders a complicated, 2D, mixed subsonic/supersonic flowfield.

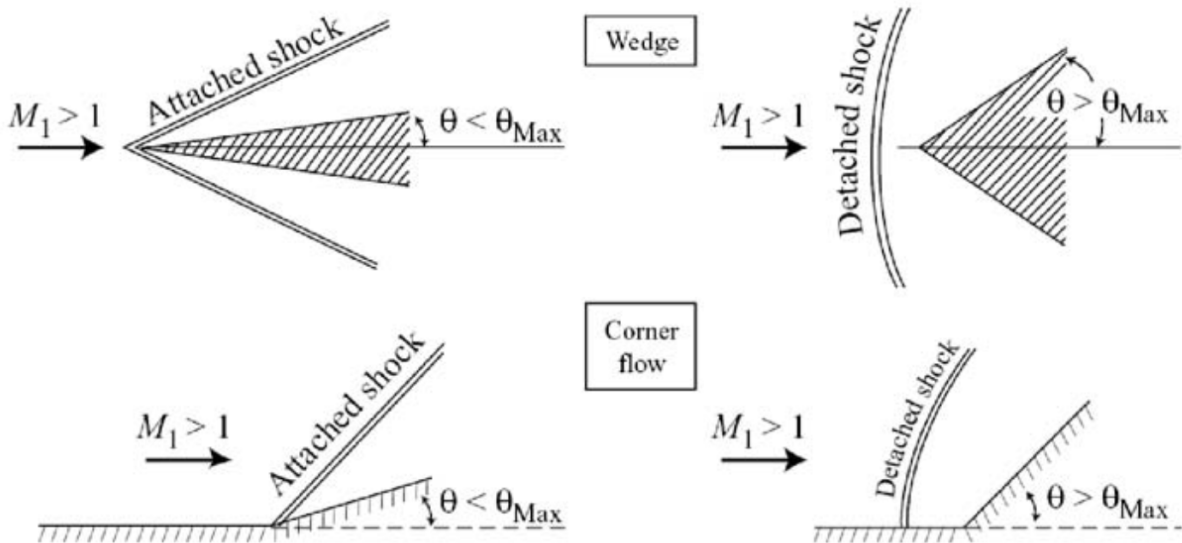


**Figure 50. Attached and detached shocks.**

### Oblique Shock Wave Reflections

We will consider two cases: (1) an OS impinging on a plane (straight) wall and (2) an OS impinging on a constant-pressure boundary.

#### 7.3.2 Reflection from a Plane Wall

A weak oblique shock is generated at the upper compression corner since the flow must be turned downward through the angle  $\theta$  (Figure 51). Thus, the streamlines in region 2 are directed downward at an angle  $\theta$  from the horizontal. Since we cannot have the flow penetrating through the lower plane wall, a reflected wave must be generated at the lower wall to turn the flow back to the horizontal (i.e., through angle  $\theta$ ). Is this wave an OS or a series of reversible P-M expansion waves? Looking at the sketch, we see that the wave must turn the flow toward the reflected wave and away from the normal, i.e., turn the flow into itself. Therefore, the normal velocity component is smaller with the tangential component unchanged, that is *the reflected wave is an oblique shock*.

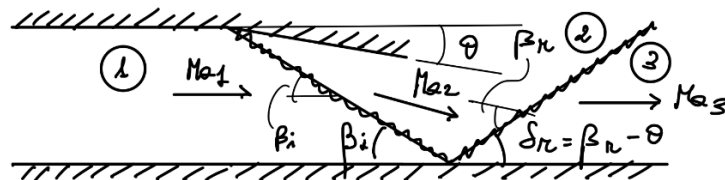


**Figure 51. Oblique shock waves reflect from solid boundaries as oblique shock waves.**

Note that (different than light waves that would have  $\beta_i = \delta_r$ ) here the boundary conditions that are enforced are the turning angles ( $\theta_{12} = \theta_{23}$ ). In fact, since  $Ma_2 < Ma_1$  and the turning angles are the same,  $\theta_{12} = \theta_{23}$ , we must have  $\beta_r = \delta_r + \theta > \beta_i$ .

### 7.3.3 Reflection from a Constant Pressure Boundary

Now suppose we have a flow from a perfectly expanded CD nozzle ( $Ma_1 > 1, p_1 = p_b$ ) impinge on a lower compression corner that generates an OS (Figure 52). The OS turns the flow up for a little bit lower wall and impinges on the constant pressure jet boundary. In this case, a wave or series of waves must be generated at the intersection of the shock and the jet boundary to satisfy that condition that the boundary pressure remains constant at  $p_b$ . Again, is this wave an OS or a series of reversible P-M expansion waves? Since the static pressure is increased across the incident shock  $p_2 > p_b$ . Therefore, the reflected wave must decrease the pressure such that  $p_3 = p_b$ , that is the reflected waves are PM expansion waves. These turn the flow toward the normal and away from the waves, since the normal velocity component is increased. In other words, the floor is turned away from itself.

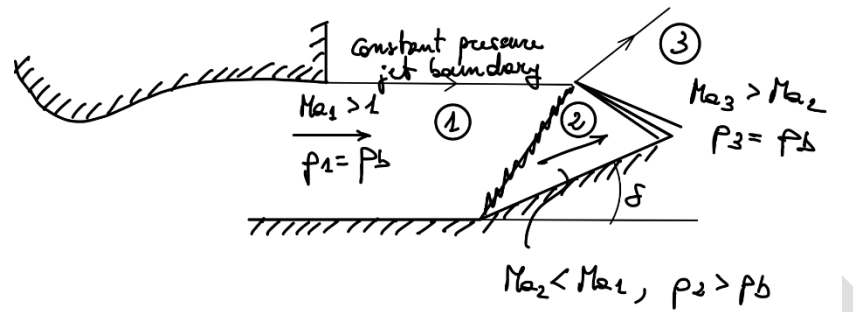


**Figure 52. Oblique shock waves reflect from constant boundaries as PM expansion waves.**

In summary, like for NS wave, OS waves reflect from solid boundaries as OS waves and from constant pressure boundaries as a series of PM expansion waves.

For an oblique shock reflection at the plane wall, the required tuning angle  $\theta < \theta_{\max}$  for  $Ma_2$  of the reflected wave may be too large for a solution to exist. In this case, rather than having a regular reflection, such as that sketched in Figure 51, a Mach reflection will occur (Figure 53). At the wall the shock curves no since we cannot have flow penetrating (nor separating) from the wall. The flow behind this part of the wave is subsonic while that behind the upper two weak oblique shocks is supersonic.

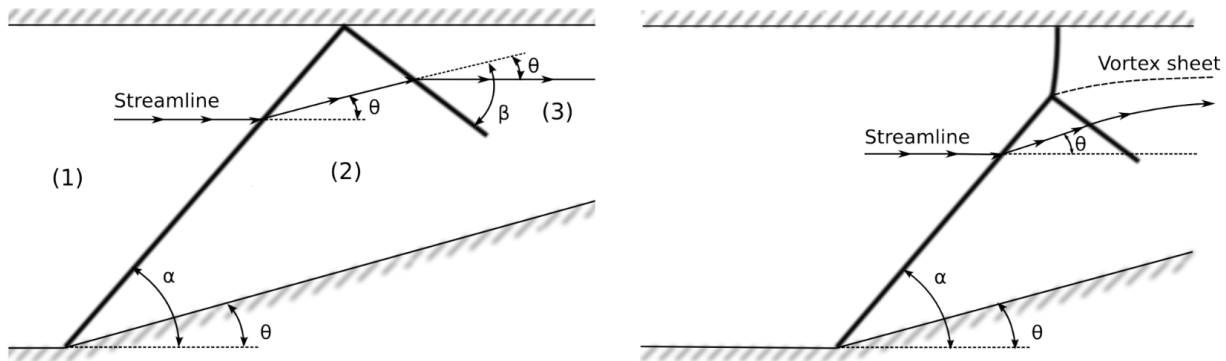


**Figure 53. Regular reflection (left) and Mach reflection (right) off of a solid wall boundary (from Schwer, 2008).**

This renders a complicated, 2D, mixed subsonic/supersonic flowfield. Note that in a real viscous flow this flowfield would be further complicated by the shock wave/boundary layer interaction.

#### 7.4 Conical Shock Waves

For a right, circular cone immersed at zero angle of attack in a uniform supersonic flow a straight conical oblique shock is generated, as for the wedge, although at a different shock angle  $\beta$ . However, unlike the 2D planar wedge case, the flow behind the conical shock is not uniform, but rather the streamlines are curved, and the flow properties vary with the spherical angle  $\theta$ , i.e. from ray to ray traced from the cone vertex. The conical shock turns the flow only part of the way parallel to the cone surface with additional turning behind a wave. Since the flow is multi-dimensional, the solution involves using the governing multi-dimensional partial differential equations (PDEs) to two coupled ordinary differential equations (ODEs) in the spherical angle  $\theta$ . The details of this derivation are covered in more advanced courses. However, it is interesting to look at the characteristics of the solution, which is shown in Chart 5 (Figure 54), Chart 6 (Figure 55) and Chart 7 (Figure 56) of NACA 1135, for  $\gamma = 1.4$ . Note that there is no straightforward calculator like *vucalc* for cones. Chart 5 gives the shock angle  $\beta = \beta(\text{Ma}_1, \theta_c)$ , where  $\theta_c$  is the cone half-angle (again, careful with the nomenclature here, our shock angle  $\beta$  is  $\theta$  in the chart, while our cone half-angle  $\theta_c$  is  $\sigma$  in the chart).

Chart 6 gives the shock surface pressure coefficient  $C_p = C_p(\text{Ma}_1, \theta_c)$ , where:

$$C_p = \frac{p_c - p_1}{q_1} = \frac{p_c - p_1}{\frac{1}{2} \rho_1 U_1^2} = \frac{p_c/p_1 - 1}{\frac{1}{2} \gamma \frac{\rho_1 U_1^2}{p_1}} = \frac{p_c/p_1 - 1}{\frac{1}{2} \gamma \text{Ma}_1^2} \quad (312)$$

Chart 7 gives the cone surface Mach number  $\text{Ma}_c = \text{Ma}_c(\text{Ma}_1, \theta_c)$ .

Even though weak and strong solution are possible for conical shocks, only the weak solution is plotted since the usual application is for external flows.

The flow properties immediately behind the conical shock can be determined as for a planar OS analysis, i.e., using NS relations evaluated at  $\text{Ma}_{n1} = \text{Ma}_1 \sin \beta$ . However, additional compression of the flow occurs between the shock and the cone surface. The flow everywhere behind the shock is isentropic.

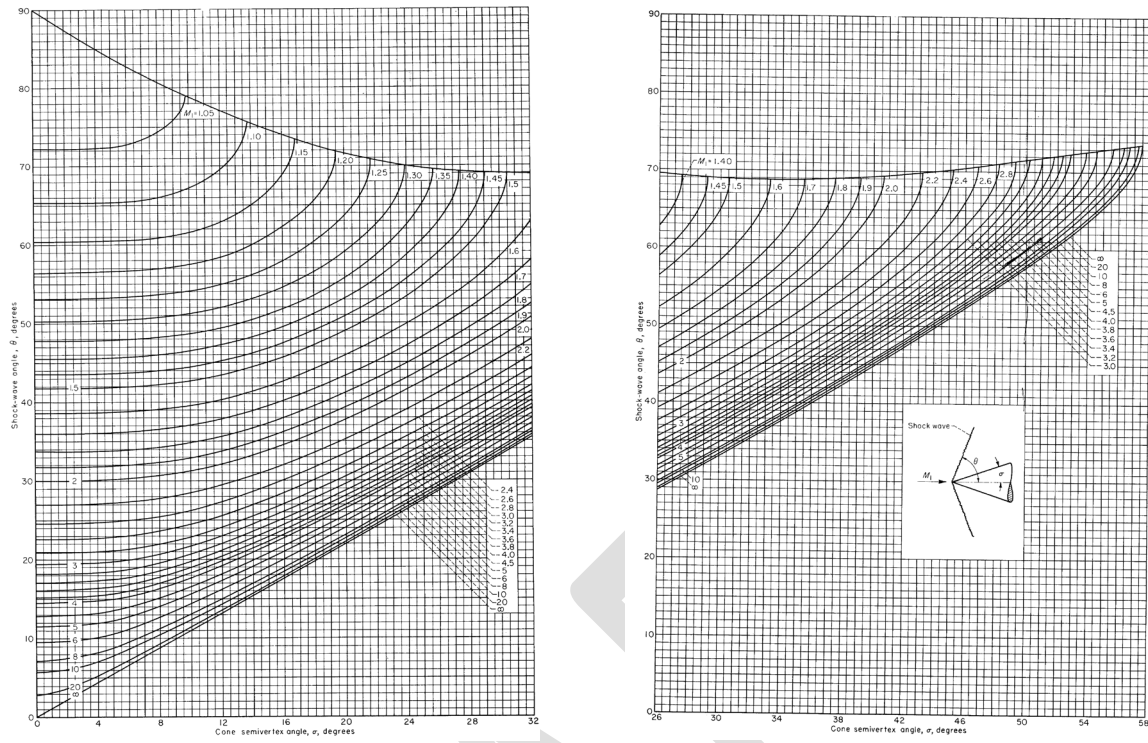


Figure 54. Chart 5 of NACA 1135.

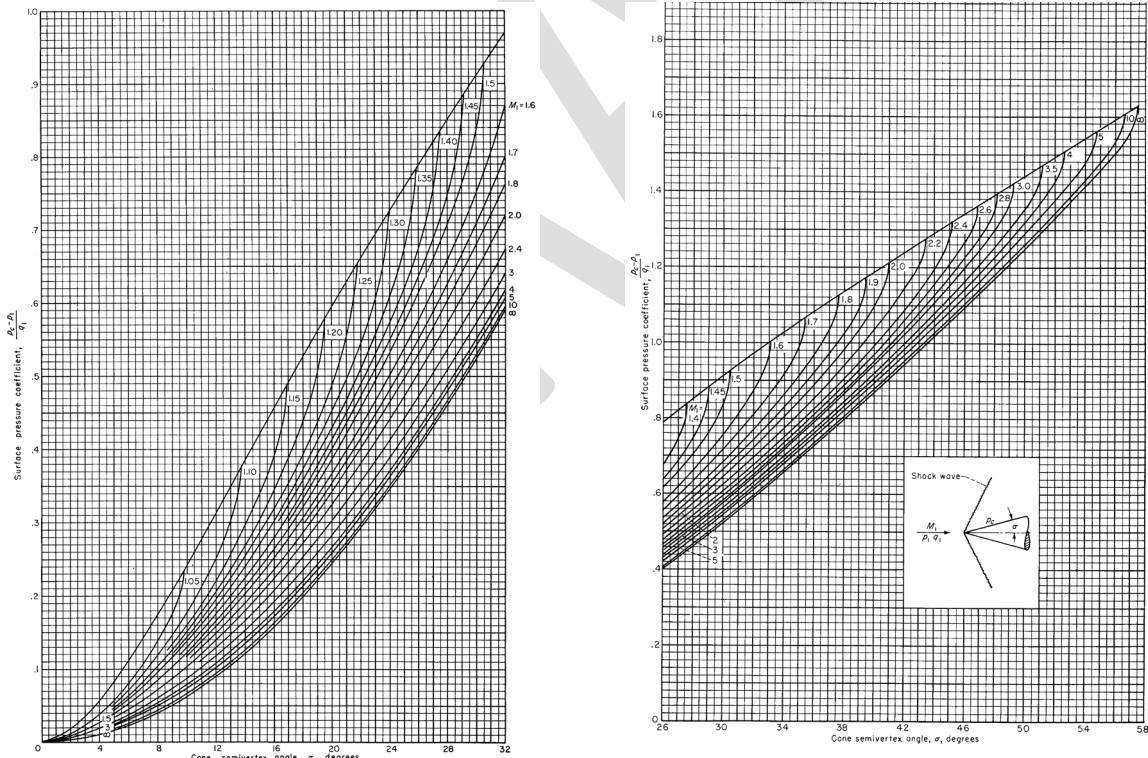


Figure 55. Chart 6 of NACA 1135.

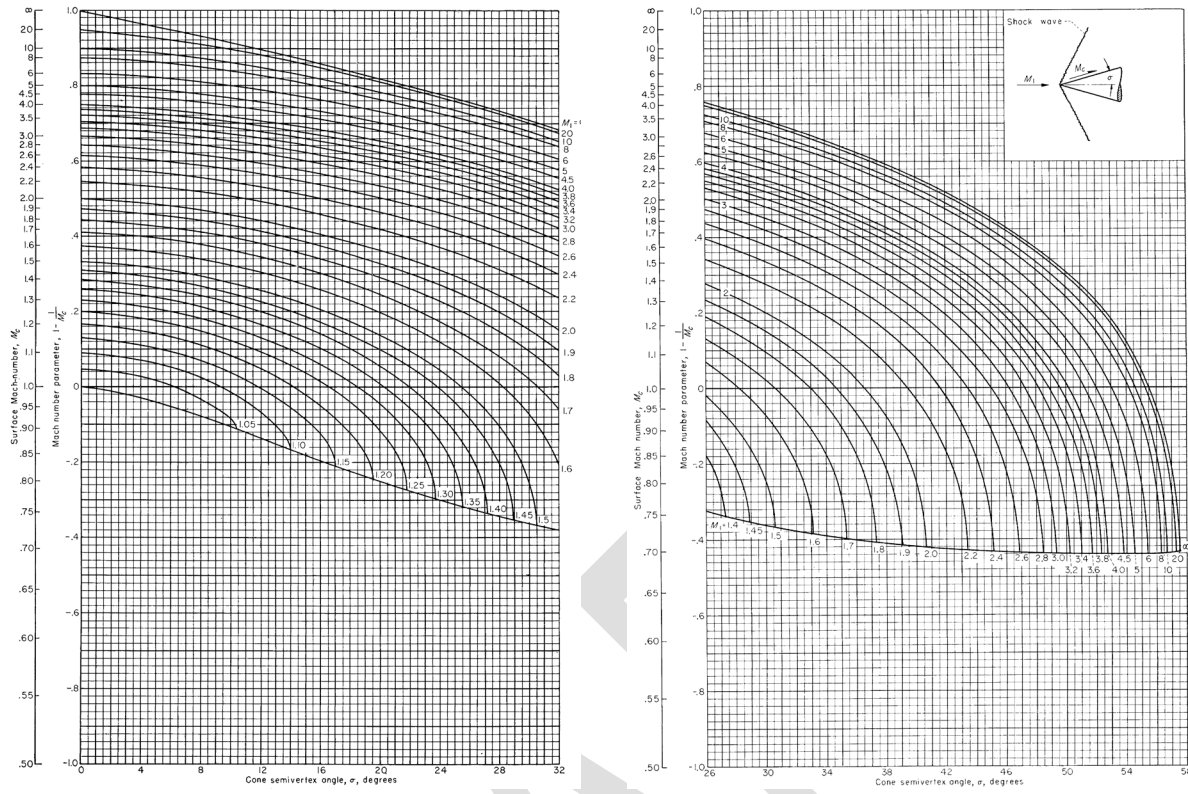


Figure 56. Chart 7 of NACA 1135.

For a given value of  $Ma_1$ , there is maximum value  $\theta_{c,\max}$  above which the conical shock is detached. However, for a given value of  $Ma_1$ ,  $\theta_{c,\max} > \theta_{w,\max}$  (with the subscript  $w$  referring to the wedge), i.e.,  $\theta_{\max,3D} > \theta_{\max,2D}$ . For given values of  $Ma_1$  and  $\theta_c$ , the shock angle for the cone is less than that of the wedge, i.e.  $\beta_c < \beta_w$  or  $\beta_{3D} < \beta_{2D}$ . Thus, conical shocks are weaker, with lower surface static pressure, static temperature, and stagnation pressure loss for the cone than for the wedge. This is the result of a three-dimensional relief effect available to the cone, i.e., the cone presents a smaller obstruction to the flow than a wedge at the same Mach number and aperture angle. For the cone, the flow can “slip around the sides” of the cone in the third dimension while this relieve is not available to the wedge.

## 8 Prandtl-Meyer Expansions

### 8.1 Introduction

In section 7 we analyzed the flowfield that occurs at a (concave) compression corner in supersonic planar flow and found that the adjustment to the required change in flow direction occurs via a finite OS wave. Now the question arises as to what occurs when a supersonic flow must adjust to the changes in flow direction imposed by a convex corner (Figure 57), *i.e.*, when the flow turns away from itself.

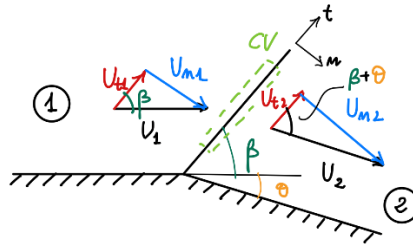


Figure 57. Supersonic flow around convex corner.

Assuming that the adjustment occurs by means of a single finite wave, we can write the governing equations just as we did for the oblique shock and obtain:

$$\text{Continuity: } \varepsilon_\rho + \varepsilon_{U_n} + \varepsilon_\rho \varepsilon_{U_n} = 0 \quad (313)$$

$$n\text{-Momentum: } \varepsilon_p + \gamma Ma_{n1}^2 \varepsilon_{U_n} = 0 \quad (314)$$

$$t\text{-Momentum: } \varepsilon_{U_t} = 0 \text{ or } U_{t1} = U_{t2} \quad (315)$$

$$\text{Energy: } \varepsilon_T + \left(\frac{\gamma-1}{2}\right) Ma_{n1}^2 (2\varepsilon_{U_n} + \varepsilon_{U_n}^2) = 0 \quad (316)$$

From the geometry of the velocity triangles in Figure 57 ( $U_{n1} = U_{t1} \tan \beta$ ,  $U_{n2} = U_{t2} \tan(\beta + \theta)$ ) and with (315), we see that  $U_{n2} > U_{n1}$ , *i.e.*,  $\varepsilon_{U_n} > 0$ . Then from (314) we see that  $\varepsilon_p < 0$ , *i.e.*,  $p_2 < p_1$ . Therefore, the adjustment must occur through and *expansion*. However, the adjustment cannot be through a finite expansion oblique shock, since we know that the normal velocity component satisfies the normal shock equation, and a finite expansion NS was found to violate the Second Law of Thermodynamics (cf. section 2.2.2). Thus, the adjustment must be by some other means.

Consider now a supersonic flow encountering an infinitesimal change in direction  $dv$  (Figure 58), either expansive or compressive. A wave will be generated at the corner in order that the flow adapts to the corner itself. Let us analyze this flow. Since the changes in flow properties must be infinitesimal (differential) across this infinitesimal turn, we can linearize our governing equations, *i.e.*, drop all the H.O.T. and obtain:

$$\text{Continuity: } \varepsilon_\rho + \varepsilon_{U_n} = 0 \quad (317)$$

$$n\text{-Momentum: } \varepsilon_p + \gamma Ma_{n1}^2 \varepsilon_{U_n} = 0 \quad (318)$$

$$t\text{-Momentum: } \varepsilon_{U_t} = 0 \text{ or } U_{t1} = U_{t2} \quad (319)$$

$$\text{Energy: } \varepsilon_T + \left(\frac{\gamma-1}{2}\right) Ma_{n1}^2 (2\varepsilon_{U_n} + \varepsilon_{U_n}^2) = 0 \quad (320)$$

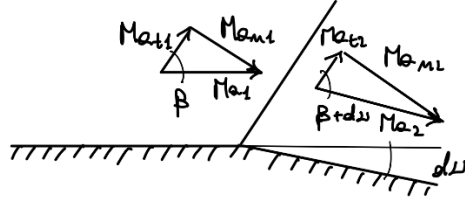


**Figure 58. Supersonic flow encountering an infinitesimal change in direction.**

These are exactly the weak wave equations that we have derived in section 2.2.3, with  $Ma_{n1}$  instead substituted for  $Ma_1$ . They are a set of four simultaneous, linear, homogeneous, algebraic equations in the unknown  $\varepsilon_p$ ,  $\varepsilon_{U_n}$ ,  $\varepsilon_T$ ,  $\varepsilon_{T_n}$ . In order to obtain a non-trivial solution to this set, we reduce the rank of the coefficient matrix, *i.e.*, set the determinant of the coefficient matrix to zero, which results in  $Ma_{n1} = 1$ . Recall that we had obtained  $Ma_1 = 1$  when we analyzed weak NS in section 2.2.3. So, what kind of wave is this? Drawing a velocity triangle, we realize that:

$$\sin \beta = \frac{Ma_{n1}}{Ma_1} = \frac{1}{Ma_1} \Rightarrow \beta = \sin^{-1} \left( \frac{1}{Ma_1} \right) = \mu \quad (321)$$

which is just the relation for the Mach angle found in (272). So the wave generated at this infinitesimal turn is a Mach wave, as we should have guessed.

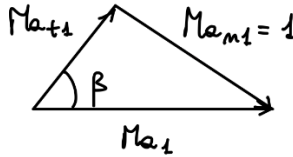


**Figure 59. Velocity triangle with unit normal Mach number.**

We can easily show that the flow through a Mach wave is isentropic:

Now let us look at the entropy change across weak waves. Using (21):

$$\begin{aligned} Tds = dh - \frac{dp}{\rho} \Rightarrow ds = c_p \frac{dT}{T} - \frac{dp}{\rho T} = c_p \frac{dT}{T} - R \frac{dp}{p} \\ \Rightarrow \frac{ds}{c_p} = \varepsilon_T - \left( \frac{\gamma - 1}{\gamma} \right) \varepsilon_p \end{aligned} \quad (322)$$

Using energy (320) and the  $n$ -momentum (318), (322) becomes:

$$\begin{aligned} \frac{ds}{c_p} = \varepsilon_T - \left( \frac{\gamma - 1}{\gamma} \right) \varepsilon_p \Rightarrow \frac{ds}{c_p} = -(\gamma - 1) Ma_{n1}^2 \varepsilon_{U_n} - \left( \frac{\gamma - 1}{\gamma} \right) (-\gamma Ma_{n1}^2 \varepsilon_{U_n}) = 0 \\ \Rightarrow \frac{ds}{c_p} = 0 \end{aligned} \quad (323)$$

The therefore either compression or expansion Mach waves are possible since they are isentropic and therefore satisfy the Second Law of Thermodynamics  $\Delta s \geq 0$ .

Now consider a series of expansions generated by a series of infinitesimal convex turns (Figure 60). In this case an infinitesimal expansion Mach wave is generated at each corner. However, the Mach waves will not interact with and reinforce each other to form a finite expansion wave for

two reasons: 1) the Mach angle is decreased across the waves and 2) the wall is turned down. Instead, they spread out and diverge. Since the flow across each infinitesimal Mach wave is isentropic and since it is uniform and isentropic between each wave, the distance between each turn is unimportant, and we could just as well have an expansion through a sharp corner of finite turning angle, i.e., we can use linear superposition of infinitesimal Mach waves to analyze finite expansion fans.

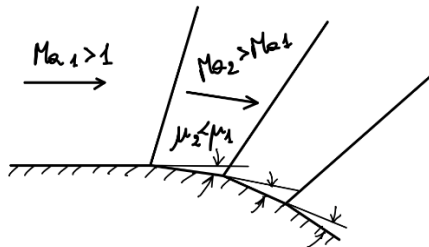


**Figure 60. Series of expansions generated by a series of infinitesimal convex turns.**

Therefore, supersonic flow adjusts to an expansion turn (either centered or non-centered) by means of a series of reversible (isentropic) expansion waves. The first and last waves are inclined and the local Mach angle to the local flow direction. The thermodynamic properties upstream and downstream of the waves are related entropy. These are Prandtl-Meyer (PM) expansions.

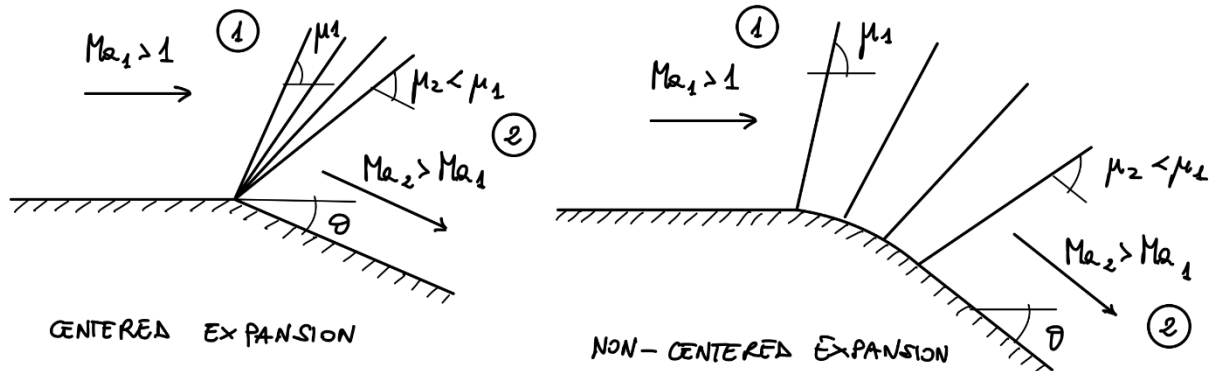


**Figure 61. Centered and non-centered PM expansion.**

## 8.2 Analysis

As described above, we already know quite a bit qualitatively and quantitatively about PM expansion waves. But there is one key piece that we are missing. We need to relate the angle  $\nu$  (finite, driving potential) to the Mach number.

Consider a single Mach wave expanding supersonic flow through an infinitesimal turning angle,  $dv$  (Figure 62). Using the  $\varepsilon$  notation for differential changes, i.e.,  $\varepsilon_\alpha = d\alpha/\alpha$ , by tangential momentum we have:  $\varepsilon_{U_t} = 0$ . Therefore, from the velocity triangles:

$$U \cos \mu = U(1 + \varepsilon_U) \cos(\mu + dv) \Rightarrow \cos \mu = (1 + \varepsilon_U)(\cos \mu \cos dv - \sin \mu \sin dv) \quad (324)$$

For infinitesimal  $dv$ :  $\sin dv \approx dv$  and  $\cos dv \approx 1$ , therefore (324) yields

$$\cos \mu = (1 + \varepsilon_U)(\cos \mu - \sin \mu dv) \Rightarrow \quad (325)$$

$$\Rightarrow \cos \mu = \cos \mu - \sin \mu dv + \varepsilon_U \cos \mu - \varepsilon_U \sin \mu dv$$

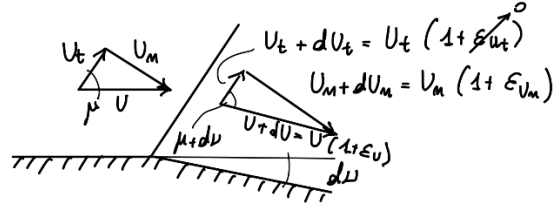


**Figure 62. Mach wave expanding through an infinitesimal turning angle.**

Here  $\varepsilon_U \sin \mu dv = \frac{dU}{U} \sin \mu dv$  is an H.O.T and can be neglected, therefore

$$\varepsilon_U = \tan \mu dv \quad (326)$$

To relate  $\tan \mu$  to  $Ma$ , we use the definition of the Mach angle:

$$\sin \mu = \frac{1}{Ma} \Rightarrow \tan \mu = \frac{1}{\sqrt{Ma^2 - 1}} \quad (327)$$

Combining (326) and (327):

$$\varepsilon_U = \tan \mu dv = \frac{dv}{\sqrt{Ma^2 - 1}} \quad (328)$$

So now if we would have an expression for  $\varepsilon_U = \frac{dU}{U}$  in terms of  $Ma$ , we would have  $dv$  in terms of  $Ma$  and could integrate. To obtain this, we use the definition of Mach number:

$$U^2 = Ma^2 (\gamma RT) \Rightarrow \ln U^2 = 2 \ln U = \ln Ma^2 + \ln \gamma R + \ln T \quad (329)$$

and differentiate to obtain:

$$2 \frac{dU}{U} = \frac{dMa^2}{Ma^2} + \frac{dT}{T} \Rightarrow \frac{dU}{U} = \frac{1}{2} \frac{dMa^2}{Ma^2} + \frac{1}{2} \frac{dT}{T} \quad (330)$$

Now we have introduced  $\frac{dT}{T}$ , which we can obtain as a function of the Mach number, because the flow is adiabatic (stagnation temperature is constant):

$$T_0 = \left(1 + \frac{\gamma - 1}{2} Ma^2\right) T = \text{const.} \Rightarrow \ln T_0 = \ln T + \ln \left(1 + \frac{\gamma - 1}{2} Ma^2\right) \quad (331)$$

Differentiating:

$$\frac{dT_0}{T_0} = \frac{dT}{T} + \frac{\frac{\gamma - 1}{2} Ma^2}{\left(1 + \frac{\gamma - 1}{2} Ma^2\right)} \frac{dMa^2}{Ma^2} = 0 \quad (332)$$

or

$$\frac{dT}{T} = -\frac{\frac{\gamma-1}{2} Ma^2}{\left(1 + \frac{\gamma-1}{2} Ma^2\right)} \frac{dMa^2}{Ma^2} = 0 \quad (333)$$

Finally, substituting (333) into (330), and then back into (328) we have:

$$dv = \frac{\sqrt{Ma^2 - 1}}{2Ma^2 \left(1 + \frac{\gamma-1}{2} Ma^2\right)} dMa^2 \quad (334)$$

We can now integrate this equation to find a relationship between the finite turning angle  $v$  and the Mach number. Integrating between a reference state where  $v = 0$  and  $Ma^2 = 1$  to a general state where  $v = v$  and  $Ma^2 = Ma^2$ :

$$\int_0^v dv = \int_1^{Ma^2} \frac{\sqrt{Ma^2 - 1}}{2Ma^2 \left(1 + \frac{\gamma-1}{2} Ma^2\right)} dMa^2 \quad (335)$$

which leads to:

$$v(\gamma, Ma) = \left(\frac{\gamma+1}{\gamma-1}\right)^{\frac{1}{2}} \tan^{-1} \left[ \frac{\gamma-1}{\gamma+1} (Ma^2 - 1) \right]^{\frac{1}{2}} - \tan^{-1} (Ma^2 - 1)^{\frac{1}{2}} \quad (336)$$

This is the key gas dynamic function for PM flow because it relates the driving potential  $v$  to the Mach number variation. With this reference state, we see that the physical interpretation of the turning angle or Prandtl-Meyer angle  $v$  is that it is the angle through which a sonic ( $Ma = 1$ ) flow must be turned to reach supersonic Mach number ( $Ma > 1$ ). To find the turning angle through which a supersonic flow at  $Ma_1 > 1$  must be turned to reach supersonic Mach number  $Ma_2 > Ma_1 > 1$ , we simply take the difference in the PM angles  $v_2 - v_1$ , since the reference state drops out. Mathematically:

$$\begin{aligned} \int_{v_1}^{v_2} dv &= v_2 - v_1 = \theta = \int_{Ma_1^2}^{Ma_2^2} \dots dMa^2 = \int_{Ma_1^2}^1 \dots dMa^2 + \int_1^{Ma_2^2} \dots dMa^2 \\ &= \int_1^{Ma_2^2} \dots dMa^2 - \int_1^{Ma_1^2} \dots dMa^2 = v(\gamma, Ma_2) - v(\gamma, Ma_1) \end{aligned} \quad (337)$$

or

$$\begin{aligned} v_2 - v_1 &= \theta = \\ &= \left(\frac{\gamma+1}{\gamma-1}\right)^{\frac{1}{2}} \tan^{-1} \left[ \frac{\gamma-1}{\gamma+1} (Ma_2^2 - 1) \right]^{\frac{1}{2}} - \tan^{-1} (Ma_2^2 - 1)^{\frac{1}{2}} \\ &\quad - \left(\frac{\gamma+1}{\gamma-1}\right)^{\frac{1}{2}} \tan^{-1} \left[ \frac{\gamma-1}{\gamma+1} (Ma_1^2 - 1) \right]^{\frac{1}{2}} - \tan^{-1} (Ma_1^2 - 1)^{\frac{1}{2}} \end{aligned} \quad (338)$$

This is a key relation to solve PM expansion. Note that for the thermodynamic properties, since the flow through the PM expansion is isentropic, we can use the IF relations in Table 5, which are summarized in Table 16 for convenience.

**Table 16. PM functions.**

$$\nu_2 - \nu_1 = \theta \quad (339)$$

$$\nu(\gamma, \text{Ma}) = \left( \frac{\gamma + 1}{\gamma - 1} \right)^{\frac{1}{2}} \tan^{-1} \left[ \frac{\gamma - 1}{\gamma + 1} (\text{Ma}^2 - 1) \right]^{\frac{1}{2}} - \tan^{-1} (\text{Ma}^2 - 1)^{\frac{1}{2}} \quad (340)$$

$$p_{01} = p_{02} \quad (341)$$

$$T_{02} = T_{01} \quad (342)$$

$$\frac{p_2}{p_1} = \frac{(p_2/p_{02})_{\text{IF}}}{(p_1/p_{01})_{\text{IF}}} = \frac{\left(1 + \frac{\gamma - 1}{2} \text{Ma}_1^2\right)^{\frac{\gamma}{\gamma-1}}}{\left(1 + \frac{\gamma - 1}{2} \text{Ma}_2^2\right)^{\frac{\gamma}{\gamma-1}}} \quad (343)$$

$$\frac{T_2}{T_1} = \frac{(T_2/T_{02})_{\text{IF}}}{(T_1/T_{01})_{\text{IF}}} = \frac{1 + \frac{\gamma - 1}{2} \text{Ma}_1^2}{1 + \frac{\gamma - 1}{2} \text{Ma}_2^2} \quad (344)$$

The PM angle  $\nu$  and the Mach angle  $\mu$  are tabulated as a function of the Mach number for  $\gamma = 1.4$  in the NACA 1135 report. The *vucalc* software also has the two angles as output (or input) parameter for supersonic Mach number in the “isentropic flow” tab for any value of the adiabatic coefficient. In all cases entries are in degrees.

### 8.3 Maximum Turning Angle for Prandtl-Meyer Flow

Let us now look at the limit as  $\text{Ma} \rightarrow \infty$  of the PM angle  $\nu$ . From (336):

$$\begin{aligned} \lim_{\text{Ma} \rightarrow \infty} \nu &= \lim_{\text{Ma} \rightarrow \infty} \left\{ \left( \frac{\gamma + 1}{\gamma - 1} \right)^{\frac{1}{2}} \tan^{-1} \left[ \frac{\gamma - 1}{\gamma + 1} (\text{Ma}^2 - 1) \right]^{\frac{1}{2}} - \tan^{-1} (\text{Ma}^2 - 1)^{\frac{1}{2}} \right\} \\ &= \left( \frac{\gamma + 1}{\gamma - 1} \right)^{\frac{1}{2}} \tan^{-1}(\infty) - \tan^{-1}(\infty) = \left( \frac{\gamma + 1}{\gamma - 1} \right)^{\frac{1}{2}} 90^\circ - 90^\circ \\ &= \left[ \left( \frac{\gamma + 1}{\gamma - 1} \right)^{\frac{1}{2}} - 1 \right] 90^\circ = (130.45^\circ \text{ for } \gamma = 1.4) \end{aligned} \quad (345)$$

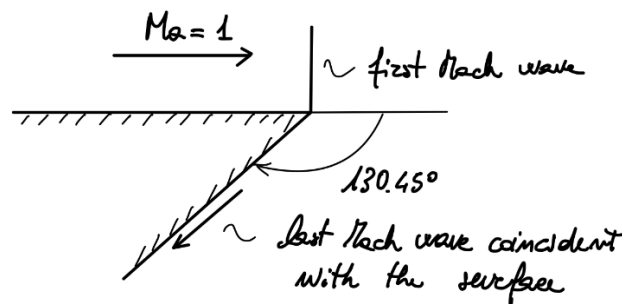


**Figure 63. Mach wave expanding through an infinitesimal turning angle.**

Therefore, theoretically, a sonic flow can be turned through a  $\sim 130^\circ$  before  $Ma \rightarrow \infty$  is reached at which point  $p$  and  $T$  approach absolute zero. However, from a practical standpoint, this can never be achieved because as absolute zero  $p$  and  $T$  are approached, the ideal gas assumption is definitely no longer valid. Also, in real viscous flow, separation will occur at least local near the corner. While an academic limit, this does point to the very large angles through which supersonic flows can expand when exposed to very low pressures.

#### 8.4 Reflections of Expansion Waves

Similar to what we have done earlier, we will consider two cases, that of reflections from plane straight walls and that of reflection from constant pressure boundaries. Note that, opposite to OS waves, PM expansion waves turn the flow toward the normal and away from the waves.

##### 8.4.1 Reflection from a Plane Wall

The supersonic approach flow at  $Ma_1 > 1$  is expanded at the upper corner by PM expansion waves to  $Ma_2 > Ma_1 > 1$  such that the flow is parallel to the upper boundary. However, at the lower boundary the flow must be turned back horizontal because the flow cannot separate from the lower wall nor penetrate it. Because the turn at the lower wall is an expansion turn (the flow turns away from itself toward normal and away from waves), we see that expansion waves reflect as expansion waves. However, in the reflection region, the expansion waves are not centered, making the analysis more difficult. Region ③ is still uniform (easy to find), but we are not exactly sure where the reflected waves are.

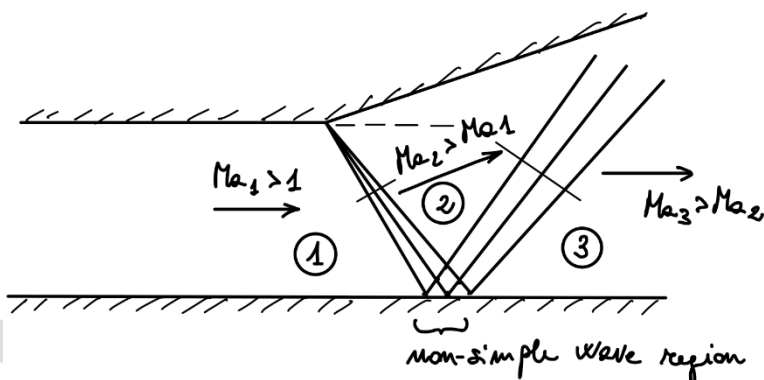
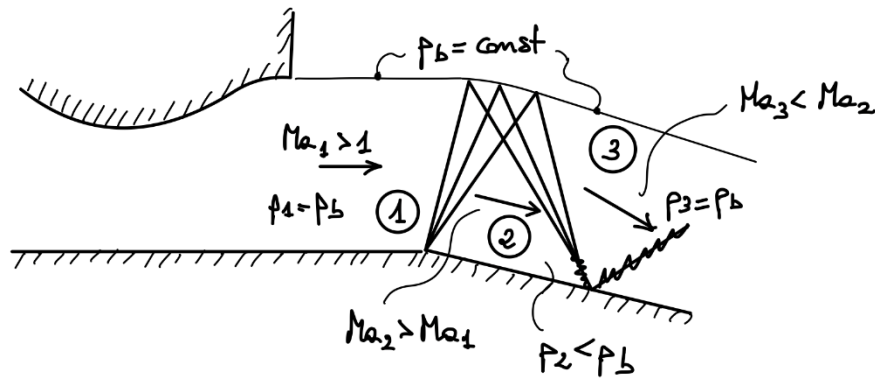


Figure 64. Prandtl-Meyer Expansions reflect from solid boundaries as expansion waves.

##### 8.4.2 Reflection from a Constant Pressure Boundary

The supersonic approach flow at  $Ma_1 > 1$  is expanded at the lower corner by PM expansion waves to  $Ma_2 > Ma_1 > 1$ ,  $p_2 < p_1 = p_b$  such that the flow is parallel to the lower boundary. However, because the boundary of the jet must be maintained at  $p_b = \text{const.}$ , and since the pressure in region ② is smaller than  $p_b$ , the expansion waves reflect at the constant pressure boundary as compression waves to return the pressure in region ③ to  $p_b$ . These reflected compression waves will eventually coalesce to form a finite oblique shock. Again, such flow features require a complicated analysis which is beyond scope here.

In summary, PM expansion waves reflect from solid boundaries as expansion waves and from constant pressure boundaries as compression waves.



**Figure 65. Prandtl-Meyer Expansions reflect from constant pressure boundaries as compression waves.**

## 8.5 Applications of Two-Dimensional Supersonic Flow

In this section we analyzed notable applications of 2D supersonic flows, involving both OS waves and PM expansion waves.

### 8.5.1 Supersonic Inlets

The purpose of supersonic inlets, also called external compression inlets is to efficiently (i.e., with high stagnation pressure recovery) diffuse supersonic flow to subsonic conditions for the compressor of a turbofan or turbojet engine.

It can be shown that a fixed-geometry converging-diverging diffuser for external supersonic flow is impractical (at least at very large Mach numbers) because startup requires overspeeding or a variable area throat. The startup problem can be eliminated by removing the internal throat, such as in the constant area NS or Pitot inlet (or by using variable area). However, a NS at the design Mach number entails a large loss in stagnation pressure except at transonic flight conditions.

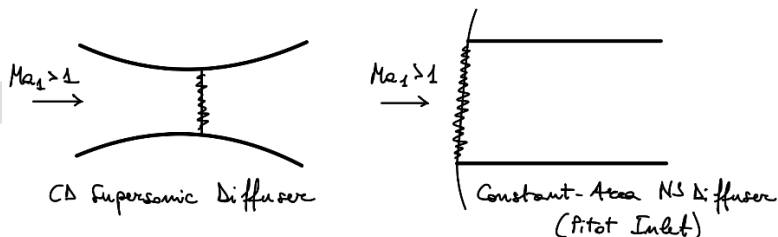


**Figure 66. Impractical supersonic inlet configurations.**

Instead of these designs, we can take the advantage of the fact that an oblique shock provides a more nearly reversible compression than does a normal shock at the same Mach number, and design an oblique shock diffuser, such as those shown in Figure 67.

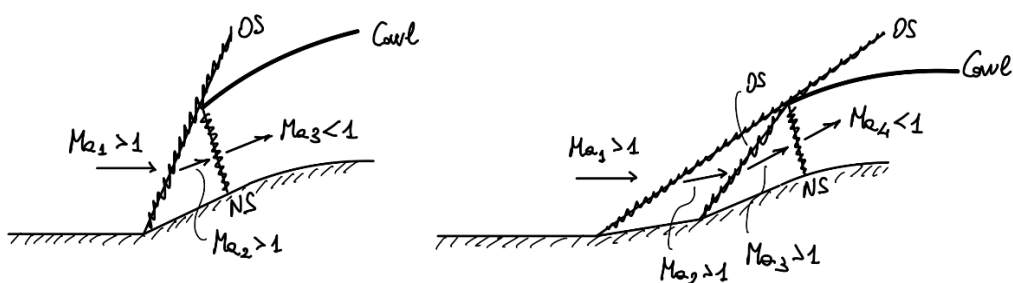


**Figure 67. Single-OS (left) and two-OS (right) supersonic inlet configurations.**

Notable examples are the planar versions on the F-15 or the cylindrical versions on the SR-71.

In both cases shown, a normal shock occurs, but since the Mach number has been lowered through the oblique shocks, the stagnation pressure loss is also lowered. Further subsonic diffusion also occurs internally behind the NS, in the diverging area of the inlet.

Theoretically in the limit of an infinite number of oblique shocks of infinitesimal turning angle, the compression could be carried out isentropically (this is the so-called “isentropic inlet”). However, this would require a very long inlet ramp and, therefore a thick boundary layer. Since the pressure gradient imposed on the boundary layer by the compression is adverse (i.e., increasing) the boundary layer would tend to separate, leading to poor inlet performance. As a rule of thumb, a single-OS diffuser is used for flight Mach numbers up to  $\sim 2.0$ , while multiple-OS diffusers are used for higher flight Mach numbers.

There are three modes of operation for the supersonic inlet depending on the back pressure imposed by the downstream flow conditions, such as the engine speed. These are shown in Figure 68

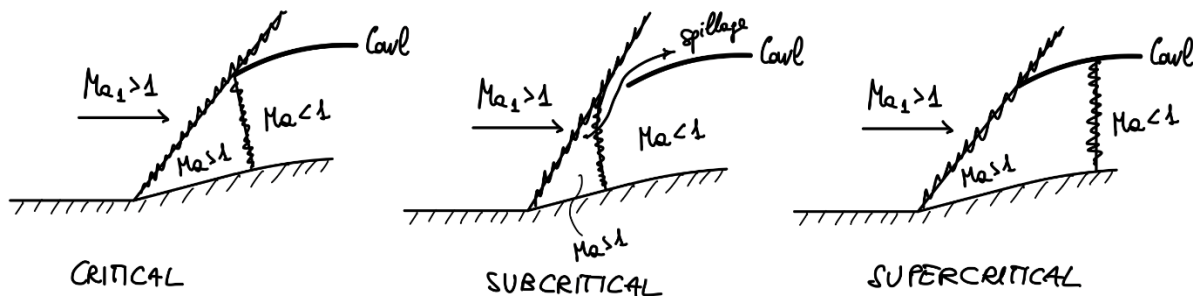


**Figure 68. Modes of operation for supersonic inlets.**

In the *critical* mode of operation, the NS is positioned right at the cowl inlet/diffuser throat so that the inlet ingests the maximum mass flow possible, and the stagnation pressure recovery is the most favorable because the minimum Mach number for the NS in the diffuser duct occurs when it is positioned at the cowl inlet (minimum area).

If the engine speed is reduced so that the back pressure increases, the NS will move out of the inlet and a *subcritical* mode will occur. This is a very unfavorable operation condition because the flow behind the shock is subsonic and will therefore spill over the cowl (creating “spillage drag”). Thus, the inlet is not handling the maximum mass flow in this case. Also, the stagnation pressure recovery is unfavorable because the stagnation pressure loss across the two shocks is large.

If the back pressure is reduced from the critical operating condition, the NS moves further into the diffuser and a *supercritical* operating condition is obtained. In this case, the inlet is handling the maximum mass flow, but the stagnation pressure recovery is not quite as good as for the critical case because the Mach number at which the NS occurs is higher (larger area). However, the supercritical mode is the preferred one because flight increases in the back pressure will not cause an initiation of the subcritical mode as they would for operation right at the critical mode (neutrally stable).

**8.5.2 Flow at the Exit of Overexpanded and Underexpanded Converging-Diverging Nozzles**  
 In section 4.5.3, we found that for overexpanded CD nozzles ( $p_e < p_b$ ), operating between the point at which a NS stands at the exit and the supersonic design point, an oblique shock occurs at the nozzle exit. Underexpanded CD nozzles ( $p_e > p_b$ ), operating at points, i.e., at back pressure ratios below the supersonic design point, PM expansions occur at the exit. We are now well positioned to analyze these exit flows.

Overexpanded case ( $p_e < p_b$ ). Consider the overexpanded mode of operation, but  $p_b/p_{01}$  is low enough ( $p_e$  large enough) that regular reflection occurs. In this case an OS occurs at the exit such that  $p_2 = p_b$ . However, the flow in region ② is directed down toward the axis (turned toward the wave). Because the axis is a plane of symmetry (i.e., treated as a plane wall) a reflected OS must occur to turn the flow in region ③ parallel to the axis. However,  $p_3 > p_b$ , so this OS must reflect from the constant pressure boundary as a centered PM expansion fan so that  $p_4 = p_b$ . The PM expansion direct the flow in region ④ up, away from the axis (turns the flow toward the normal), so that these expansions must reflect from the symmetry plane as expansions to turn the flow back horizontal. In region ⑤, we are essentially back to the conditions in region ①, with horizontal flow and  $p_5 = p_b$ . The flow pattern between ① and ⑤ will theoretically repeat indefinitely, but in reality breaks down after only a few cycles due to viscous mixing of the jet with the ambient.

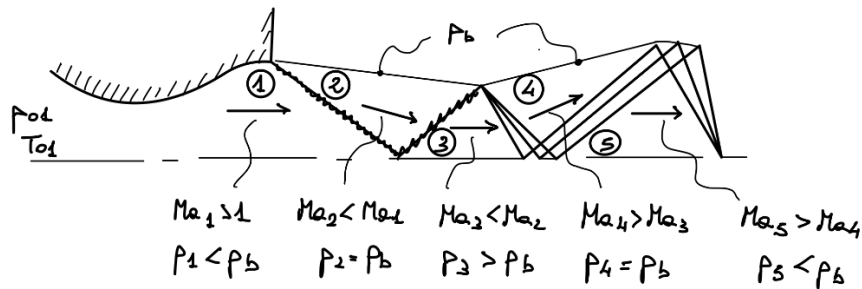


Figure 69. Overexpanded nozzle flow.

If  $p_e$  is too much less than  $p_b$  (i.e., “too overexpanded”), regular reflection is impossible and Mach reflection occurs. In this case, we have a 2D, mixed subsonic/supersonic flow that cannot be analyzed with our simple methods. Note that the breakoff between regular and Mach reflection occurs at the maximum  $\theta$  for which there is just barely a solution possible for the reflected shock, with  $\theta_r = \theta_i$ . This also give a maximum  $p_b/p_e$  for regular reflection.

Underexpanded case ( $p_e > p_b$ ). In the underexpanded mode of operation, the flow exits the nozzle with  $p_1 = p_e > p_b$ . Since  $p_1 > p_b$  a centered PM expansion fan is generated at the exit lip such that  $p_2 = p_b$ . This expansion fan turns the flow in region ② up, away from the axis (turned toward the normal), so that the expansion waves must reflect as expansion waves from the plane of symmetry to turn the flow in region ③ back to the horizontal. However,  $p_3 < p_b$ , so these reflected expansions must reflect as compressions from the jet pressure boundary so that  $p_4 = p_b$ . These compressions turn the flow in region ④ down, towards the axis (turn the flow toward the waves), so that they must reflect from the symmetry plane as compression (or coalesced OS), into order to turn the flow in region ⑤ back horizontal. In region ⑤, the flow is similar to that in region ①, with horizontal flow and  $p_5 > p_b$ . Theoretically, this pattern is again repeated indefinitely, but in reality it breaks down due to viscous mixing.

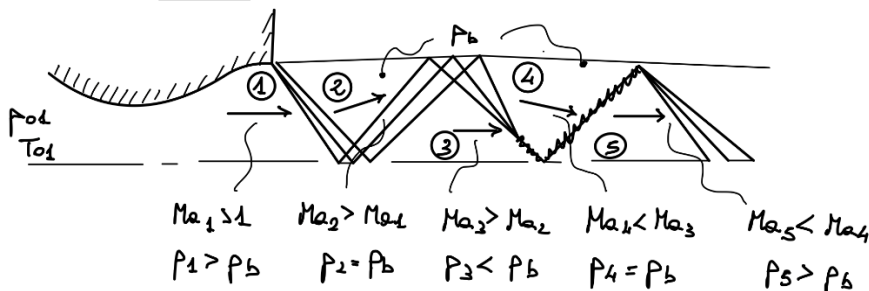
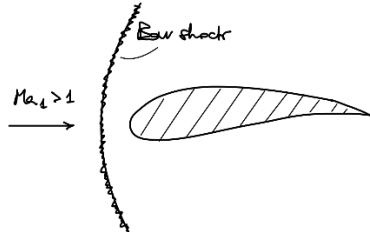


Figure 70. Overexpanded nozzle flow.

### 8.5.3 Supersonic Airfoils

The purpose of an airfoil is to provide lift (force normal to the approach flow) with a minimum drag (force parallel to the approach flow). In low speed, subsonic flow, the drag is composed of skin friction and some pressure drag due to separation near the trailing edge. The optimum airfoil shape that results from these considerations is a streamlined teardrop shape.



**Figure 71.** A detached bow shock forms in front of a teardrop airfoil in supersonic flow.

In supersonic flow, a detached shock wave (bow shock) would occur due to the rounded blunt nature of the leading edge. The drag associated with the high pressure occurring behind the bow shock (*wave drag*) would be prohibitive, so the design must be modified accordingly. The technical solution is to use a *sharp leading edge*.

One possibility is a flat plate flying at an angle of attack (Figure 72). Due to the expansion turn required of the flow on the top surface of the leading edge, a PM expansion fan is generated that lowers the pressure on the upper surface below that of the incoming flow,  $p_2 > p_1$ . The flow is forced to undergo a compression turn at the leading edge of the lower surface, so an oblique shock is formed. This compresses the flow such that  $p_3 > p_1$ . The result of these pressures is a net lift ( $p_3 > p_2$ ) and drag (wave drag). Lift and drag coefficients can be evaluated as:

$$C_L = \frac{\left(\frac{p_3}{p_1} - \frac{p_2}{p_1}\right) \cos \alpha}{\frac{1}{2} \gamma Ma_1^2} \quad (346)$$

$$C_D = \frac{\left(\frac{p_3}{p_1} - \frac{p_2}{p_1}\right) \sin \alpha}{\frac{1}{2} \gamma Ma_1^2} = C_L \tan \alpha \quad (347)$$

where  $\alpha$  is the plate angle of attack.

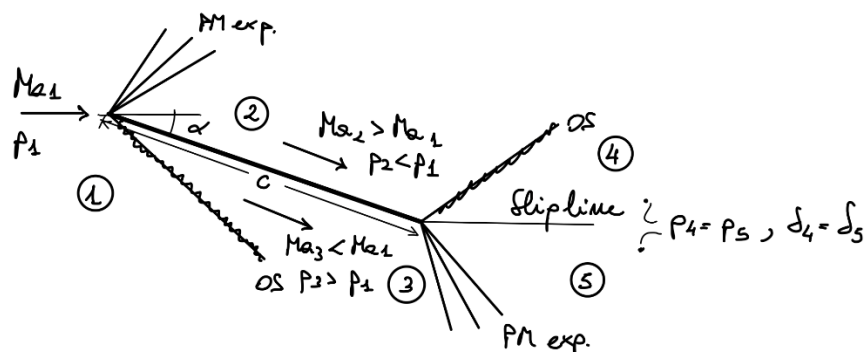


**Figure 72.** Flat plate at an angle of attack in supersonic flow.

However, the flat plate is an idealization, since of course it is structurally unsound. Another possibility that still involves a sharp leading edge to avoid a detached bow shock is the *diamond*

airfoil flying at an angle of attack  $\alpha$ . Depending on  $\alpha$  and on the thickness of the airfoil (i.e., its half-angle  $\epsilon$ ), and OS ( $\alpha < \epsilon$ ) or a PM expansion ( $\alpha > \epsilon$ ) may occur at the top surface leading edge.

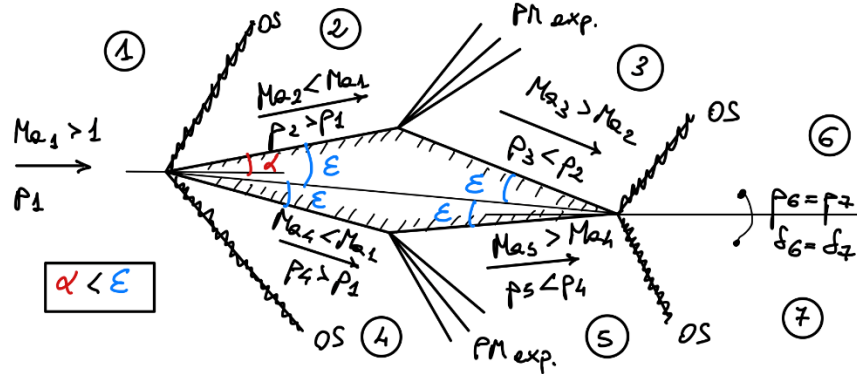


**Figure 73. Diamond airfoil at an angle of attack in supersonic flow.**

For the case illustrated in Figure 73, and OS occurs so  $p_2 > p_1$ . A PM expansion occurs at the expansion turn in the middle of the top surface, such that  $p_3 < p_2$ . On the bottom surface leading edge, a stronger OS occurs than on the top surface, due to the larger turning angle required by the angle of attack, so that  $p_4 > p_1$ . At the expansion turn, in the middle of the bottom surface, a PM expansion occurs,  $p_5 < p_4$ . As a result of these interactions, net lift and (wave) drag are created. The expressions for lift and drag coefficients are a bit more involved than those of the flat plate, but in each case they revert to the basic definitions:

$$C_L = \frac{L/\text{span}}{\frac{1}{2} \rho_1 U_1^2 c} \quad (348)$$

$$C_D = \frac{D/\text{span}}{\frac{1}{2} \rho_1 U_1^2 c} \quad (349)$$

For the flat plate, the flows on the upper and lower surfaces have the same flow direction, but different static pressures. When the flows reach the trailing edge, where we have an OS on the upper surface and a PM expansion on the lower surface, discontinuities must be generated so that across the *slipline* the static pressures are equal,  $p_4 = p_5$ , and the flow directions are the same,  $\delta_4 = \delta_5$ .

For the diamond airfoil, not only are the static pressures different in regions ③ and ⑤, but so are the flow directions. Again, discontinuities must be generated at the trailing edge, such that across the slipline  $p_6 = p_7$  and  $\delta_6 = \delta_7$ . In both cases the flow over the upper and lower surfaces encounters shocks of different strengths so that the stagnation pressures and entropies in regions ④ and ⑤ for the flat plate and regions ⑥ and ⑦ for the diamond airfoil are slightly different. This results in slightly different velocities, static temperatures, densities, etc. in these regions, which are separated by a slipline (a line of infinite vorticity). The boundary conditions to be applied across the slipline are equality of static pressure and flow direction. The deviations of the pressures from  $p_1$  and the flow directions from the approach flow direction in these regions are generally small.